

HAZARD MAPPING OF THE PHILIPPINES USING LIDAR (PHIL-LIDAR I)

LiDAR Surveys and Flood Mapping of Mayo River



University of the Philippines Training Center
for Applied Geodesy and Photogrammetry
University of the Philippines Mindanao

APRIL 2017



© University of the Philippines Diliman and University of the Philippines Mindanao 2017

Published by the UP Training Center for Applied Geodesy and Photogrammetry (TCAGP)
College of Engineering
University of the Philippines – Diliman
Quezon City
1101 PHILIPPINES

This research project is supported by the Department of Science and Technology (DOST) as part of its Grants-in-Aid Program and is to be cited as:

E.C. Paringit, and J.E. Acosta, (Eds.). (2017), *LiDAR Surveys and Flood Mapping of Mayo River*. Quezon City: University of the Philippines Training Center for Applied Geodesy and Photogrammetry-130 pp.

The text of this information may be copied and distributed for research and educational purposes with proper acknowledgement. While every care is taken to ensure the accuracy of this publication, the UP TCAGP disclaims all responsibility and all liability (including without limitation, liability in negligence) and costs which might incur as a result of the materials in this publication being inaccurate or incomplete in any way and for any reason.

For questions/queries regarding this report, contact:

Dr. Joseph E. Acosta

Project Leader, Phil-LiDAR 1 Program
University of the Philippines Mindanao
Davao City, Davao del Sur, 8000
E-mail: jacosta_96140@yahoo.com

Enrico C. Paringit, Dr. Eng.

Program Leader, Phil-LiDAR 1 Program
University of the Philippines Diliman
Quezon City, Philippines 1101
E-mail: ecparingit@up.edu.ph

National Library of the Philippines
ISBN: 987-621-430-196-0

TABLE OF CONTENTS

| | |
|--|------------|
| TABLE OF CONTENTS | iii |
| LIST OF TABLES | v |
| LIST OF FIGURES | vii |
| LIST OF ACRONYMS AND ABBREVIATIONS | x |
| CHAPTER 1: OVERVIEW OF THE PROGRAM AND MAYO RIVER | 1 |
| 1.1 Background of the Phil-LiDAR 1 Program..... | 1 |
| 1.2 Overview of the Mayo River Basin..... | 1 |
| CHAPTER 2: LIDAR DATA ACQUISITION OF THE MAYO FLOODPLAIN | 5 |
| 2.1 Flight Plans..... | 5 |
| 2.2 Ground Base Stations..... | 7 |
| 2.3 Flight Missions..... | 12 |
| 2.4 Survey Coverage..... | 13 |
| CHAPTER 3: LIDAR DATA PROCESSING OF THE MAYO FLOODPLAIN | 15 |
| 3.1 Overview of the LiDAR Data Pre-Processing..... | 15 |
| 3.2 Transmittal of Acquired LiDAR Data..... | 16 |
| 3.3 Trajectory Computation..... | 16 |
| 3.4 LiDAR Point Cloud Computation..... | 18 |
| 3.5 LiDAR Data Quality Checking..... | 19 |
| 3.6 LiDAR Point Cloud Classification and Rasterization..... | 23 |
| 3.7 LiDAR Image Processing and Orthophotograph Rectification..... | 25 |
| 3.8 DEM Editing and Hydro-Correction..... | 26 |
| 3.9 Mosaicking of Blocks..... | 28 |
| 3.10 Calibration and Validation of Mosaicked LiDAR Digital Elevation Model (DEM)..... | 30 |
| 3.11 Integration of Bathymetric Data into the LiDAR Digital Terrain Model..... | 33 |
| 3.12 Feature Extraction..... | 35 |
| 3.12.1 Quality Checking of Digitized Features' Boundary | 35 |
| 3.12.2 Height Extraction | 36 |
| 3.12.3 Feature Attribution | 36 |
| 3.12.4 Final Quality Checking of Extracted Features..... | 37 |
| CHAPTER 4: LIDAR VALIDATION SURVEY AND MEASUREMENTS OF THE MAYO RIVER BASIN | 38 |
| 4.1 Summary of Activities..... | 38 |
| 4.2 Control Survey..... | 40 |
| 4.3 Baseline Processing..... | 45 |
| 4.4 Network Adjustment..... | 46 |
| 4.5 Cross-section and Bridge As-Built survey and Water Level Marking..... | 49 |
| 4.6 Validation Points Acquisition Survey..... | 54 |
| 4.7 River Bathymetric Survey..... | 56 |
| CHAPTER 5: FLOOD MODELING AND MAPPING | 61 |
| 5.1 Data Used for Hydrologic Modeling..... | 61 |
| 5.1.1 Hydrometry and Rating Curves..... | 61 |
| 5.1.2 Precipitation..... | 61 |
| 5.1.3 Rating Curves and River Outflow..... | 63 |
| 5.2 RIDF Station..... | 64 |
| 5.3 HMS Model..... | 66 |
| 5.4 Cross-section Data..... | 71 |
| 5.5 Flo2D Model..... | 72 |
| 5.6 Results of HMS Calibration..... | 73 |
| 5.7 Calculated outflow hydrographs and discharge values for different rainfall return periods..... | 75 |
| 5.7.1 Hydrograph using the Rainfall Runoff Model | 75 |
| 5.8 River Analysis (RAS) Model Simulation..... | 77 |
| 5.9 Flow Depth and Flood Hazard..... | 78 |
| 5.10 Inventory of Areas Exposed to Flooding..... | 85 |
| 5.11 Flood Validation..... | 92 |
| REFERENCES | 95 |
| ANNEXES | 96 |
| Annex 1. Optech Technical Specification of the Gemini Sensor..... | 96 |
| Annex 2. NAMRIA Certification of Reference Points Used in the LIDAR Survey..... | 97 |
| Annex 3. Baseline Processing Reports of Control Points used in the LIDAR Survey..... | 99 |
| Annex 4. The LIDAR Survey Team Composition..... | 101 |

| | |
|---|-----|
| Annex 5. Data Transfer Sheet for Mayo Floodplain..... | 102 |
| Annex 6. Flight Logs for the Flight Missions..... | 104 |
| Annex 7. Flight Status Reports..... | 108 |
| Annex 8. Mission Summary Reports..... | 113 |
| Annex 9. Mayo Model Basin Parameters..... | 118 |
| Annex 10. Mayo Model Reach Parameters..... | 120 |
| Annex 11. Mayo Field Validation Points..... | 121 |
| Annex 12. Educational Institutions affected by flooding in Mayo Floodplain..... | 127 |
| Annex 13. Health Institutions affected by flooding in Mayo Floodplain..... | 127 |

LIST OF TABLES

| | |
|---|----|
| Table 1. Flight planning parameters for the Gemini LiDAR system..... | 5 |
| Table 2. Details of the recovered NAMRIA horizontal control point DVE-42 used as base station for the LiDAR acquisition..... | 8 |
| Table 3. Details of the recovered NAMRIA horizontal control point DVE-61 used as base station for the LiDAR acquisition..... | 9 |
| Table 4. Details of the recovered NAMRIA horizontal control point DVE-3088 used as base station for the LiDAR acquisition with established coordinates..... | 10 |
| Table 5. Details of the recovered NAMRIA horizontal control point DVE-3118 used as base station for the LiDAR acquisition with established coordinates..... | 11 |
| Table 6. Ground control points used during the LiDAR data acquisition..... | 12 |
| Table 7. Flight missions for the LiDAR data acquisition in Mayo Floodplain..... | 12 |
| Table 8. Actual parameters used during the LiDAR data acquisition of the Mayo Floodplain..... | 12 |
| Table 9. List of municipalities and cities surveyed of the Mayo Floodplain LiDAR acquisition..... | 13 |
| Table 10. Self-calibration Results values for Mayo flights..... | 18 |
| Table 11. List of LiDAR blocks for Mayo Floodplain..... | 19 |
| Table 12. Mayo classification results in TerraScan..... | 23 |
| Table 13. LiDAR blocks with its corresponding areas..... | 26 |
| Table 14. Shift values of each LiDAR block of Mayo Floodplain..... | 28 |
| Table 15. Calibration Statistical Measures..... | 32 |
| Table 16. Validation Statistical Measures..... | 33 |
| Table 17. Quality Checking Ratings for Mayo Building Features..... | 35 |
| Table 18. Building Features Extracted for Mayo Floodplain..... | 36 |
| Table 19. Total Length of Extracted Roads for Mayo Floodplain..... | 37 |
| Table 20. Number of Extracted Water Bodies for Mayo Floodplain..... | 37 |
| Table 21. List of Reference and Control Points occupied for Mayo River Survey..... | 40 |
| Table 22. Baseline Processing Summary Report for Mayo River Survey..... | 45 |
| Table 23. Constraints applied to the adjustment of the control points..... | 46 |
| Table 24. Adjusted grid coordinates for the control points used in the Mayo River Floodplain survey..... | 46 |
| Table 25. Adjusted geodetic coordinates for control points used in the Mayo River Floodplain validation..... | 47 |
| Table 26. The reference and control points utilized in the Balamban River Static Survey, with their corresponding locations (Source: NAMRIA, UP-TCAGP)..... | 48 |
| Table 27. RIDF values for Davao Rain Gauge computed by PAGASA..... | 64 |
| Table 28. Range of calibrated values for the Mayo River Basin..... | 73 |
| Table 29. Summary of the Efficiency Test of the Balamban HMS Model..... | 74 |
| Table 30. Peak values of the Mayo HEC-HMS Model outflow using the Davao RIDF 24-hour values..... | 76 |
| Table 31. Municipalities affected in Mayo Floodplain..... | 78 |
| Table 32. Affected areas in Mati City, Davao Oriental during a 5-Year Rainfall Return Period..... | 85 |
| Table 33. Affected areas in Tarragona, Davao Oriental during a 5-Year Rainfall Return Period..... | 86 |
| Table 34. Affected areas in Mati City, Davao Oriental during a 25-Year Rainfall Return Period..... | 87 |
| Table 35. Affected areas in Tarragona, Davao Oriental during a 25-Year Rainfall Return Period..... | 88 |
| Table 36. Affected areas in Mati City, Davao Oriental during a 100-Year Rainfall Return Period..... | 89 |

| | |
|---|----|
| Table 37. Affected areas in Tarragona, Davao Oriental during a 100-Year Rainfall Return Period..... | 90 |
| Table 38. Areas covered by each warning level with respect to the rainfall scenarios..... | 91 |
| Table 39. Actual flood vs simulated flood depth at different levels in the Mayo River Basin..... | 93 |
| Table 40. Summary of the Accuracy Assessment in the Mayo River Basin Survey..... | 94 |

LIST OF FIGURES

| | |
|---|----|
| Figure 1. Map of Mayo River Basin (in brown) | 2 |
| Figure 2. Mayo River flood history | 3 |
| Figure 3. Flight Plan and base station used for the Mayo Floodplain survey..... | 6 |
| Figure 4. GPS set-up over DVE-42 located inside the premises of Don Enrique Elementary School, in front of the flagpole (a) and NAMRIA reference point DVE-42 (b) as recovered by the field team. | 8 |
| Figure 5. GPS set-up over DVE-61 located at the center of the playground of Zign Elementary School, about 10 m W of school flagpole (a) and NAMRIA reference point DVE-61 (b) as recovered by the field team..... | 9 |
| Figure 6. GPS set-up over DVE-3088 located inside Don Enrique Lopez Elementary School (a) and NAMRIA reference point DVE-3088 (b) as recovered by the field team. | 10 |
| Figure 7. GPS set-up over DVE-3118 located along the boundary of Barangays Dawan and Badas (a) and NAMRIA reference point DVE-3118 (b) as recovered by the field team.... | 11 |
| Figure 8. Actual LiDAR survey coverage of the Mayo Floodplain. | 14 |
| Figure 9. Schematic diagram for Data Pre-Processing Component..... | 15 |
| Figure 10. Smoothed Performance Metric Parameters of Mayo Flight 7362GC | 16 |
| Figure 11. Solution Status Parameters of Mayo Flight 7362GC..... | 17 |
| Figure 12. Best Estimated Trajectory of the LiDAR missions conducted over the Mayo Floodplain..... | 18 |
| Figure 13. Boundary of the processed LiDAR data over Mayo Floodplain | 19 |
| Figure 14. Image of data overlap for Mayo Floodplain..... | 20 |
| Figure 15. Pulse density map of merged LiDAR data for Mayo Floodplain..... | 21 |
| Figure 16. Elevation Difference Map between flight lines for Mayo Floodplain Survey. | 22 |
| Figure 17. Quality checking for Mayo Flight 7362GC using the Profile Tool of QT Modeler. | 23 |
| Figure 18. Tiles for Mayo Floodplain (a) and classification results (b) in TerraScan. | 24 |
| Figure 19. Point cloud before (a) and after (b) classification..... | 24 |
| Figure 20. The production of last return DSM (a) and DTM (b), first return DSM (c) and secondary DTM (d) in some portion of Mayo Floodplain. | 25 |
| Figure 21. Portions in the DTM of Mayo Floodplain – a bridge before (a) and after (b) manual editing..... | 27 |
| Figure 22. Map of Processed LiDAR Data for Mayo Floodplain | 29 |
| Figure 23. Map of Mayo Floodplain with validation survey points in green. | 31 |
| Figure 24. Correlation plot between calibration survey points and LiDAR data..... | 32 |
| Figure 25. Correlation plot between validation survey points and LiDAR data. | 33 |
| Figure 26. Map of Mayo Floodplain with bathymetric survey points shown in blue. | 34 |
| Figure 27. Blocks (in blue) of Mayo building features that were subjected to QC | 35 |
| Figure 28. Extracted features for Mayo Floodplain. | 37 |
| Figure 29. Extent of the bathymetric survey (in blue line) in Mayo River | 39 |
| and the LiDAR data validation survey (in red). | 39 |
| Figure 30. The GNSS Network established in the Mayo River Survey..... | 41 |
| Figure 31. GNSS base set up, Trimble® SPS 852, at DVE-42, located in front of the flagpole inside Don Enrique Lopez Elementary School in Brgy. Don Enrique Lopez, Mati City, Davao Oriental..... | 42 |
| Figure 32. GNSS receiver set up, Trimble® SPS 985, at DE-160, located at approach of Calinan Bridge in Brgy. Mayo, City of Mati, Davao Oriental..... | 43 |
| Figure 33. GNSS receiver set up, Trimble® SPS 852, at UP_BIT-1, located at the side of the railing near the approach of Bitanagan Bridge in Brgy. Don Enrique Lopez, City of Mati, Davao Oriental | 43 |

| | |
|---|----|
| Figure 34. GNSS receiver set up, Trimble® SPS 985, at UP_MAY-1, located beside the approach of Mayo Bridge in Brgy. Mayo, City of Mati, Province of Davao Oriental | 44 |
| Figure 35. GNSS receiver set up, Trimble® SPS 882, at UP QUI-1, located beside the approach of Quinonoan Bridge in Brgy. San Ignacio, Municipality of Manay, Province of Davao Oriental | 44 |
| Figure 36. Mayo Bridge facing downstream | 49 |
| Figure 37. As-built survey of Mayo Bridge..... | 50 |
| Figure 38. Mayo Bridge cross-section diagram..... | 51 |
| Figure 39. As-built survey of Mayo Bridge..... | 52 |
| Figure 40. Water level markings on Mayo Bridge..... | 53 |
| Figure 41. Validation points acquisition survey set-up for Mayo River..... | 54 |
| Figure 42. Validation point acquisition survey of Mayo River basin | 55 |
| Figure 43. Manual bathymetric survey of ABSD at Bugnan Mayo River using Horizon® Total Station .. | 56 |
| Figure 44. Gathering of random bathymetric points along Bugnan Mayo River | 57 |
| Figure 45. Extent of the Mayo River Bathymetry Survey..... | 58 |
| Figure 46. Quality checking points gathered along Mayo River by DVBC..... | 59 |
| Figure 47. Mayo riverbed profile. | 60 |
| Figure 48. Location map of the Balamban HEC-HMS model used for calibration. | 62 |
| Figure 49. Cross-section plot of Mayo Bridge..... | 63 |
| Figure 50. Rating curve at Mayo Bridge, Tarragona, Davao Oriental..... | 63 |
| Figure 51. Rainfall and outflow data at Mayo Bridge used for modeling | 64 |
| Figure 52. Location of Davao RIDF Station relative to Mayo River Basin | 65 |
| Figure 53. Synthetic storm generated for a 24-hr period rainfall for various return periods. | 65 |
| Figure 54. Soil Map of Mayo River Basin used for the estimation of the CN parameter. | 66 |
| Figure 55. Land Cover Map of Mayo River Basin used for the estimation of the Curve Number (CN) and the watershed lag parameters of the rainfall-runoff model..... | 67 |
| Figure 56. Slope Map of Mayo River Basin | 68 |
| Figure 57. Stream Delineation Map of Mayo River Basin | 69 |
| Figure 58. Mayo River Basin model generated in HEC-HMS..... | 70 |
| Figure 59. River cross-section of Mayo River generated through Arcmap HEC GeoRAS tool..... | 71 |
| Figure 60. Screenshot of the river sub-catchment with the computational area to be modeled in FLO-2D Grid Developer System Pro (FLO-2D GDS Pro) | 72 |
| Figure 61. Outflow hydrograph of Balamban produced by the HEC-HMS model compared with observed outflow | 73 |
| Figure 62. Outflow hydrograph at Mayo Station generated using the Davao RIDF simulated in HEC-HMS. | 75 |
| Figure 63. Sample output map of Mayo RAS Model | 77 |
| Figure 64. 100-year Flood Hazard Map for Mayo Floodplain overlaid on Google Earth imagery..... | 79 |
| Figure 65. 100-year Flow Depth Map for Mayo Floodplain overlaid on Google Earth imagery | 80 |
| Figure 66. 25-year Flood Hazard Map for Mayo Floodplain overlaid on Google Earth imagery..... | 81 |
| Figure 67. 25-year Flow Depth Map for Mayo Floodplain overlaid on Google Earth imagery | 82 |
| Figure 68. 5-year Flood Hazard Map for Mayo Floodplain overlaid on Google Earth imagery..... | 83 |
| Figure 69. 5-year Flood Depth Map for Mayo Floodplain overlaid on Google Earth imagery | 84 |
| Figure 70. Affected Areas in Mati City, Davao Oriental during 5-Year Rainfall Return Period..... | 85 |
| Figure 71. Affected Areas in Tarragona, Davao Oriental during 5-Year Rainfall Return Period..... | 86 |
| Figure 72. Affected Areas in Mati City, Davao Oriental during 25-Year Rainfall Return Period..... | 87 |
| Figure 73. Affected Areas in Tarragona, Davao Oriental during 25-Year Rainfall Return Period..... | 88 |
| Figure 74. Affected Areas in Mati City, Davao Oriental during 100-Year Rainfall Return Period..... | 89 |
| Figure 75. Affected Areas in Tarragona, Davao Oriental during 100-Year Rainfall Return Period..... | 90 |

Figure 76. Mayo Flood Validation Points 92
Figure 77. Flood map depth vs. actual flood depth..... 93

LIST OF ACRONYMS AND ABBREVIATIONS

| | | | |
|---------|---|----------|--|
| AAC | Asian Aerospace Corporation | IMU | Inertial Measurement Unit |
| Ab | abutment | kts | knots |
| ALTM | Airborne LiDAR Terrain Mapper | LAS | LiDAR Data Exchange File format |
| ARG | automatic rain gauge | LC | Low Chord |
| AWLS | Automated Water Level Sensor | LGU | local government unit |
| BA | Bridge Approach | LiDAR | Light Detection and Ranging |
| BM | benchmark | LMS | LiDAR Mapping Suite |
| CAD | Computer-Aided Design | m AGL | meters Above Ground Level |
| CN | Curve Number | MMS | Mobile Mapping Suite |
| CSRS | Chief Science Research Specialist | MSL | mean sea level |
| DA-BSWM | Department of Agriculture - Bureau of Soil and Water Management | NSTC | Northern Subtropical Convergence |
| DAC | Data Acquisition Component | PAF | Philippine Air Force |
| DEM | Digital Elevation Model | PAGASA | Philippine Atmospheric Geophysical and Astronomical Services Administration |
| DENR | Department of Environment and Natural Resources | PDOP | Positional Dilution of Precision |
| DOST | Department of Science and Technology | PPK | Post-Processed Kinematic [technique] |
| DPPC | Data Pre-Processing Component | PRF | Pulse Repetition Frequency |
| DREAM | Disaster Risk and Exposure Assessment for Mitigation [Program] | PTM | Philippine Transverse Mercator |
| DRRM | Disaster Risk Reduction and Management | QC | Quality Check |
| DSM | Digital Surface Model | QT | Quick Terrain [Modeler] |
| DTM | Digital Terrain Model | RA | Research Associate |
| DVBC | Data Validation and Bathymetry Component | RIDF | Rainfall-Intensity-Duration-Frequency |
| FMC | Flood Modeling Component | RMSE | Root Mean Square Error |
| FOV | Field of View | SAR | Synthetic Aperture Radar |
| GiA | Grants-in-Aid | SCS | Soil Conservation Service |
| GCP | Ground Control Point | SRTM | Shuttle Radar Topography Mission |
| GNSS | Global Navigation Satellite System | SRS | Science Research Specialist |
| GPS | Global Positioning System | SSG | Special Service Group |
| HEC-HMS | Hydrologic Engineering Center - Hydrologic Modeling System | TBC | Thermal Barrier Coatings |
| HEC-RAS | Hydrologic Engineering Center - River Analysis System | UP-TCAGP | University of the Philippines – Training Center for Applied Geodesy and Photogrammetry |
| HC | High Chord | UTM | Universal Transverse Mercator |
| IDW | Inverse Distance Weighted [interpolation method] | USC | University of San Carlos |
| | | WGS | World Geodetic System |

CHAPTER 1: OVERVIEW OF THE PROGRAM AND MAYO RIVER

Enrico C. Paringit, Dr. Eng., Dr. Joseph E. Acosta, and Dr. Ruth James

1.1 Background of the Phil-LiDAR 1 Program

The University of the Philippines Training Center for Applied Geodesy and Photogrammetry (UP-TCAGP) launched a research program entitled “Nationwide Hazard Mapping using LiDAR” or Phil-LiDAR 1 in 2014, supported by the Department of Science and Technology (DOST) Grant-in-Aid (GiA) Program. The program was primarily aimed at acquiring a national elevation and resource dataset at sufficient resolution to produce information necessary to support the different phases of disaster management. Particularly, it targeted to operationalize the development of flood hazard models that would produce updated and detailed flood hazard maps for the major river systems in the country.

Also, the program was aimed at producing an up-to-date and detailed national elevation dataset suitable for 1:5,000 scale mapping, with 50 cm and 20 cm horizontal and vertical accuracies, respectively. These accuracies were achieved through the use of the state-of-the-art Light Detection and Ranging (LiDAR) airborne technology procured by the project through DOST. The methods described in this report are thoroughly described in a separate publication entitled “Flood Mapping of Rivers in the Philippines Using Airborne LiDAR: Methods (Paringit, et. al., 2017) available separately.

The implementing partner university for the Phil-LiDAR 1 Program is the University of the Philippines Mindanao (USC) is in charge of processing LiDAR data and conducting data validation reconnaissance, cross section, bathymetric survey, validation, river flow measurements, flood height and extent data gathering, flood modeling, and flood map generation for the 13 river basins in the Southern Mindanao Region. The university is located in Davao City in the province of Davao del Sur.

1.2 Overview of the Mayo River Basin

The Mayo River Basin covers two (2) municipalities and one (1) city in Davao Oriental, namely the Municipalities of Lupon and Tarragona and the City of Mati on the southeastern side of Mindanao. The DENR River Basin Control Office (RBCO) states that the Mayo River Basin has a drainage area of 146 km² and an estimated 292 cubic meter (MCM) annual run-off (RBCO, 2015).

The Mayo Watershed traverses between the City of Mati and the Municipality of Tarragona with the Pacific Ocean and Mayo Bay on its east and south. It has a total drainage area of 294 square kilometers. It has 22 junctions, 22 reaches, and 45 subbasins. The Mayo River, the main stem of Mayo River Basin, is part of the fourteen (14) river systems under the PHIL-LIDAR 1 Program partner HEI, UP Mindanao.

Mayo River serves as one of the major drainage systems in the area of the Mt. Mayo mountain range. It is described as generally dendritic abound with vegetation. The Mt. Mayo Range is bounded to the west by Lupon, to the South by Mati, and to the east by Tarragona. It is the closest forest neighbor from Mt. Hamiguitan which is a national park and wildlife sanctuary. From Mount Mayo, the river flows downstream to Mayo bay facing the Pacific Ocean where local sea turtles known as pawikans and dugongs can be found (Republic Act No. 4755, 1966; Lasco, 2014; Ibanez, 2015).

The Mineral Production Sharing Agreement (MPSA) 184 XI between the Municipalities of Lupon and Tarragona is considered to be a gold-rush site and is host to artisan mining activities. It has been explored for copper and gold until 2012 when the Mines and Geosciences Bureau (MGB) issued a cease and desist order against all small-scale mining operations in the area (Oro East, 2011; ABS-CBN, 2014).

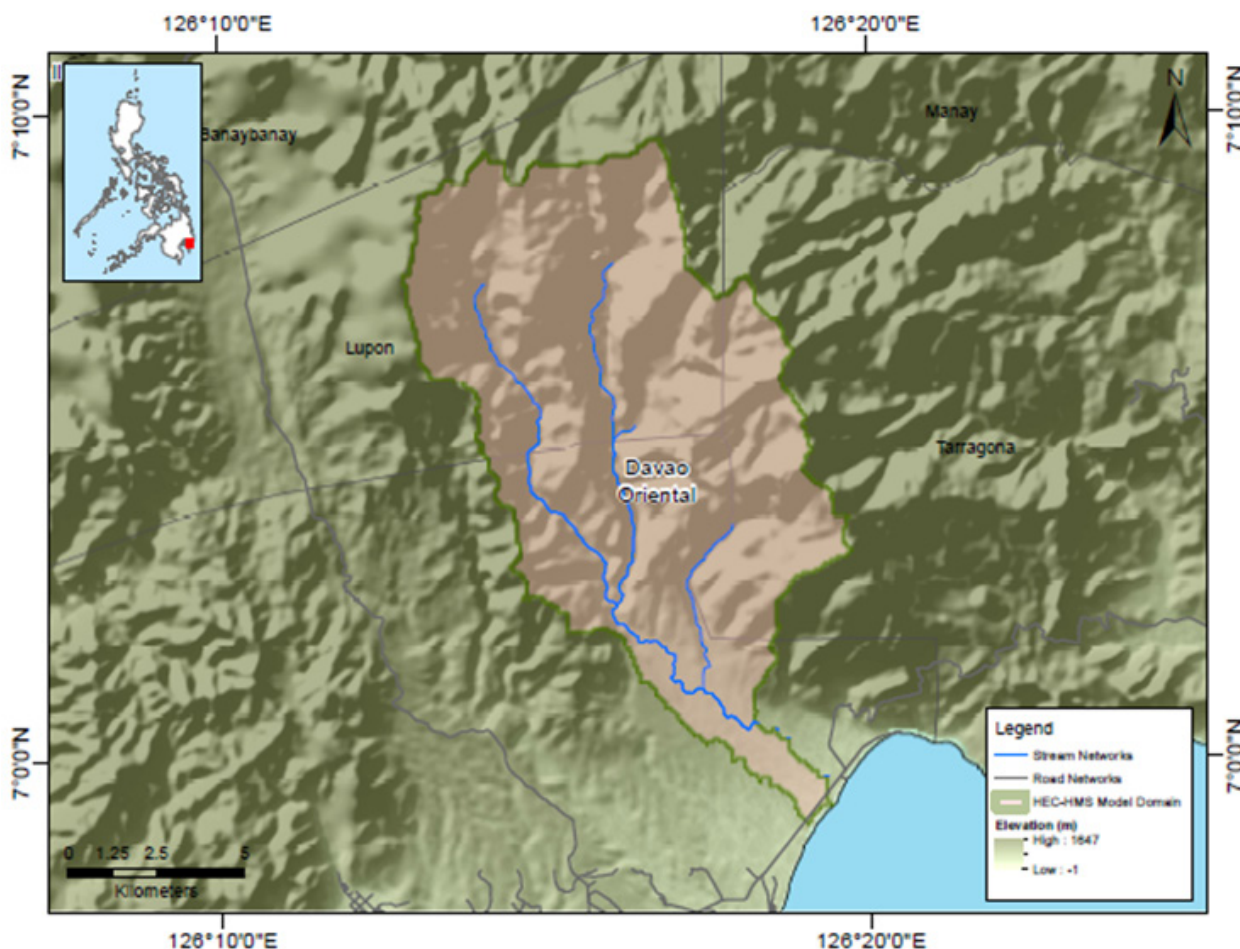


Figure 1. Map of Mayo River Basin (in brown)

Mati comes from the Mandayan word “Maa-ti” which refers to the creek that dries up easily even after heavy rain. The river flows towards the Pacific Ocean into Mayo Bay where rich marine life and various species of sea turtles, sea cows, dolphins, and whale sharks can be seen (Lim, 2014). Based on local history, the site of Dahican was settled by Moro pirates as an anchoring place for their vintas due to its fine harbor. It had no particular name yet but they gradually called it Dahican from the word “dahic” which “means to set on shore a boat”. It has been the official name of the barrio since the advent of the American regime (Capili, 2014). Currently, Dahican is known for its rich marine life and ecotourism. Its 7 kilometers of white sand beach offers a wide range of activities including skimboarding and surfing which invites a diverse crowd: from small kids and local hobbyists to first-time tourists (Triptheislands, 2013).

Historical accounts indicate that the early residents of the locality include the Mandayans along the river and on Mt. Mayo, Kalagans, and Maranaos at the harbor of Mati. These tribes’ indigenous culture carries strong traces of Indo-Malayan and Arabic influences (Official Website of the City of Mati, 2017; Philippine Cities, 2017; Travelgrove Inc., 2017).

Mayo River has been part of the Mandaya tribe’s history and culture. In fact, the river is a key element in the tribe’s creation myth. The Children of Limokon (Cole, 1916; Gale, 2002) tells the story of the Limokon, a kind of dove that was powerful and could talk like men. One limokon laid two eggs in Mayo River and when they hatched, became a man and a woman. Their children are now the Mandaya still living along the Mayo River. In the oral traditions of the Kaagan, their early civilization is situated at “Bawiy” which is now called the Mayo River in Mati City (Sunstar, 2015).

Another pioneering settler is the Kaagan or Kalagan tribe. Kaagan came from the word “kaag” which means “to inform,” “to secure,” “to warn,” or “secrecy”. It is a native word used to inform other members of the tribe when something is about to happen. The Kaagans, also called Tagakaolo-Kaagan, were part of the Tagakaolo tribe converted to Islam. Kaagans lived along the riverbanks of Mayo River, Mati, Davao Oriental; Summog (Sumlog), Lupon, Davao Oriental; Mamuyapoy, Tarragona, Davao Oriental; Bingcungan; Hijo and Pantukan, Compostela Valley Province (Manuel, 2010; Lasco, 2014).



UPMIn Phil-LiDAR 1, 2015

MAYO RIVER FLOOD HISTORY

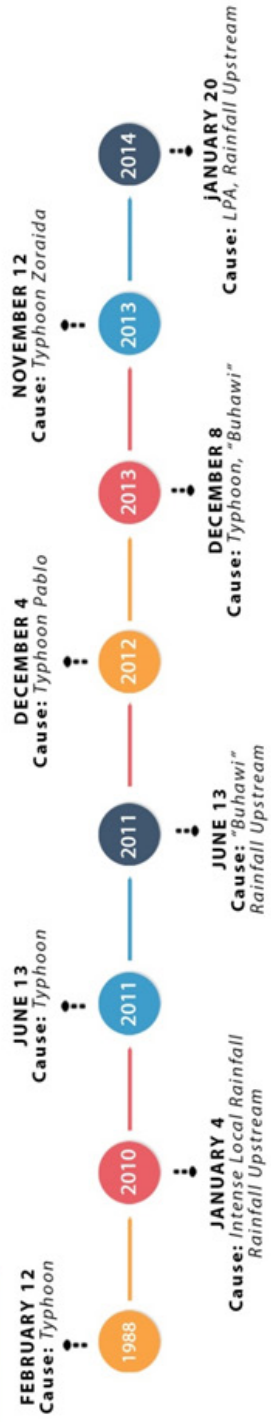


Figure 2. Mayo River flood history

According to the 2015 national census of PSA, a total of 12,581 persons distributed among Barangay Don Salvador Lopez, Sr., Mayo, and Don Enrique Lopez in the City of Mati are residing within the immediate vicinity of the river.

Locals say that from the year 1988 to 2014, local rainfall and “buhawi” are the usual cause of flooding near the river. However, PAGASA only noted typhoon events such as Pablo in 2012 and Yolanda and Zoraida in 2013. Also, on November 8, 2011, heavy rains brought by the Inter Tropical Convergence Zone (ITCZ) flooded Mati City with one (1) house in Brgy. Central partially damaged as per NDRRMC report (National Disaster Risk Reduction and Management Council, 2011).

Nevertheless, Brgy. Mayo was hailed on November 2015 as one of the best prepared barangays in terms of disaster risk prevention. Upon inspection, all 26 barangays in the City of Mati have their own fully-functional Barangay Disaster Operations Center (Deloso, 2015).

CHAPTER 2: LIDAR DATA ACQUISITION OF THE MAYO FLOODPLAIN

Engr. Louie P. Balicanta, Engr. Christopher Cruz, Lovely Acuna, Engr. Gerome Hipolito, Ms. Pauline Joanne G. Arceo, and Engr. Kenneth A. Quisado.

The methods applied in this Chapter were based on the DREAM methods manual (Sarmiento, et al., 2014) and further enhanced and updated in Paringit, et al. (2017).

2.1 Flight Plans

Plans were made to acquire LiDAR data within the delineated priority area for Mayo Floodplain in Davao Oriental. These missions were planned for 14 lines and ran for at most four and a half (4.5) hours including take-off, landing and turning time. The flight planning parameters for the LiDAR system is found in Table 1. Figure 3 shows the flight plans and base stations used for Mayo Floodplain.

Table 1. Flight planning parameters for the Gemini LiDAR system.

| Block Name | Flying Height (m AGL) | Overlap (%) | Field of view (ϕ) | Pulse Repetition Frequency (PRF) (kHz) | Scan Frequency (Hz) | Average Speed (kts) | Average Turn Time (Minutes) |
|------------|-----------------------|-------------|--------------------------|--|---------------------|---------------------|-----------------------------|
| BLK84B | 1000 | 40 | 40 | 100 | 50 | 130 | 5 |
| BLK84C | 1200 | 30 | 26 | 70 | 60 | 130 | 5 |
| BLK85B | 1200 | 30 | 26 | 70 | 60 | 130 | 5 |

¹ The explanation of the parameters used are in the volume "LiDAR Surveys and Flood Mapping in the Philippines: Methods."

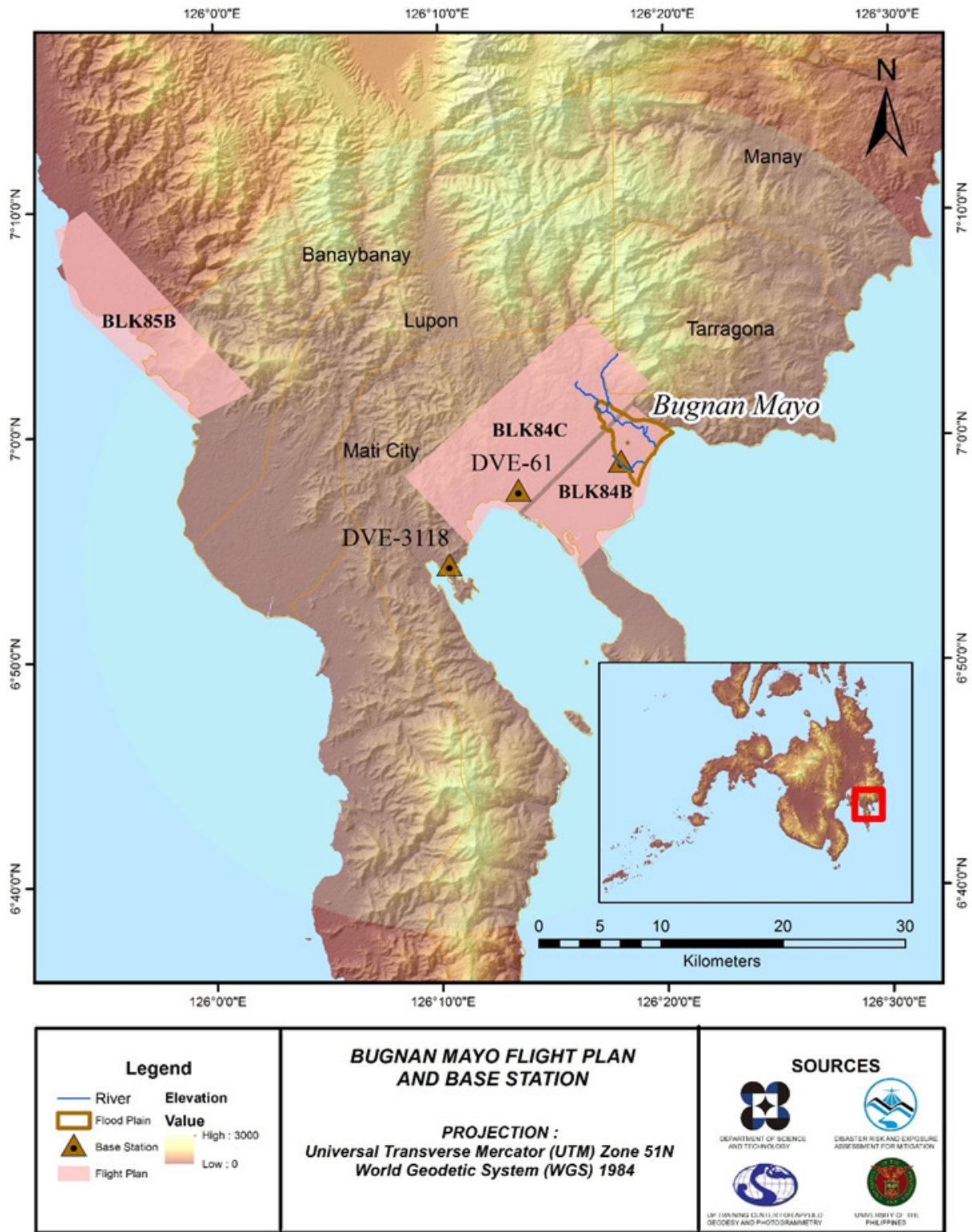


Figure 3. Flight Plan and base station used for the Mayo Floodplain survey.

2.2 Ground Base Stations

The project team was able to recover four (4) NAMRIA ground control points: DVE-42 and DVE-61 which are of second (2nd) order accuracy, and DVE-3088 and DVE-3118 which are of fourth (4th) order accuracy. Fourth (4th) order ground control points were then re-processed to obtain coordinates of second (2nd) order accuracy. The certifications for the NAMRIA reference points are found in Annex 2 while the baseline processing reports for the re-processed control points are found in Annex 3. These were used as base stations during flight operations for the entire duration of the survey (June 19 – July 11, 2014). Base stations were observed using dual frequency GPS receivers, TRIMBLE SPS 882 and SPS 985. Flight plans and location of base stations used during the aerial LiDAR acquisition in Mayo Floodplain are shown in Figure 3.

Figure 4 to Figure 7 show the recovered NAMRIA reference points within the area. In addition, Table 2 to Table 5 present the details about the following NAMRIA control stations and established points while Table 6 lists all ground control points occupied during the acquisition with the corresponding dates of utilization. The list of team members are found in Annex 4.

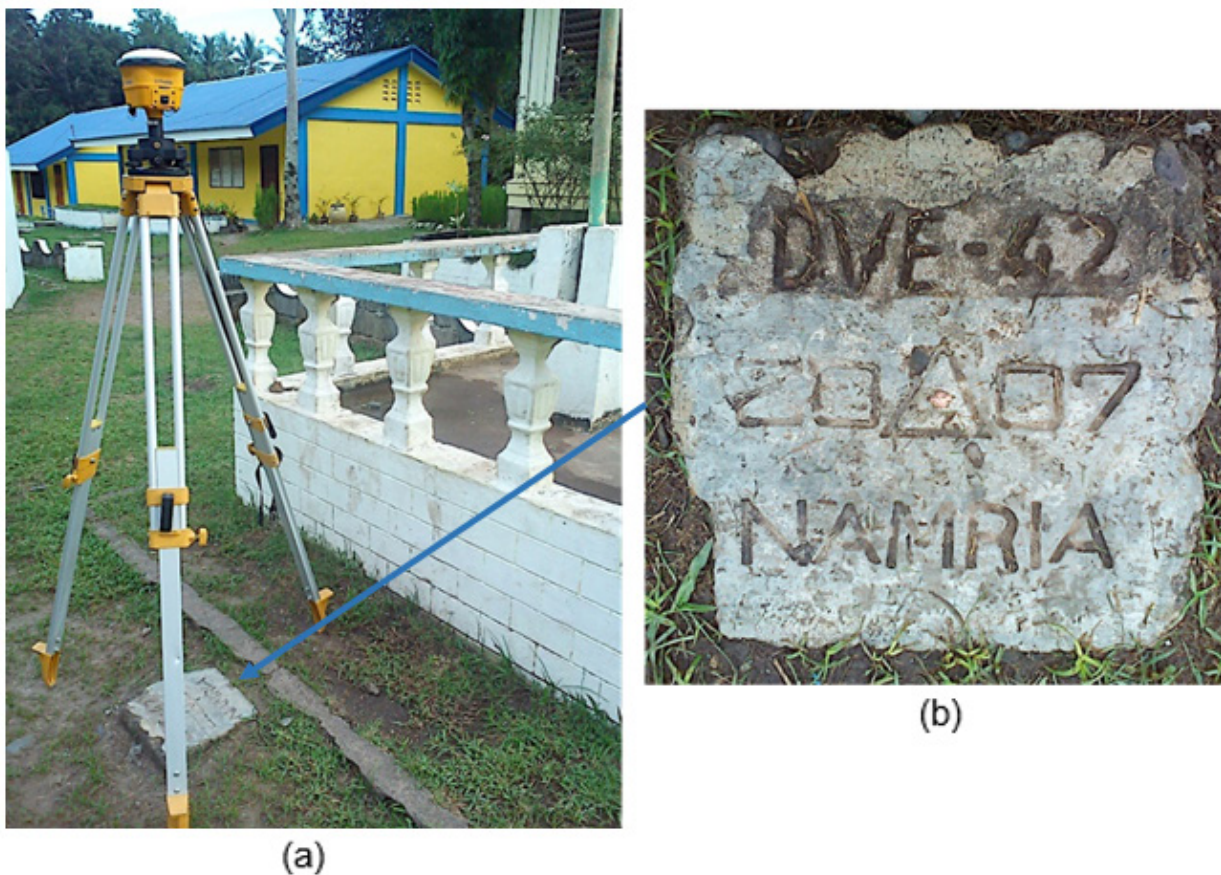


Figure 4. GPS set-up over DVE-42 located inside the premises of Don Enrique Elementary School, in front of the flagpole (a) and NAMRIA reference point DVE-42 (b) as recovered by the field team.

Table 2. Details of the recovered NAMRIA horizontal control point DVE-42 used as base station for the LiDAR acquisition.

| Station Name | DVE-42 | |
|---|---|---|
| Order of Accuracy | 2nd | |
| Relative Error (Horizontal positioning) | 1 in 50,000 | |
| Geographic Coordinates, Philippine Reference Of 1992 Datum (PRS 92) | Latitude Longitude Ellipsoidal Height | 6°58'54.82726" North 126°17'56.05259" East 6.395 meters |
| Grid Coordinates, Philippine Transverse Mercator Zone 5 (PTM Zone 5 PRS 92) | Easting Northing | 643534.636 meters 772166.69 meters |
| Geographic Coordinates, World Geodetic System 1984 Datum (WGS 84) | Latitude Longitude Ellipsoidal Height | 6°58'51.79295" North 126°18'1.57690" East 81.025 meters |
| Grid Coordinates, Philippine Transverse Mercator Zone 51 North (UTM 51N PRS 1992) | Easting Northing | 201538.20 meters 772554.34 meters |

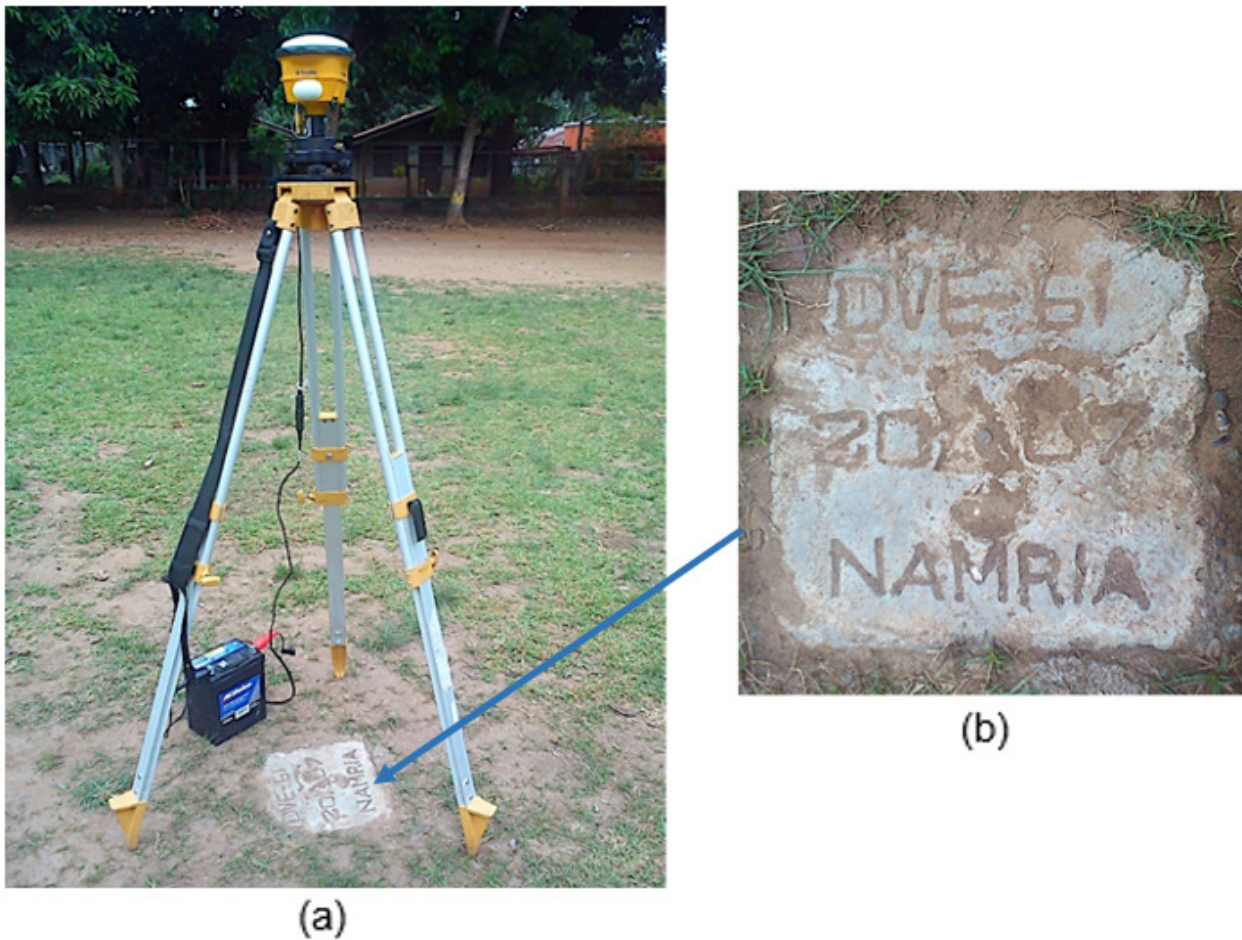


Figure 5. GPS set-up over DVE-61 located at the center of the playground of Zign Elementary School, about 10 m W of school flagpole (a) and NAMRIA reference point DVE-61 (b) as recovered by the field team.

Table 3. Details of the recovered NAMRIA horizontal control point DVE-61 used as base station for the LiDAR acquisition.

| Station Name | DVE-61 | |
|---|---|---|
| Order of Accuracy | 2nd | |
| Relative Error (Horizontal positioning) | 1 in 50,000 | |
| Geographic Coordinates, Philippine Reference of 1992 Datum (PRS 92) | Latitude Longitude Ellipsoidal Height | 6°57'39.37336" North 126°13'22.44550" East 48.474 meters |
| Grid Coordinates, Philippine Transverse Mercator Zone 3 (PTM Zone 5 PRS 92) | Easting Northing | 635140.8 meters 769826.046 meters |
| Geographic Coordinates, World Geodetic System 1984 Datum (WGS 84) | Latitude Longitude Ellipsoidal Height | 6°57'36.33777" North 126°13'27.97256" East 122.953 meters |
| Grid Coordinates, Philippine Transverse Mercator Zone 51 North (UTM 51N PRS 1992) | Easting Northing | 193120.25 meters 770283.71 meters |

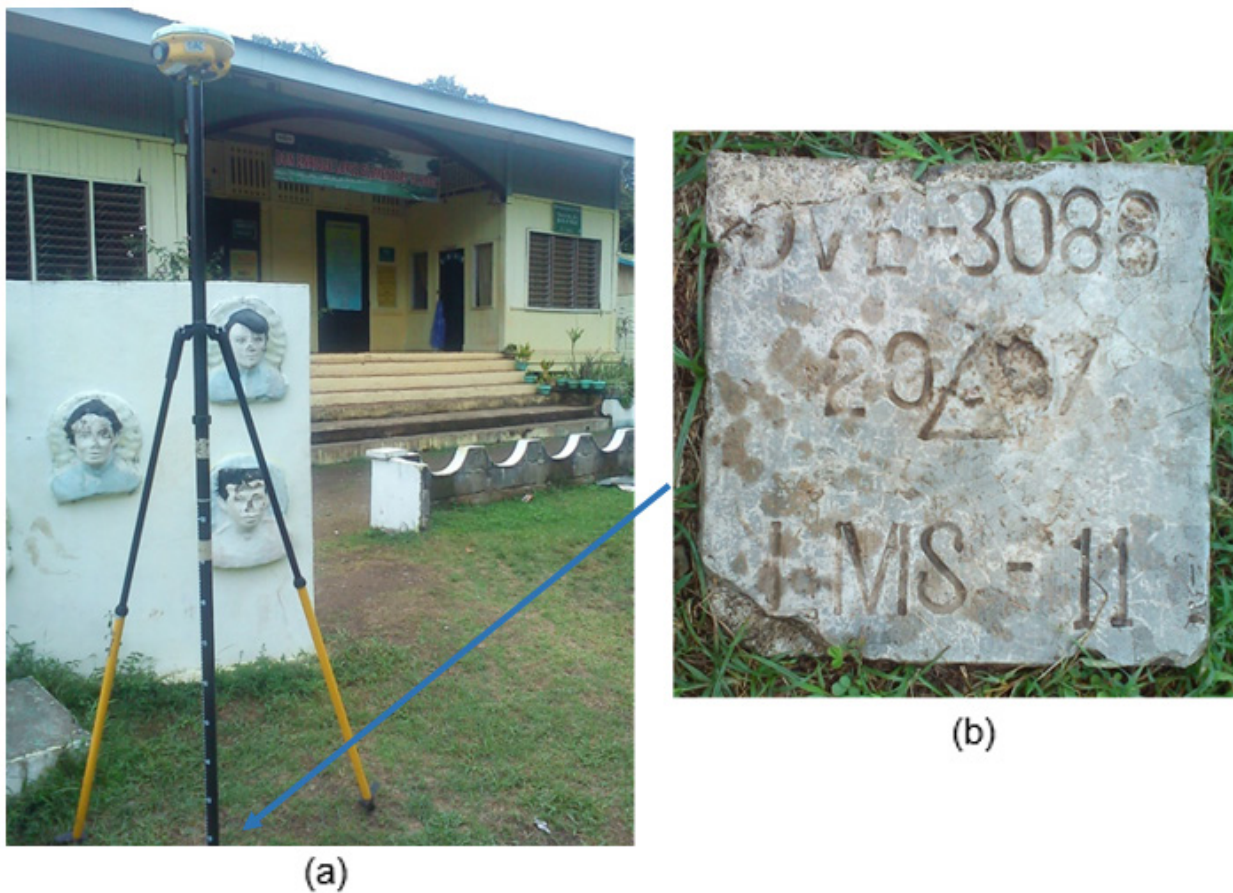


Figure 6. GPS set-up over DVE-3088 located inside Don Enrique Lopez Elementary School (a) and NAMRIA reference point DVE-3088 (b) as recovered by the field team.

Table 4. Details of the recovered NAMRIA horizontal control point DVE-3088 used as base station for the LiDAR acquisition with established coordinates.

| Station Name | DVE-3088 | |
|--|---|---|
| Order of Accuracy | 2nd | |
| Relative Error (horizontal positioning) | 1 in 50,000 | |
| Geographic Coordinates, Philippine Reference of 1992 Datum (PRS 92) | Latitude Longitude Ellipsoidal Height | 6°58'54.82726" North 126°17'56.05259" East 6.395 meters |
| Geographic Coordinates, World Geodetic System 1984 Datum (WGS 84) | Latitude Longitude Ellipsoidal Height | 6°58'51.79294" North 126°18'1.57690" East 81.024 meters |
| Grid Coordinates, Universal Transverse Mercator Zone 51 North (UTM 52N PRS 1992) | Easting Northing | 864582.336 meters 772975.574 meters |

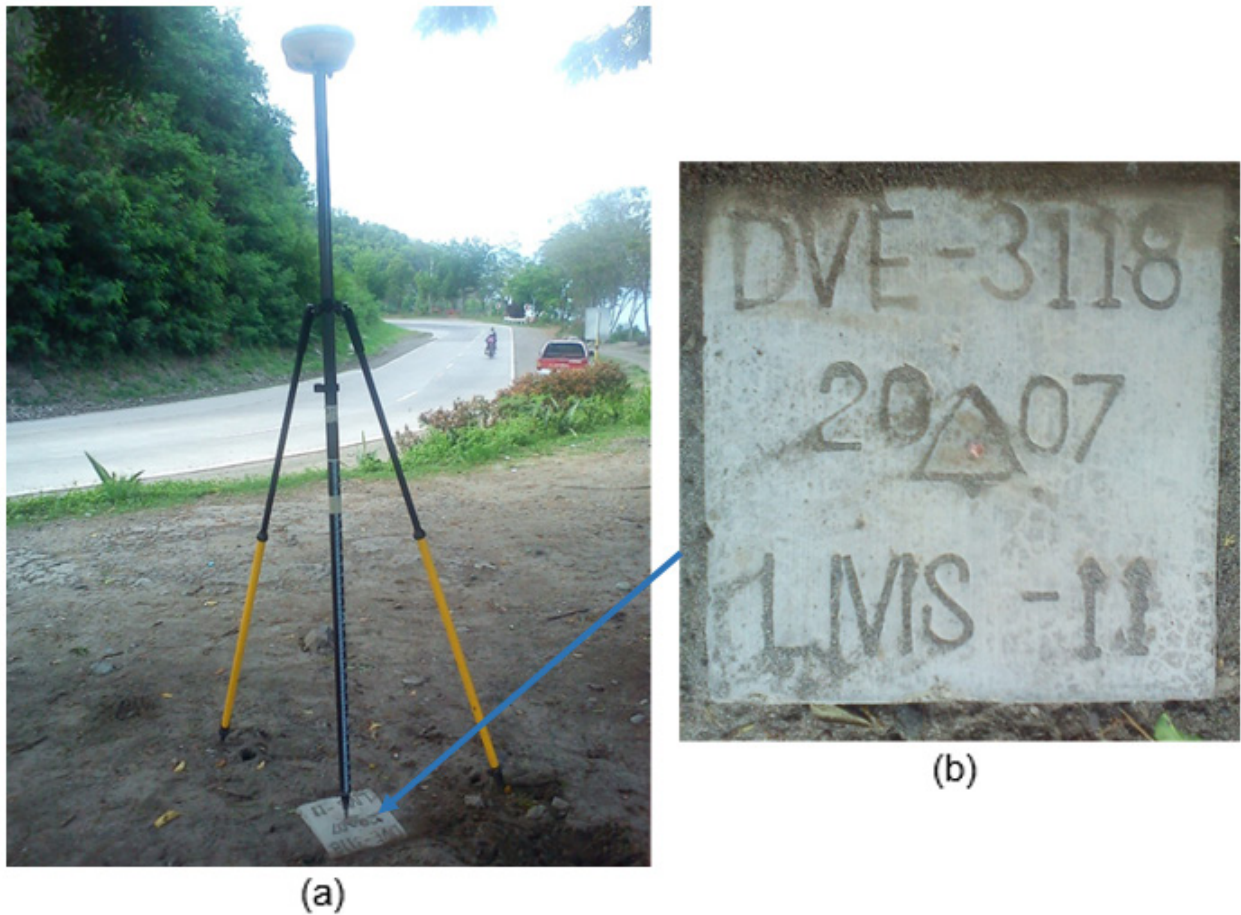


Figure 7. GPS set-up over DVE-3118 located along the boundary of Barangays Dawan and Badas (a) and NAMRIA reference point DVE-3118 (b) as recovered by the field team.

Table 5. Details of the recovered NAMRIA horizontal control point DVE-3118 used as base station for the LiDAR acquisition with established coordinates.

| Station Name | DVE-3118 | |
|--|---|---|
| Order of Accuracy | 2nd | |
| Relative Error (horizontal positioning) | 1 in 50,000 | |
| Geographic Coordinates, Philippine Reference of 1992 Datum (PRS 92) | Latitude Longitude Ellipsoidal Height | 6°54'21.10869" North 126°10'17.73141" East 48.474 meters |
| Geographic Coordinates, World Geodetic System 1984 Datum (WGS 84) | Latitude Longitude Ellipsoidal Height | 6°54'18.08333" North 126°10'23.26402" East 204.434 meters |
| Grid Coordinates, Universal Transverse Mercator Zone 51 North (UTM 52N PRS 1992) | Easting Northing | 850554.409 meters 764461.564 meters |

Table 6. Ground control points used during the LiDAR data acquisition.

| Date Surveyed | Flight Number | Mission Name | Ground Control Points |
|---------------|---------------|----------------|-----------------------|
| June 19, 2014 | 7320GC | 2BLK83A84B170A | DVE-42 & DVE-3088 |
| July 01, 2014 | 7344GC | 2BLK84BCR182A | DVE-42 & DVE-3088 |
| July 10, 2014 | 7362GC | 2BLK85CS191A | DVE-61 & DVE-3118 |
| July 11, 2014 | 7364GC | 2BLK85V192A | DVE-61 & DVE-3118 |

2.3 Flight Missions

Four (4) missions were conducted to complete the LiDAR data acquisition in Mayo Floodplain, for a total of thirteen hours and forty four minutes (13+44) of flying time for RP-C9322. All missions were acquired using the Gemini LiDAR system. Table 7 shows the total area of actual coverage and the corresponding flying hours per mission, while Table 8 presents the actual parameters used during the LiDAR data acquisition.

Table 7. Flight missions for the LiDAR data acquisition in Mayo Floodplain.

| Date Surveyed | Flight Number | Flight Plan Area (km ²) | Surveyed Area (km ²) | Area Surveyed within the Floodplain (km ²) | Area Surveyed Outside the Floodplain (km ²) | No. of Images (Frames) | Flying Hours | |
|---------------|---------------|-------------------------------------|----------------------------------|--|---|------------------------|--------------|-----------|
| | | | | | | | Hr | Min |
| June 19, 2014 | 7320GC | 71.239 | 121.572 | 1.611 | 119.961 | NA | 3 | 47 |
| July 01, 2014 | 7344GC | 156.234 | 74.469 | 0.121 | 74.348 | NA | 3 | 11 |
| July 10, 2014 | 7362GC | 103.499 | 68.350 | 21.768 | 46.582 | NA | 3 | 11 |
| July 11, 2014 | 7364GC | 103.499 | 195.195 | 4.415 | 190.780 | NA | 3 | 35 |
| TOTAL | | 629.683 | 459.586 | 27.915 | 431.671 | NA | 13 | 44 |

Table 8. Actual parameters used during the LiDAR data acquisition of the Mayo Floodplain.

| Flight Number | Flying Height (m AGL) | Overlap (%) | FOV (θ) | PRF (khz) | Scan Frequency (Hz) | Average Speed (kts) | Average Turn Time (Minutes) |
|---------------|-----------------------|-------------|------------------|-----------|---------------------|---------------------|-----------------------------|
| 7320GC | 1000 | 40 | 40 | 100 | 50 | 130 | 5 |
| 7344GC | 1200 | 45 | 24 | 70 | 60 | 130 | 5 |
| 7362GC | 1200 | 40 | 26 | 70 | 60 | 130 | 5 |
| 7364GC | 1200 | 40 | 40, 24 | 70 | 50, 60 | 130 | 5 |

2.4 Survey Coverage

This certain LiDAR acquisition survey covered the Mayo Floodplain (See Annex 7). Mayo Floodplain is located in the province of Davao Oriental, specifically within the city of Mati. The list of municipalities/cities surveyed, with at least one (1) square kilometer coverage is shown in Table 9. The actual coverage of the LiDAR acquisition for Bugnan Mayo floodplain is presented in Figure 8.

Table 9. List of municipalities and cities surveyed of the Mayo Floodplain LiDAR acquisition.

| Province | Municipality/ City | Area of Municipality/City (km ²) | Total Area Surveyed (km ²) | Percentage of Area Surveyed |
|----------------|-----------------------|--|--|--------------------------------|
| Davao Oriental | Manay | 430.894 | 137.905 | 32.00% |
| | Banaybanay | 385.281 | 113.955 | 29.58% |
| | Mati | 797.379 | 175.831 | 22.05% |
| | Tarragona | 277.903 | 38.11 | 13.71% |
| | Lupon | 356.281 | 40.392 | 11.34% |
| Total | | 1891.457 | 506.193 | 26.76% |

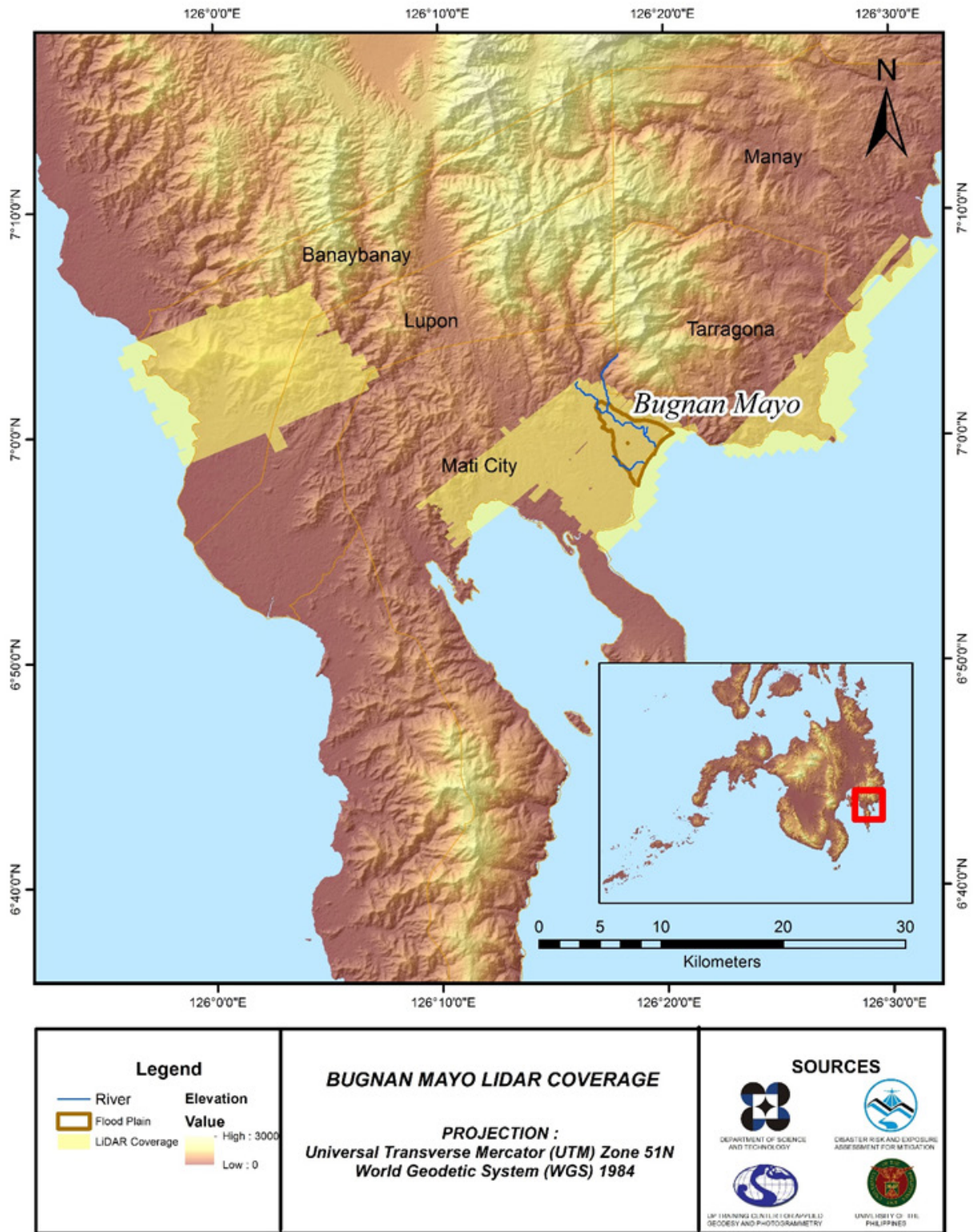


Figure 8. Actual LiDAR survey coverage of the Mayo Floodplain.

CHAPTER 3: LIDAR DATA PROCESSING OF THE MAYO FLOODPLAIN

Engr. Ma. Rosario Concepcion O. Ang, Engr. John Louie D. Fabila, Engr. Sarah Jane D. Samalburo, Engr. Harmond F. Santos, Engr. John Dill P. Macapagal, Engr. Ma. Ailyn L. Olanda, Engr. Chelou P. Prado, Engr. Krisha Marie Bautista, Engr. Ben Joseph J. Harder, and Engr. Karl Adrian P. Vergara

The methods applied in this Chapter were based on the DREAM methods manual (Ang, et al., 2014) and further enhanced and updated in Paringit, et al. (2017)

3.1 Overview of the LiDAR Data Pre-Processing

The data transmitted by the Data Acquisition Component are checked for completeness based on the list of raw files required to proceed with the pre-processing of the LiDAR data. Upon acceptance of the LiDAR field data, georeferencing of the flight trajectory is done in order to obtain the exact location of the LiDAR sensor when the laser was shot. Point cloud georectification is performed to incorporate correct position and orientation for each point acquired. The georectified LiDAR point clouds are subject for quality checking to ensure that the required accuracies of the program, which are the minimum point density, vertical and horizontal accuracies, are met. The point clouds are then classified into various classes before generating Digital Elevation Models such as Digital Terrain Model and Digital Surface Model.

Using the elevation of points gathered in the field, the LiDAR-derived digital models are calibrated. Portions of the river that are barely penetrated by the LiDAR system are replaced by the actual river geometry measured from the field by the Data Validation and Bathymetry Component. LiDAR acquired temporally are then mosaicked to completely cover the target river systems in the Philippines. Orthorectification of images acquired simultaneously with the LiDAR data is done through the help of the georectified point clouds and the metadata containing the time the image was captured.

These processes are summarized in the flowchart shown in Figure 9.

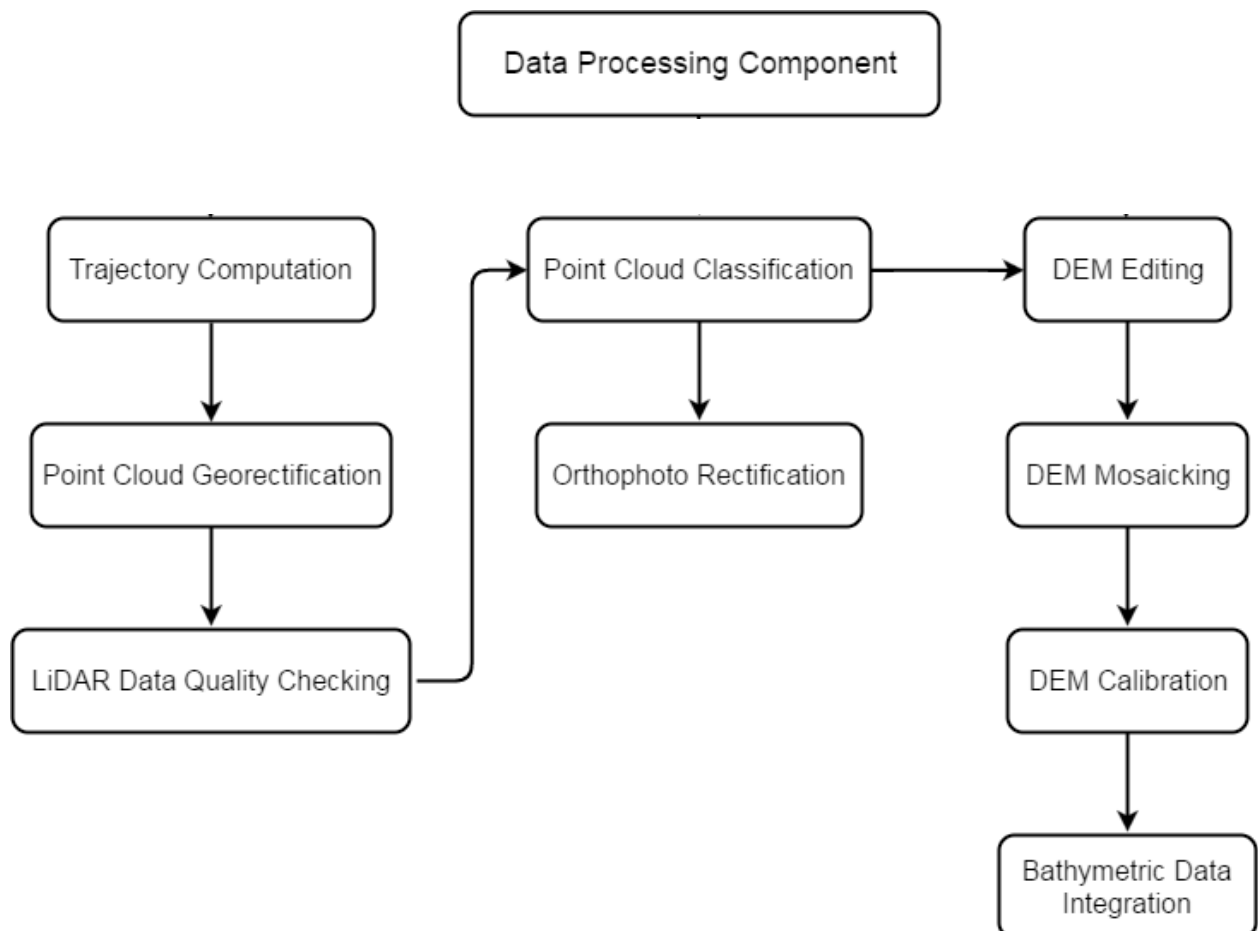


Figure 9. Schematic diagram for Data Pre-Processing Component.

3.2 Transmittal of Acquired LiDAR Data

Data transfer sheets for all the LiDAR missions for Mayo floodplain can be found in Annex 5. Missions flown during the first survey conducted on June 2014 used the Airborne LiDAR Terrain Mapper (ALTM™ Optech Inc.) Gemini system over Mati City, Davao Oriental.

The Data Acquisition Component (DAC) transferred a total of 58.14 Gigabytes of Range data, 0.79 Gigabytes of POS data, 21.07 Megabytes of GPS base station data, and 0 Gigabytes of raw image data to the data server on July 28, 2014 for the first survey. The Data Pre-processing Component (DPPC) verified the completeness of the transferred data. The whole dataset for Mayo was fully transferred on July 28, 2014, as indicated on the Data Transfer Sheets for Mayo Floodplain.

3.3 Trajectory Computation

The Smoothed Performance Metric parameters of the computed trajectory for flight 7362GC, one of the Mayo flights, which is the North, East, and Down position RMSE values are shown in Figure B-2. The x-axis corresponds to the time of flight, which is measured by the number of seconds from the midnight of the start of the GPS week, which on that week fell on July 28, 2014 00:00AM. The y-axis is the RMSE value for that particular position.

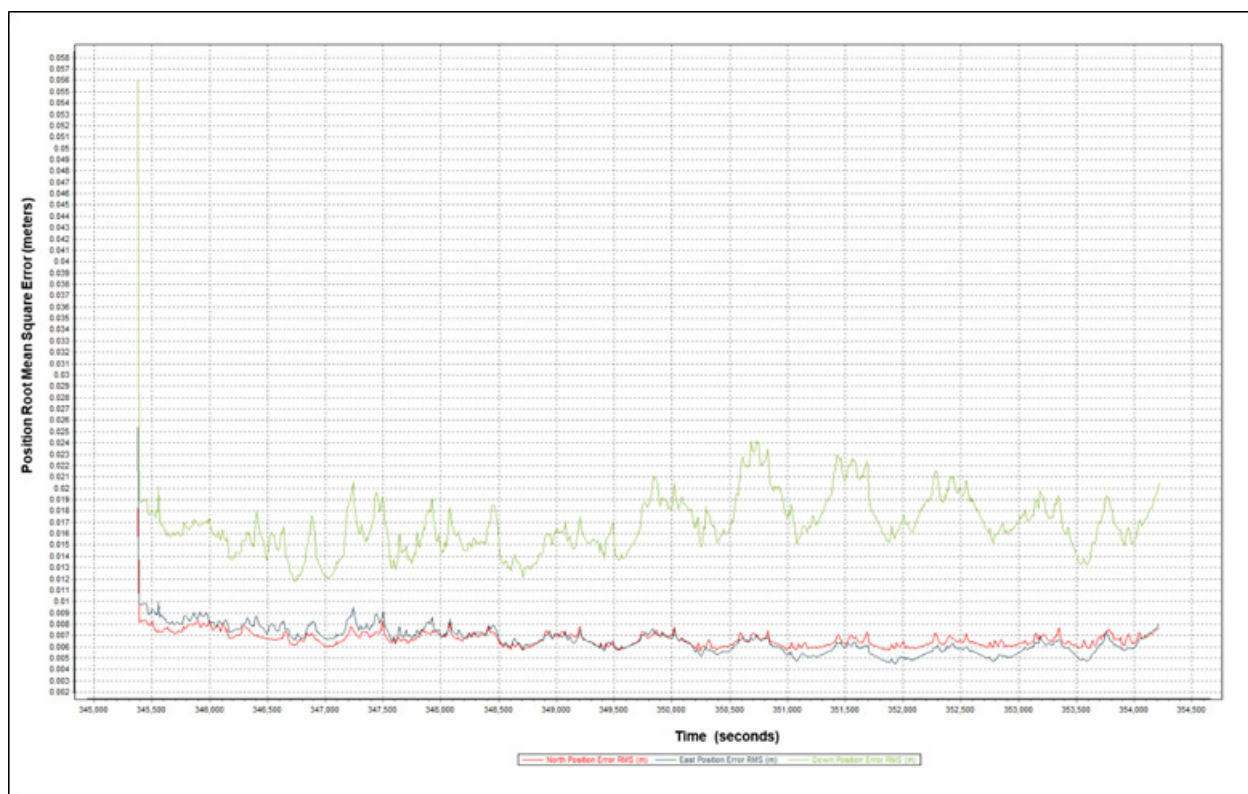


Figure 10. Smoothed Performance Metric Parameters of Mayo Flight 7362GC

The time of flight was from 345,400 seconds to 354,200 seconds, which corresponds to morning of July 28, 2014. The initial spike that is seen on the data corresponds to the time that the aircraft was getting into position to start the acquisition, and the POS system starts computing for the position and orientation of the aircraft.

Redundant measurements from the POS system quickly minimized the RMSE value of the positions. The periodic increase in RMSE values from an otherwise smoothly curving RMSE values correspond to the turn-around period of the aircraft, when the aircraft makes a turn to start a new flight line. Figure 10 shows that the North position RMSE peaks at 0.80 centimeters, the East position RMSE peaks at 1.00 centimeters, and the Down position RMSE peaks at 2.40 centimeters, which are within the prescribed accuracies described in the methodology.



Figure 11. Solution Status Parameters of Mayo Flight 7362GC.

The Solution Status parameters of flight 7362GC, one of the Mayo flights, which are the number of GPS satellites, Positional Dilution of Precision (PDOP), and the GPS processing mode used, are shown in Figure 11. The graphs indicate that the number of satellites during the acquisition. Majority of the time, the number of satellites tracked was between 5 and 10. The PDOP value also did not go above the value of 3, which indicates optimal GPS geometry. The processing mode stayed at the value of 0 for majority of the survey with some peaks up to 1 attributed to the turns performed by the aircraft. The value of 0 corresponds to a Fixed, Narrow-Lane mode, which is the optimum carrier-cycle integer ambiguity resolution technique available for POSPAC MMS. All of the parameters adhered to the accuracy requirements for optimal trajectory solutions, as indicated in the methodology. The computed best estimated trajectory for all Mayo flights is shown in Figure 12.

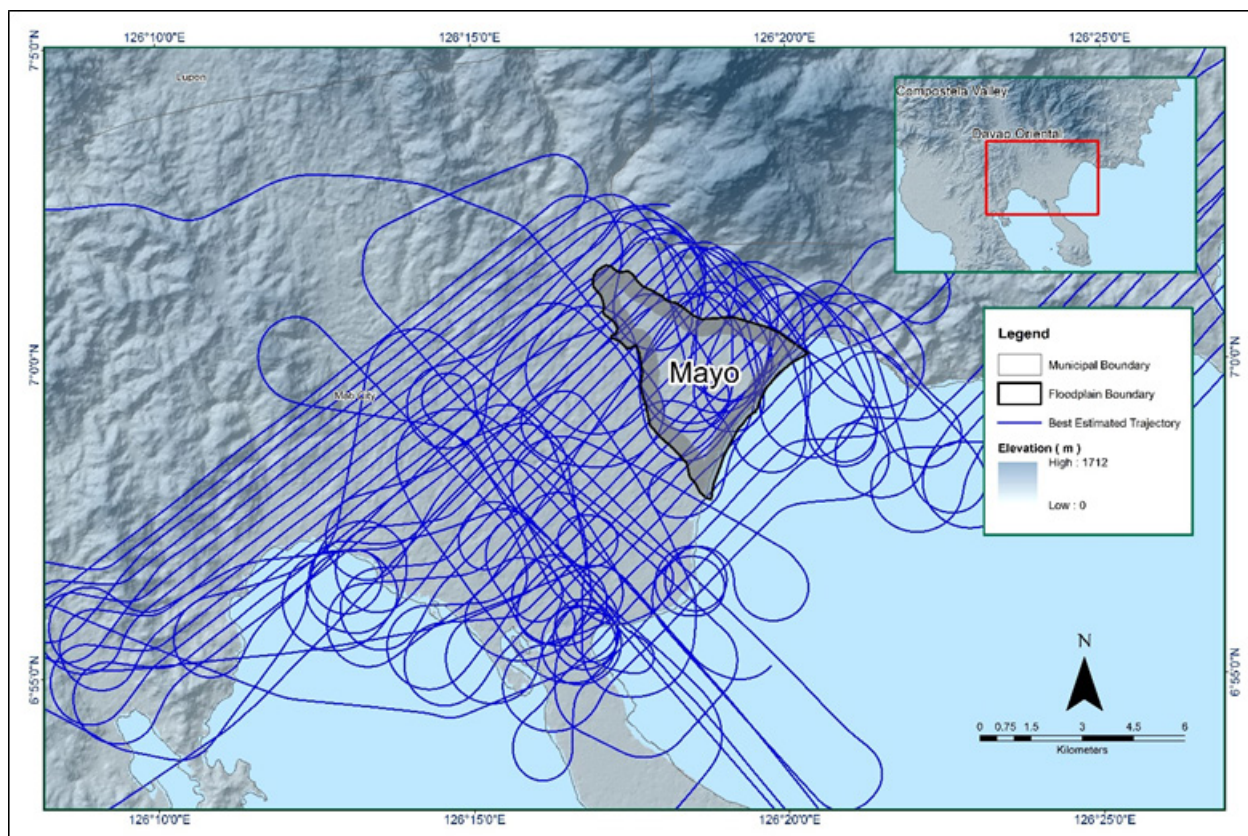


Figure 12. Best Estimated Trajectory of the LiDAR missions conducted over the Mayo Floodplain.

3.4 LiDAR Point Cloud Computation

The produced LAS data contains 44 flight lines, with each flight line containing one channel, since the Gemini system contains one channel only. The summary of the self-calibration results obtained from LiDAR processing in LiDAR Mapping Suite (LMS) software for all flights over Mayo Floodplain are given in Table 10.

Table 10. Self-calibration Results values for Mayo flights.

| Parameter | Acceptable Value | Computed Value |
|---|------------------|----------------|
| Boresight Correction stdev | <0.001degrees | 0.000237 |
| IMU Attitude Correction Roll and Pitch Correction stdev | <0.001degrees | 0.000612 |
| GPS Position Z-correction stdev | <0.01meters | 0.0074 |

The optimum accuracy is obtained for all Mayo flights based on the computed standard deviations of the corrections of the orientation parameters. Standard deviation values for individual blocks are available in Annex 8: Mission Summary Report.

3.5 LiDAR Data Quality Checking

The boundary of the processed LiDAR data on top of a SAR Elevation Data over Mayo Floodplain is shown in Figure 13. The map shows gaps in the LiDAR coverage that are attributed to cloud coverage.

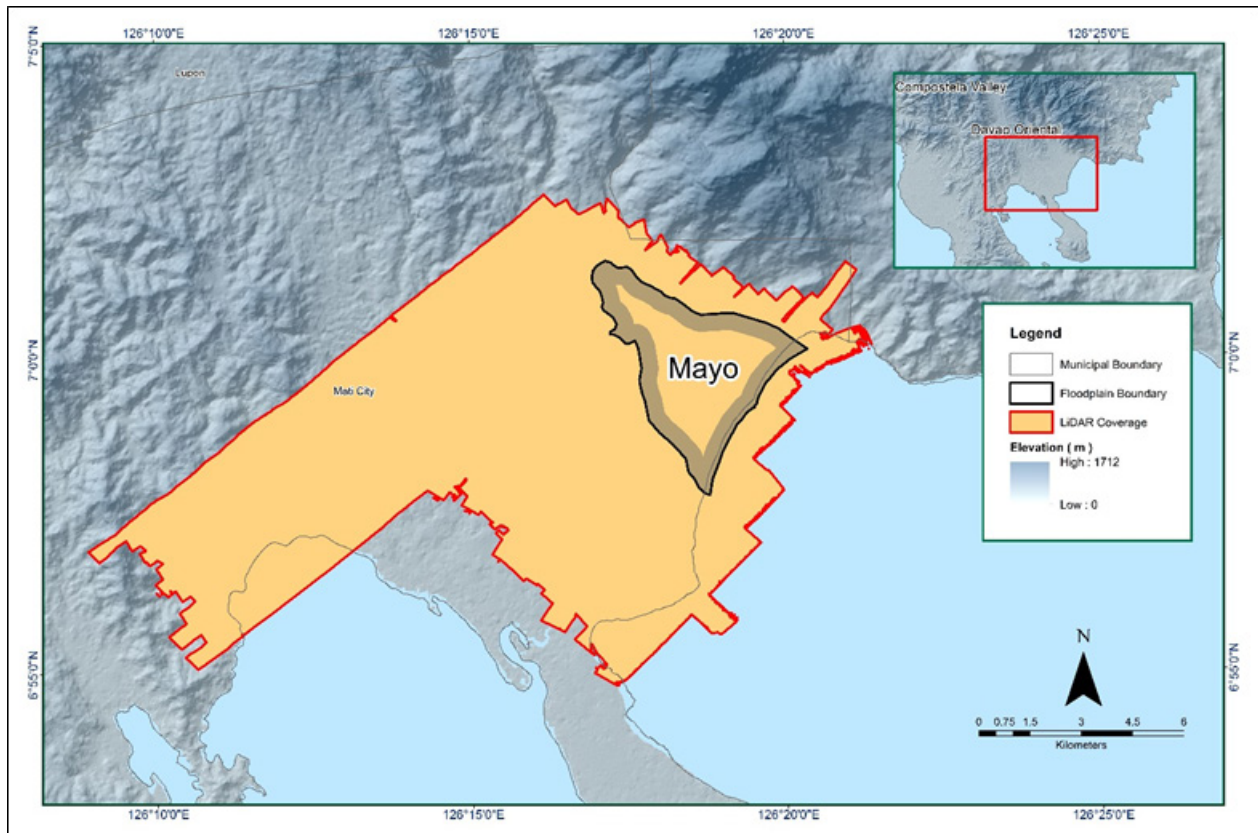


Figure 13. Boundary of the processed LiDAR data over Mayo Floodplain

The total area covered by the Mayo missions is 165.28 sq.km that is comprised of four (4) flight acquisitions grouped and merged into three (3) blocks as shown in Table 11.

Table 11. List of LiDAR blocks for Mayo Floodplain.

| LiDAR Blocks | Flight Numbers | Area (sq. km) |
|---------------------------------|----------------|---------------------|
| Davao_Oriental_Bl85B_additional | 7362G | 69.62 |
| | 7364G | |
| Davao_Oriental_Bl84C | 7344G | 68.56 |
| Davao_Oriental_Bl84B | 7320G | 27.10 |
| TOTAL | | 165.28 sq.km |

The overlap data for the merged LiDAR blocks, showing the number of channels that pass through a particular location is shown in Figure 14. Since the Gemini system employs one channel, an average value of 1 (blue) for areas where there is limited overlap, and a value of 2 (yellow) or more (red) for areas with three or more overlapping flight lines are expected.

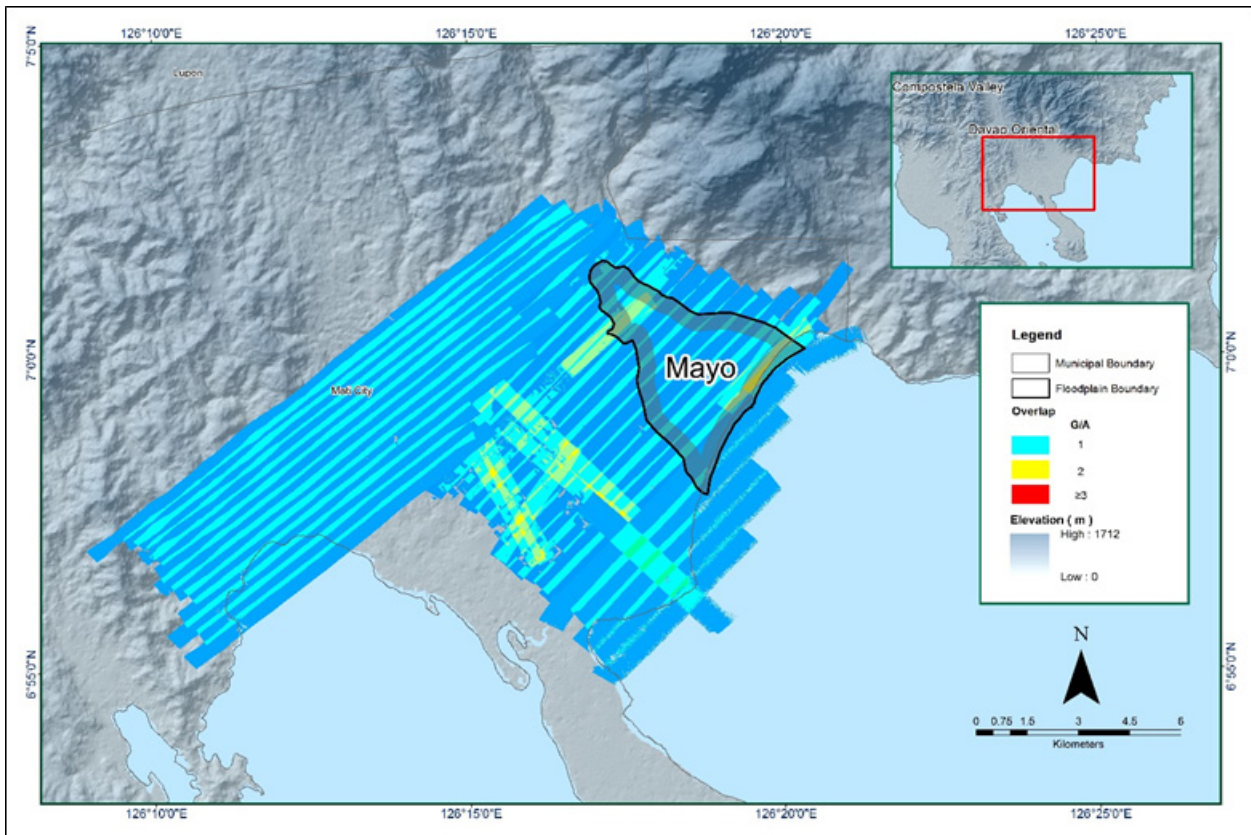


Figure 14. Image of data overlap for Mayo Floodplain.

The overlap statistics per block for the Mayo Floodplain can be found in Annex 5. One pixel corresponds to 25.0 square meters on the ground. For this area, the minimum and maximum percent overlaps are 33.97% and 42.20% respectively, which passed the 25% requirement.

The pulse density map for the merged LiDAR data, with the red parts showing the portions of the data that satisfy the 2 points per square meter criterion is shown in Figure 15. It was determined that all LiDAR data for Mayo Floodplain satisfy the point density requirement, and the average density for the entire survey area is 3.06 points per square meter.

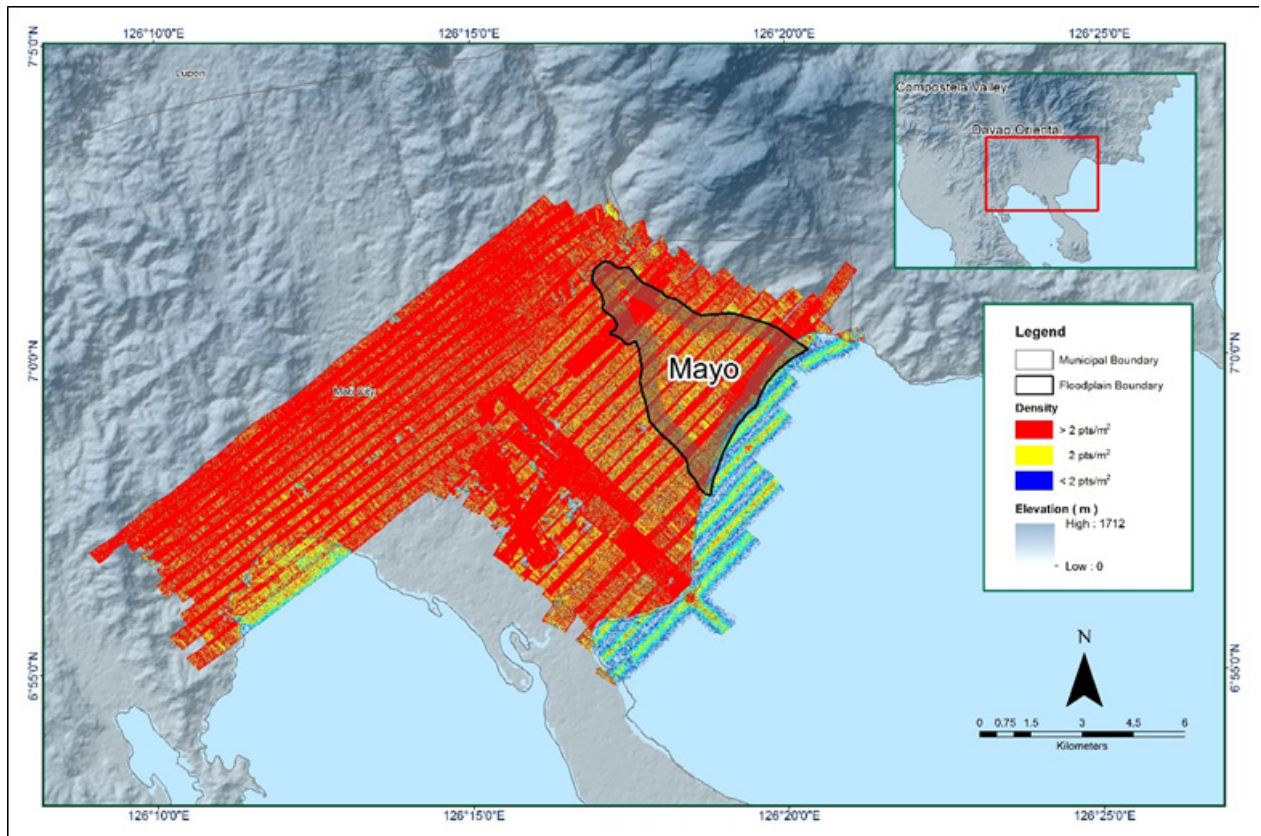


Figure 15. Pulse density map of merged LiDAR data for Mayo Floodplain.

The elevation difference between overlaps of adjacent flight lines is shown in Figure 16. The default color range is from blue to red, where bright blue areas correspond to portions where elevations of a previous flight line, identified by its acquisition time, are higher by more than 0.20m relative to elevations of its adjacent flight line. Bright red areas indicate portions where elevations of a previous flight line are lower by more than 0.20m relative to elevations of its adjacent flight line. Areas with bright red or bright blue need to be investigated further using Quick Terrain Modeler software.

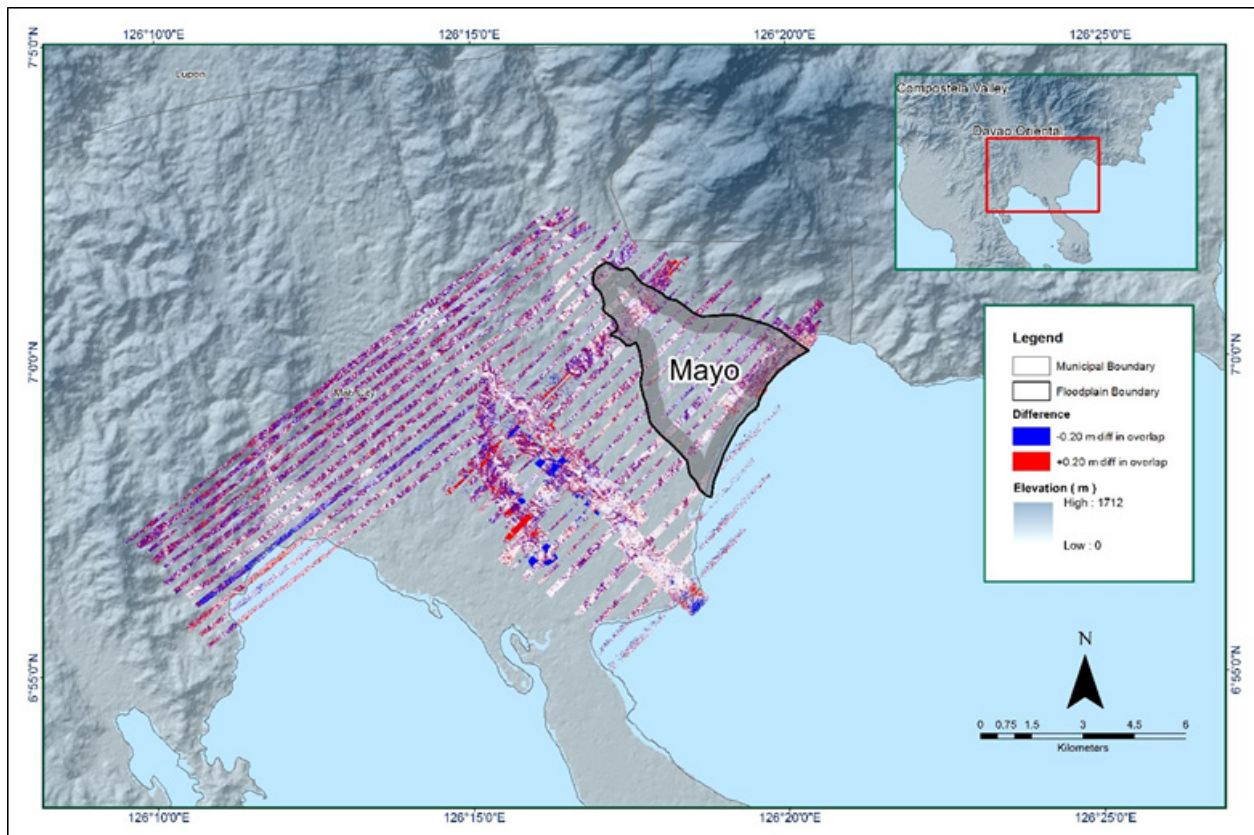


Figure 16. Elevation Difference Map between flight lines for Mayo Floodplain Survey.

A screen capture of the processed LAS data from a Mayo flight 7362GC loaded in QT Modeler is shown in Figure 17. The upper left image shows the elevations of the points from two overlapping flight strips traversed by the profile, illustrated by a dashed yellow line. The x-axis corresponds to the length of the profile. It is evident that there are differences in elevation, but the differences do not exceed the 20-centimeter mark. This profiling was repeated until the quality of the LiDAR data becomes satisfactory. No reprocessing was done for this LiDAR dataset.

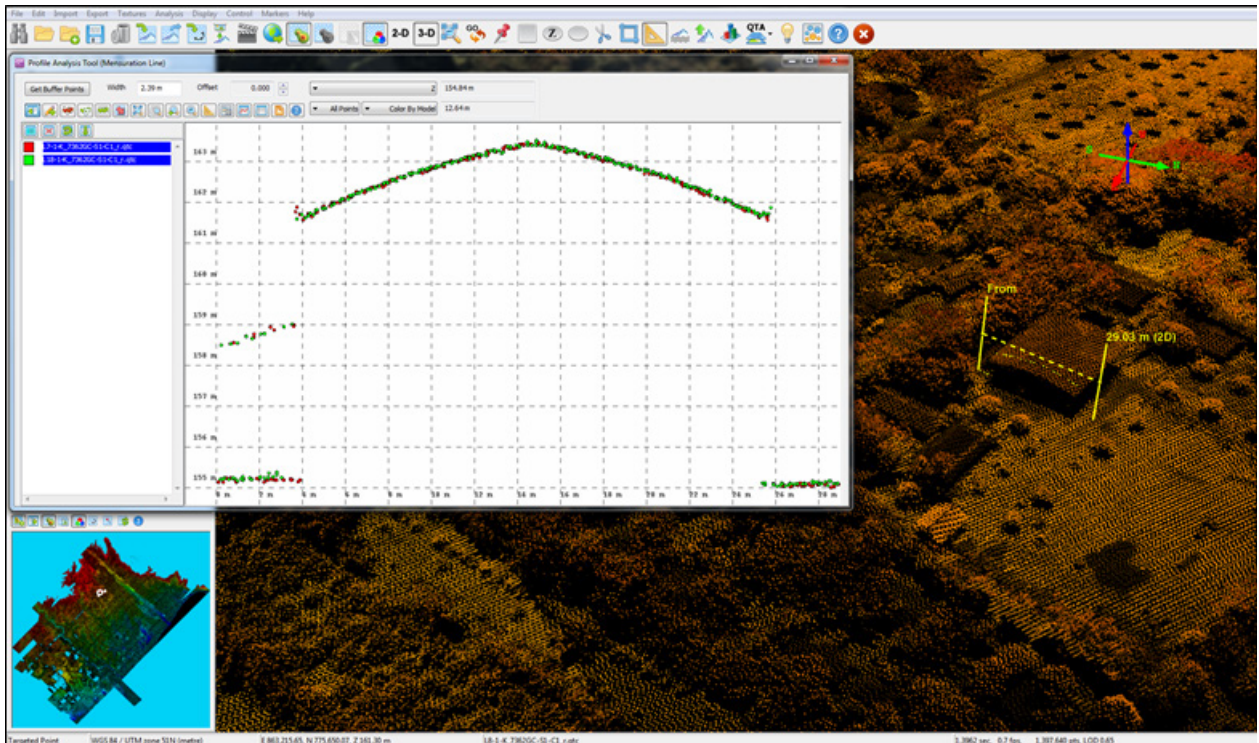


Figure 17. Quality checking for Mayo Flight 7362GC using the Profile Tool of QT Modeler.

3.6 LiDAR Point Cloud Classification and Rasterization

Table 12. Mayo classification results in TerraScan

| Pertinent Class | Total Number of Points |
|-------------------|------------------------|
| Ground | 73,335,366 |
| Low Vegetation | 54,578,389 |
| Medium Vegetation | 89,720,916 |
| High Vegetation | 230,029,114 |
| Building | 6,380,663 |

The tile system that TerraScan employed for the LiDAR data and the final classification image for a block in Mayo Floodplain is shown in Figure 18. A total of 262 1km by 1km tiles were produced. The number of points classified to the pertinent categories is illustrated in Table 12. The point cloud has a maximum and minimum height of 623.53 meters and 64.32 meters, respectively.

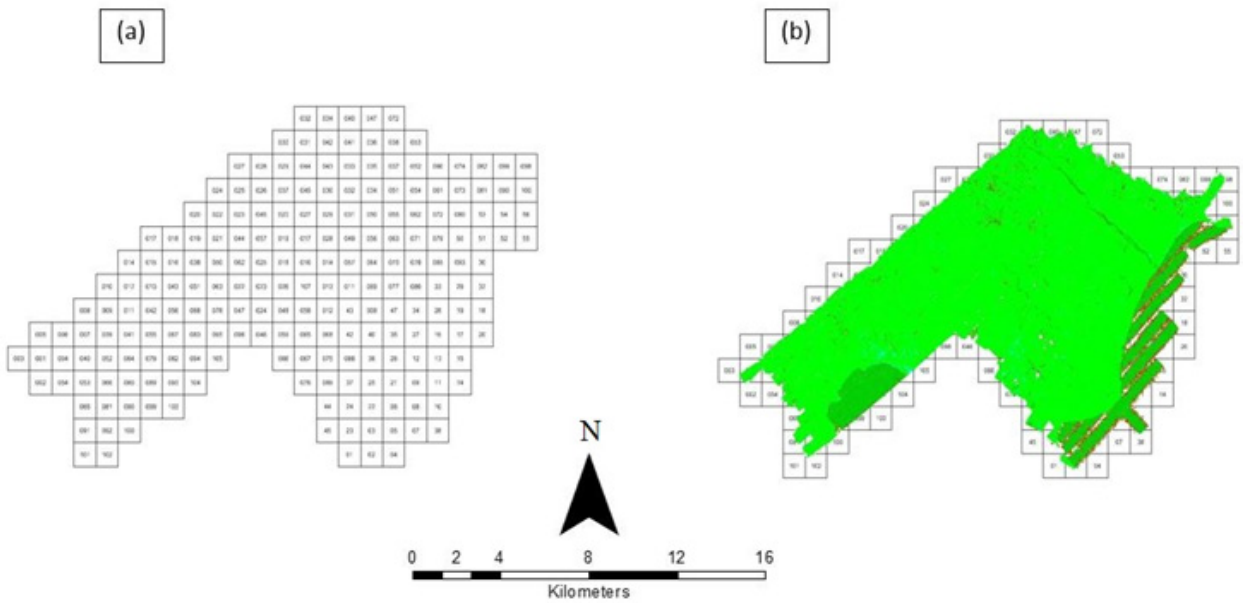


Figure 18. Tiles for Mayo Floodplain (a) and classification results (b) in TerraScan.

An isometric view of an area before and after running the classification routines is shown in Figure 19. The ground points are in orange, the vegetation is in different shades of green, and the buildings are in cyan. It can be seen that residential structures adjacent or even below canopy are classified correctly, due to the density of the LiDAR data.

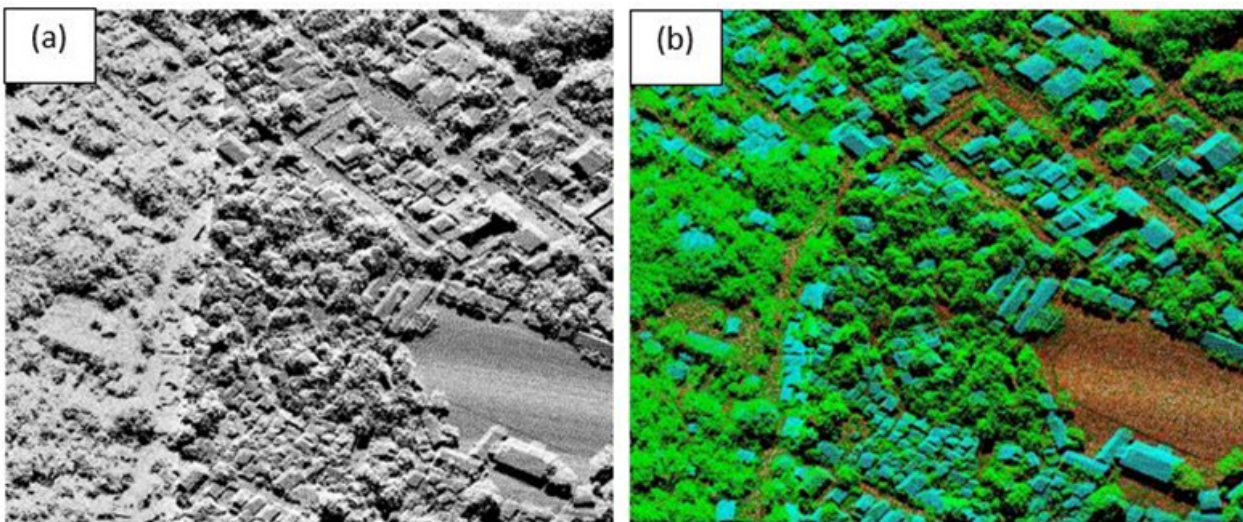


Figure 19. Point cloud before (a) and after (b) classification

The production of last return (V_ASCII) and the secondary (T_ASCII) DTM, first (S_ASCII) and last (D_ASCII) return DSM of the area in top view display are shown in Figure 20. It shows that DTMs are the representation of the bare earth while on the DSMs, all features are present such as buildings and vegetation.

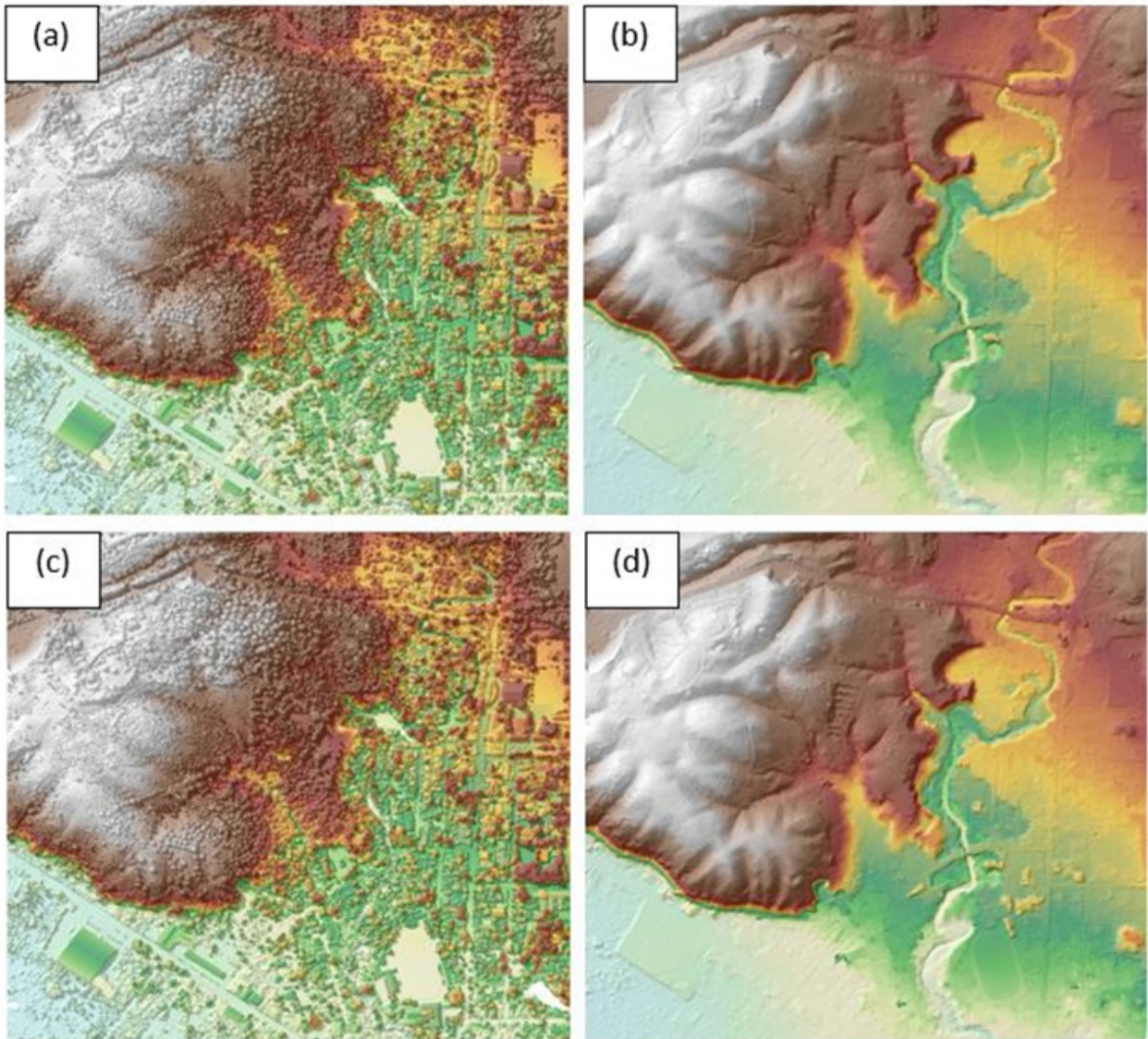


Figure 20. The production of last return DSM (a) and DTM (b), first return DSM (c) and secondary DTM (d) in some portion of Mayo Floodplain.

3.7 LiDAR Image Processing and Orthophotograph Rectification

There are no available orthophotographs for the Mayo floodplain.

3.8 DEM Editing and Hydro-Correction

Three (3) mission blocks were processed for Mayo flood plain. These blocks are composed of Davao_Oriental blocks with a total area of 165.28 square kilometers. Table 13 shows the name and corresponding area of each block in square kilometers.

Table 13. LiDAR blocks with its corresponding areas.

| LiDAR Blocks | Area (sq.km) |
|---------------------------------|---------------------|
| Davao_Oriental_Bl85B_additional | 69.62 |
| Davao_Oriental_Bl84B | 27.10 |
| Davao_Oriental_Bl84C | 68.56 |
| TOTAL | 165.28 |

Portions of DTM before and after manual editing are shown in Figure 21. The bridge (Figure 21a) is considered to be an impedance to the flow of water along the river and has to be removed (Figure 21) in order to hydrologically correct the river.

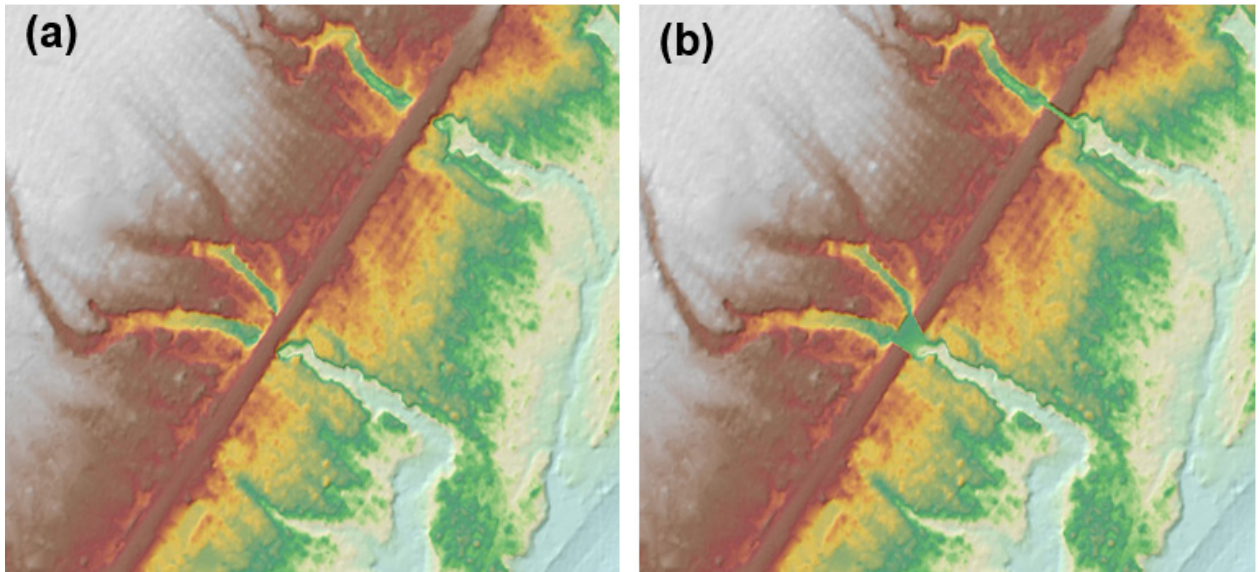


Figure 21. Portions in the DTM of Mayo Floodplain – a bridge before (a) and after (b) manual editing..

3.9 Mosaicking of Blocks

Davao_Oriental_86A was used as the reference block at the start of mosaicking because it was referred to a base station with an acceptable order of accuracy. Table 14 shows the shift values applied to each LiDAR block during mosaicking.

Table 14. Shift values of each LiDAR block of Mayo Floodplain.

| Mission Blocks | Shift Values (meters) | | |
|---------------------------------|-----------------------|-------|-------|
| | x | y | z |
| Davao_Oriental_Bl85B_additional | 1.30 | 0.00 | -0.22 |
| Davao_Oriental_Bl84B | 0.50 | -0.10 | 0.59 |
| Davao_Oriental_Bl84C | 1.10 | -0.20 | 0.15 |

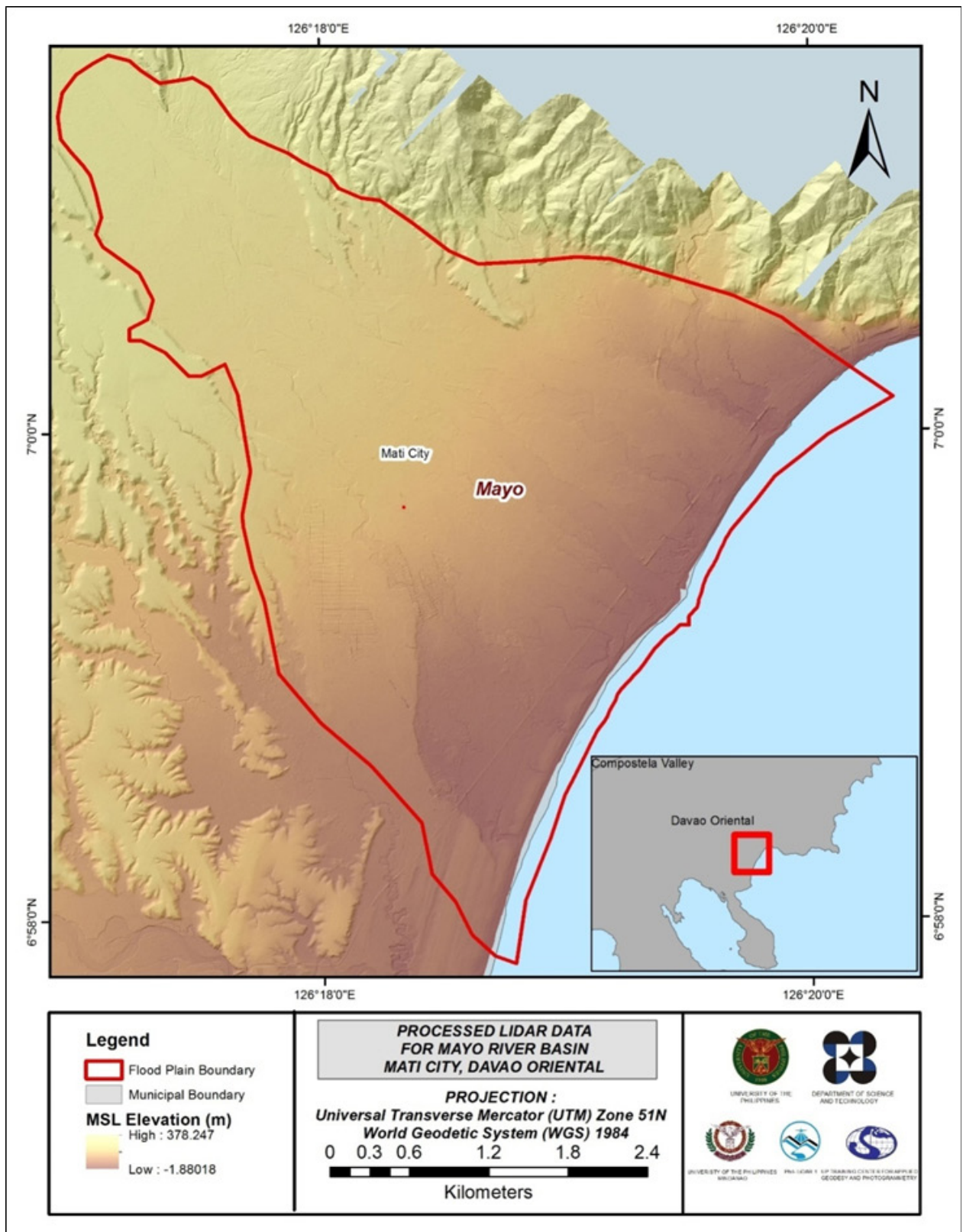


Figure 22. Map of Processed LiDAR Data for Mayo Floodplain

3.10 Calibration and Validation of Mosaicked LiDAR Digital Elevation Model (DEM)

The extent of the validation survey done by the Data Validation and Bathymetry Component (DVBC) in Mayo to collect points with which the LiDAR dataset is validated is shown in Figure 23. A total of 1,367 survey points were used for calibration and validation of Mayo LiDAR data. Random selection of 80% of the survey points, resulting to 1,094 points, were used for calibration.

A good correlation between the uncalibrated mosaicked LiDAR elevation values and the ground survey elevation values are shown in Figure 24. Statistical values were computed from extracted LiDAR values using the selected points to assess the quality of data and obtain the value for vertical adjustment. The computed height difference between the LiDAR DTM and calibration elevation values is 0.68 meters with a standard deviation of 0.17 meters. Calibration of Mayo LiDAR data was done by subtracting the height difference value, 0.68 meters, to Mayo mosaicked LiDAR data. Table 15 shows the statistical values of the compared elevation values between LiDAR data and calibration data.

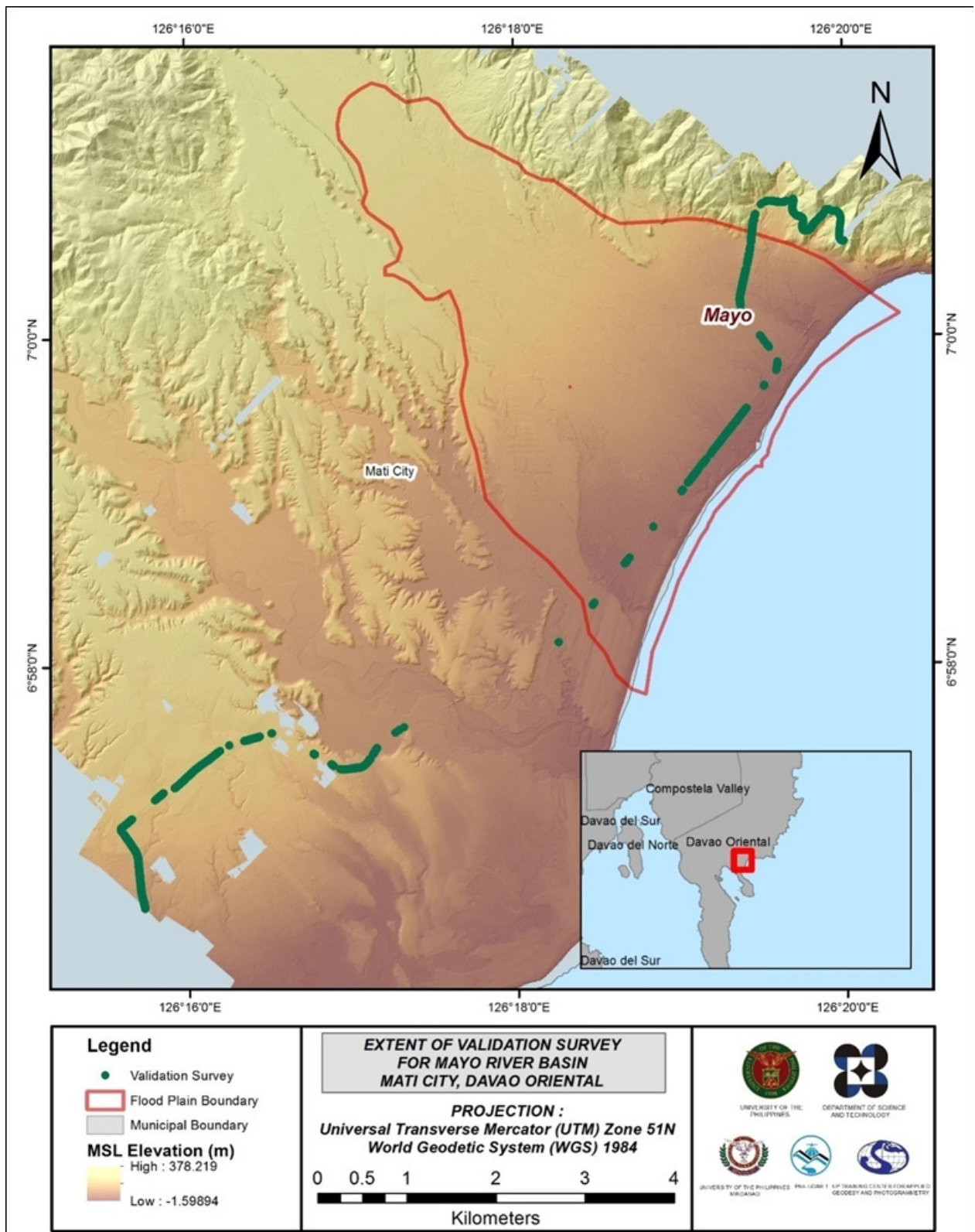


Figure 23. Map of Mayo Floodplain with validation survey points in green.

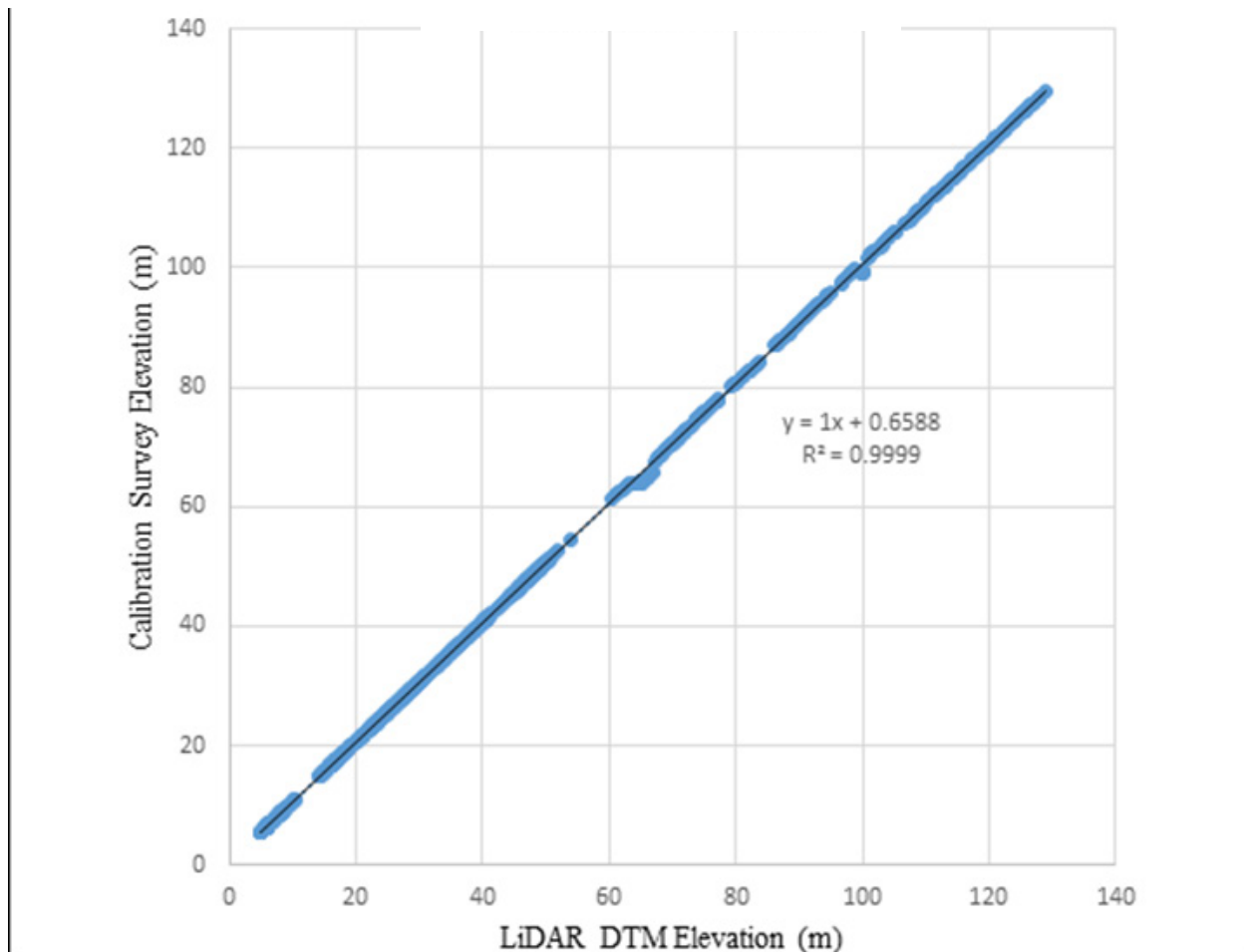


Figure 24. Correlation plot between calibration survey points and LiDAR data.

Table 15. Calibration Statistical Measures

| Calibration Statistical Measures | Value (meters) |
|----------------------------------|----------------|
| Height Difference | 0.68 |
| Standard Deviation | 0.17 |
| Average | -0.66 |
| Minimum | -1.00 |
| Maximum | -0.31 |

The remaining 20% of the total survey points, resulting to 273 points, were used for the validation of calibrated Mayo DTM. A good correlation between the calibrated mosaicked LiDAR elevation values and the ground survey elevation, which reflects the quality of the LiDAR DTM is shown in Figure 25. The computed RMSE between the calibrated LiDAR DTM and validation elevation values is 0.18 meters with a standard deviation of 0.18 meters, as shown in Table 16.

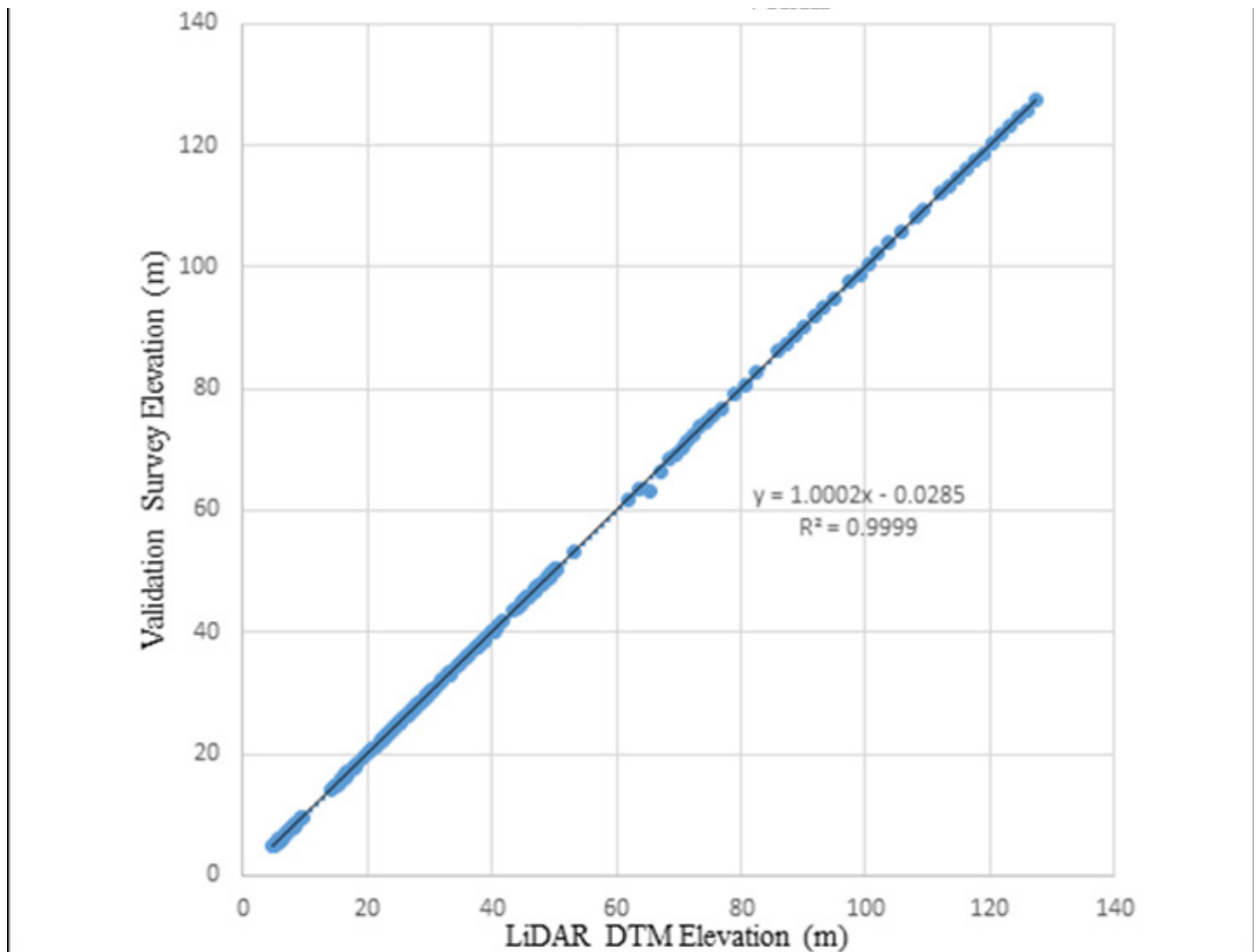


Figure 25. Correlation plot between validation survey points and LiDAR data.

Table 16. Validation Statistical Measures

| Validation Statistical Measures | Value (meters) |
|---------------------------------|----------------|
| RMSE | 0.18 |
| Standard Deviation | 0.18 |
| Average | 0.02 |
| Minimum | -0.33 |
| Maximum | 0.37 |

3.11 Integration of Bathymetric Data into the LiDAR Digital Terrain Model

For bathy integration, only centerline data was available for Mayo with 3,785 bathymetric survey points. The resulting raster surface produced was done by Kernel interpolation method. After burning the bathymetric data to the calibrated DTM, assessment of the interpolated surface is represented by the computed RMSE value of 0.43 meters. The extent of the bathymetric survey done by the Data Validation and Bathymetry Component (DVBC) in Mayo integrated with the processed LiDAR DEM is shown in Figure 26.

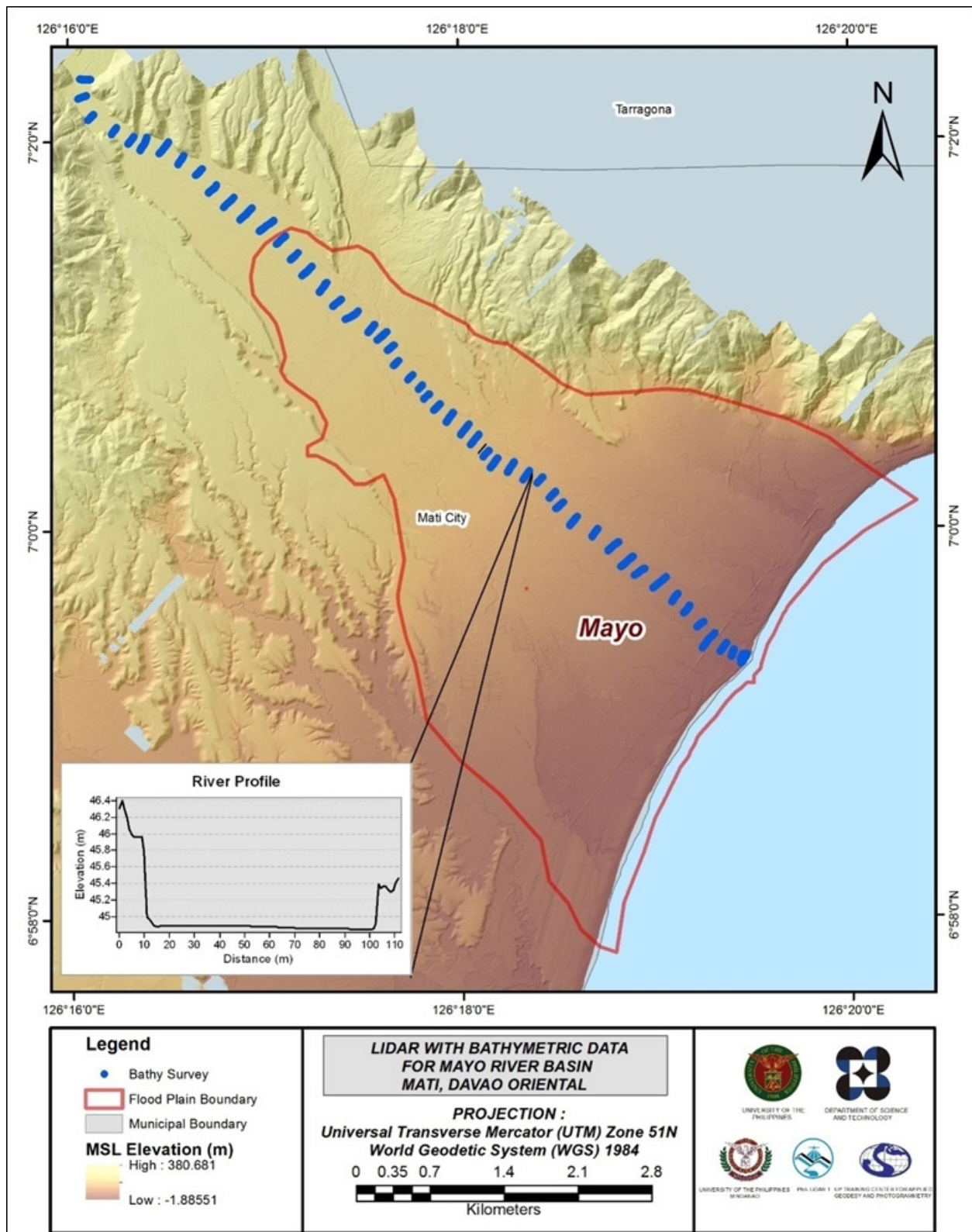


Figure 26. Map of Mayo Floodplain with bathymetric survey points shown in blue.

3.12 Feature Extraction

The features salient in flood hazard exposure analysis include buildings, road networks, bridges and water bodies within the floodplain area with 200 m buffer zone. Mosaicked LiDAR DEM with 1 m resolution was used to delineate footprints of building features, which consist of residential buildings, government offices, medical facilities, religious institutions, and commercial establishments, among others. Road networks comprise of main thoroughfares such as highways and municipal and barangay roads essential for routing of disaster response efforts. These features are represented by a network of road centerlines.

3.12.1 Quality Checking of Digitized Features' Boundary

Mayo Floodplain, including its 200 m buffer, has a total area of 22.07 sq km. For this area, a total of 5.0 sq km, corresponding to a total of 553 building features, are considered for QC. Figure 27 shows the QC blocks for Mayo Floodplain.

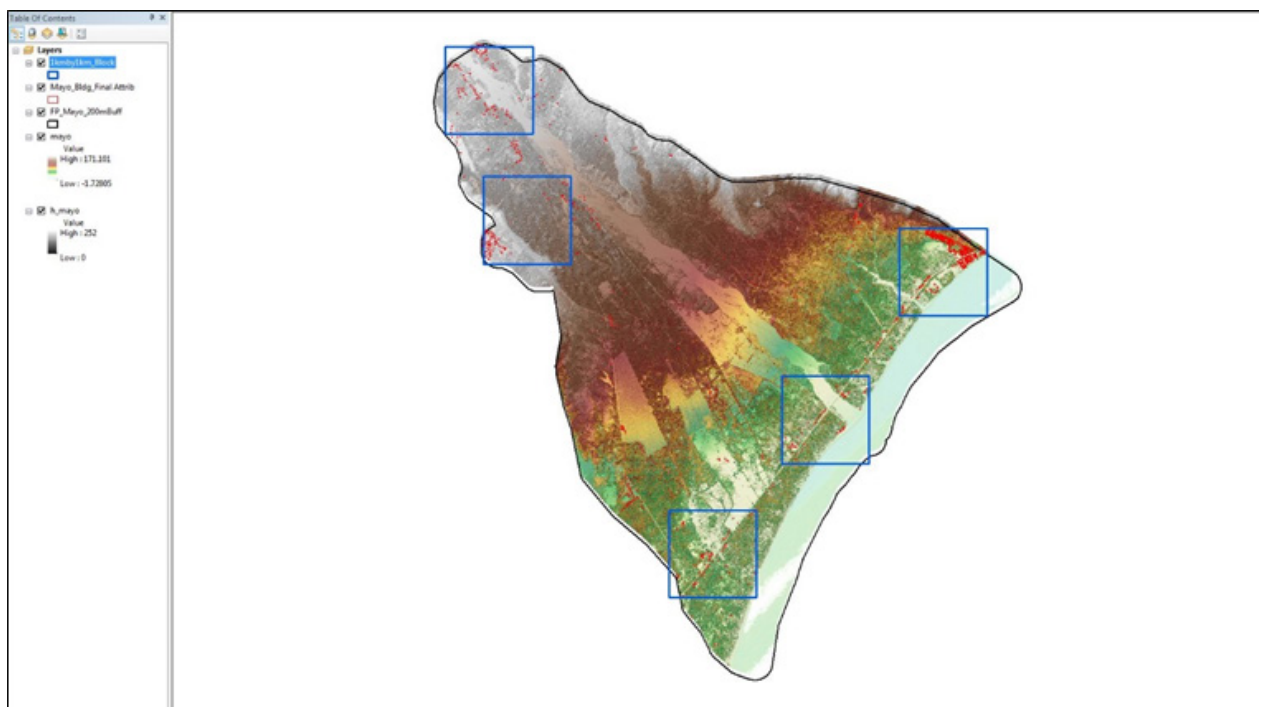


Figure27. Blocks (in blue) of Mayo building features that were subjected to QC

Quality checking of Mayo building features resulted in the ratings shown in Table 17.

Table 17. Quality Checking Ratings for Mayo Building Features

| FLOODPLAIN | COMPLETENESS | CORRECTNESS | QUALITY | REMARKS |
|------------|--------------|-------------|---------|---------|
| Mayo | 99.88 | 99.76 | 99.52 | PASSED |

3.12.2 Height Extraction

Height extraction was done for 1,108 building features in Mayo Floodplain. Of these building features, 148 was filtered out after height extraction, resulting in 960 buildings with height attributes. The lowest building height is at 2.00 m, while the highest building is at 19.87 m.

3.12.3 Feature Attribution

Before the actual field validation, courtesy calls were conducted to seek permission and assistance from the Local Government Units of each barangay. This was done to ensure the safety and security in the area for the field validation process to go smoothly. Verification of barangay boundaries was also done to finalize the distribution of features for each barangay.

The courtesy calls and project presentations were done on May 26, 2016. Barangay Health Workers (BHWs) were requested and hired to guide the University of the Philippines Mindanao Phil-LiDAR1 field enumerators during validation. The field work activity was conducted from June 6-7, 2016. The local hires deployed by the barangay captains were given a brief orientation by the field enumerators before the actual field work. The team surveyed the three (3) barangays covered by the floodplain namely Dahican, Don Enrique Lopez and Don Martin Marundan, Mati City.

Table 18 summarizes the number of building features per type. On the other hand, Table 19 shows the total length of each road type, while Table 20 presents the number of water features extracted per type.

Table 18. Building Features Extracted for Mayo Floodplain.

| Facility Type | No. of Features |
|---|-----------------|
| Residential | 806 |
| School | 39 |
| Market | 0 |
| Agricultural/Agro-Industrial Facilities | 63 |
| Medical Institutions | 2 |
| Barangay Hall | 2 |
| Military Institution | 0 |
| Sports Center/Gymnasium/Covered Court | 3 |
| Telecommunication Facilities | 0 |
| Transport Terminal | 0 |
| Warehouse | 0 |
| Power Plant/Substation | 0 |
| NGO/CSO Offices | 0 |
| Police Station | 0 |
| Water Supply/Sewerage | 1 |
| Religious Institutions | 18 |
| Bank | 0 |
| Factory | 0 |
| Gas Station | 0 |
| Fire Station | 0 |
| Other Government Offices | 2 |
| Other Commercial Establishments | 24 |
| Total | 960 |

Table 19. Total Length of Extracted Roads for Mayo Floodplain.

| Floodplain | Road Network Length (km) | | | | | Total |
|------------|--------------------------|---------------------|-----------------|---------------|--------|-------|
| | Barangay Road | City/Municipal Road | Provincial Road | National Road | Others | |
| Mayo | 20.41 | 0.00 | 0.00 | 5.66 | 0.00 | 26.07 |

Table 20. Number of Extracted Water Bodies for Mayo Floodplain.

| Floodplain | Water Body Type | | | | | Total |
|------------|-----------------|-------------|-----|-----|----------|-------|
| | Rivers/Streams | Lakes/Ponds | Sea | Dam | Fish Pen | |
| Mayo | 1 | 0 | 0 | 0 | 0 | 1 |

One (1) bridge was also extracted for the floodplain.

3.12.4 Final Quality Checking of Extracted Features

All extracted ground features were completely given the required attributes. All these output features comprise the flood hazard exposure database for the floodplain. This completes the feature extraction phase of the project.

Figure 28 shows the Digital Surface Model (DSM) of Mayo Floodplain overlaid with its ground features.

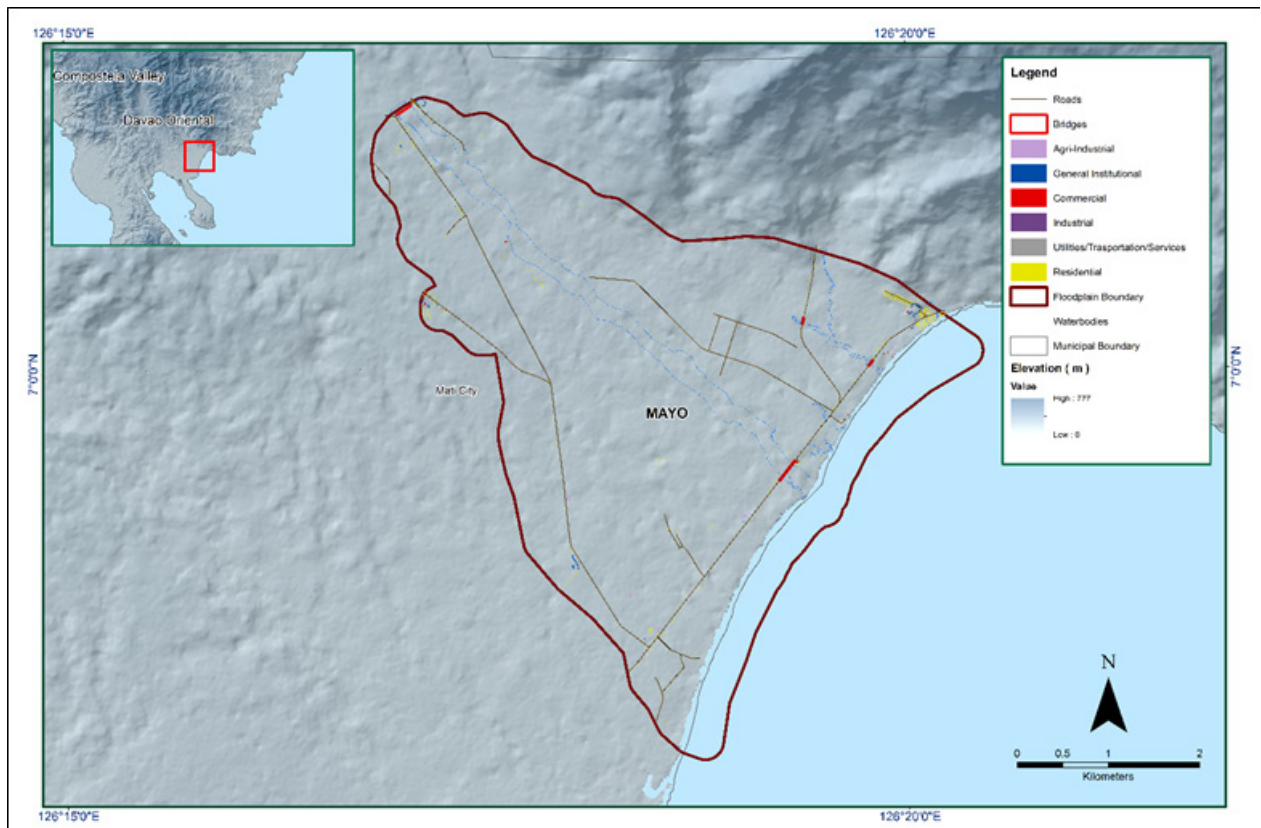


Figure 28. Extracted features for Mayo Floodplain.

CHAPTER 4: LIDAR VALIDATION SURVEY AND MEASUREMENTS OF THE MAYO RIVER BASIN

Engr. Louie P. Balicanta, Engr. Joemarie Caballero, Patrizcia Mae. P. dela Cruz, Engr. Kristine Ailene B. Borromeo, Ms. Jeline M. Amante, Marie Angelique R. Estipona, Charie Mae V. Manliguez, Engr. Janina Jupiter, and Vie Marie Paola M. Rivera

The methods applied in this Chapter were based on the DREAM methods manual (Balicanta, et al., 2014) and further enhanced and updated in Paringit, et al. (2017).

4.1 Summary of Activities

The AB Surveying and Development (ABSD) conducted a field survey in Mayo River on February 27, 2016, March 4-6, 2016, and March 20, 2016 with the following scope: reconnaissance; control survey; cross-section and as-built survey at Mayo Bridge in Brgy. Mayo, Mati City, Davao Oriental; and bathymetric survey from its upstream in Brgy. Don Salvador Lopez, Sr. to the mouth of the river located in Brgy. Don Enrique Lopez, Mati City, with an approximate length of 8.53 km using a Horizon® Total Station. Random checking points for the contractor's cross-section and bathymetry data were gathered by DVBC on May 10-24, 2016 using a survey grade GNSS receiver Trimble® SPS 985 GNSS PPK survey technique. In addition to this, validation points acquisition survey was conducted covering the Mayo River Basin area. The entire survey extent is illustrated in Figure 29.

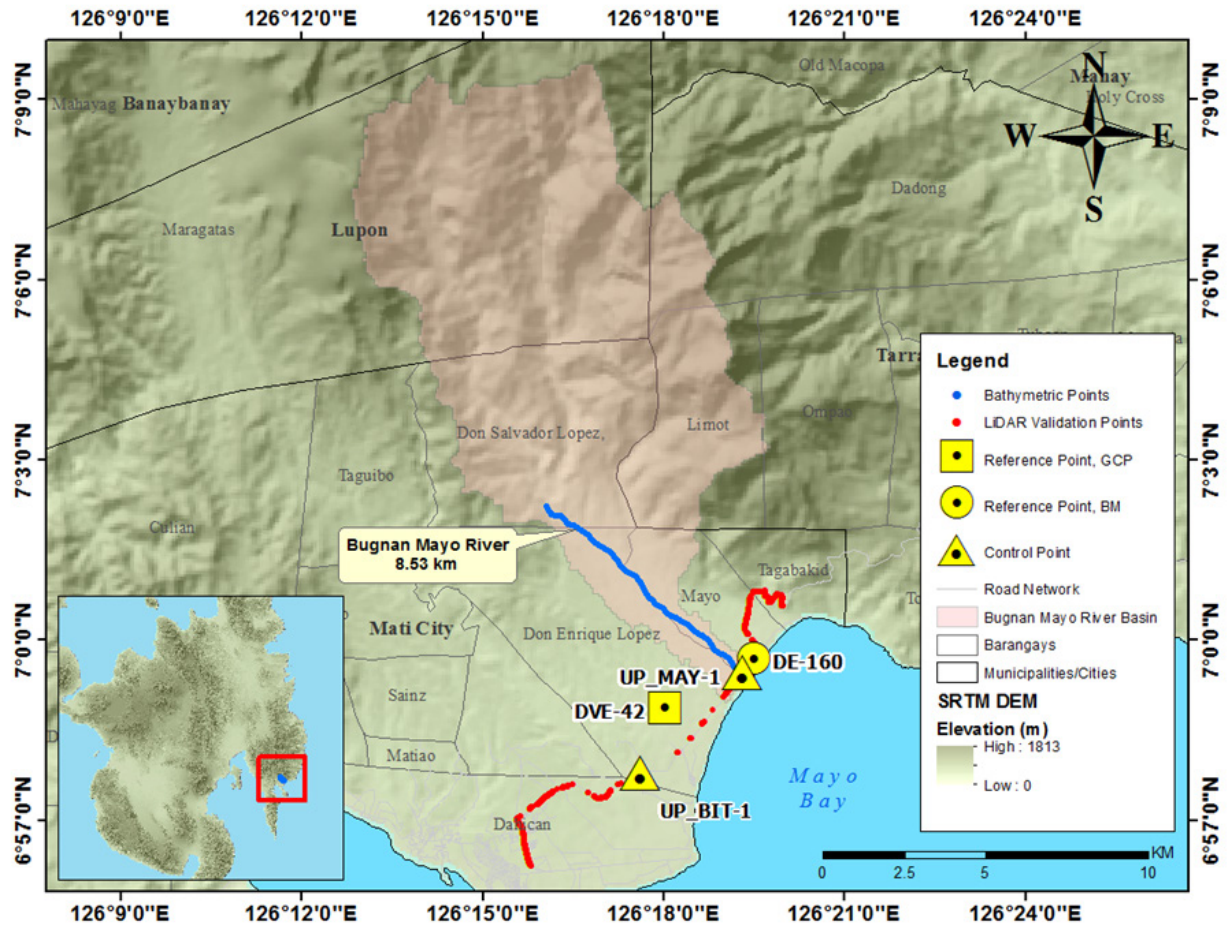


Figure 29. Extent of the bathymetric survey (in blue line) in Mayo River and the LiDAR data validation survey (in red).

4.2 Control Survey

The GNSS network used for Mayo River is composed of seven (7) loops established on May 22, 2016 occupying the following reference points: DVE-42 a second-order GCP, in Brgy. Don Enrique Lopez, Mati City, Davao Oriental and DE-160, a first-order BM, in Brgy. Mayo, Mati City, Davao Oriental.

Three (3) control points established in the area by ABSD were also occupied: UP_BIT-1 beside the approach of Bitanagan Bridge in Brgy. Don Enrique Lopez, Mati City, Province of Davao Oriental, UP_MAY-1 beside the approach of Mayo Bridge in Brgy. Mayo, Mati City, Davao Oriental, and UP_QUI-1 located beside the approach of Quinonoan Bridge in Brgy. San Ignacio, Manay, Davao Oriental.

The summary of reference and control points and its location is summarized in Table 21 while GNSS network established is illustrated in Figure 30.

Table 21. List of Reference and Control Points occupied for Mayo River Survey

(Source: NAMRIA; UP-TCAGP)

| Control Point | Order of Accuracy | Geographic Coordinates (WGS 84) | | | | |
|---------------|-------------------|---------------------------------|-------------------|----------------------------|--------------------------|------------------|
| | | Latitude | Longitude | Ellipsoidal Height (Meter) | Elevation in MSL (Meter) | Date Established |
| DVE-42 | 2nd order, GCP | 6°58'51.79295"N | 126°18'01.57690"E | 80.539 | 15.122 | 2007 |
| DE-160 | 1st order, BM | 6°59'41.20398"N | 126°19'30.03464"E | 71.754 | 6.419 | 2009 |
| UP_BIT-1 | Established | 6°57'46.30507"N | 126°17'35.96635"E | 80.537 | 15.21 | 2-26-16 |
| UP_MAY-1 | Established | 6°59'26.93722"N | 126°19'18.72092"E | 73.478 | 8.152 | 2-27-16 |
| UP_QUI-1 | Established | 7°05'25.95862"N | 126°27'58.08622"E | 70.854 | 6.305 | 2-20-16 |

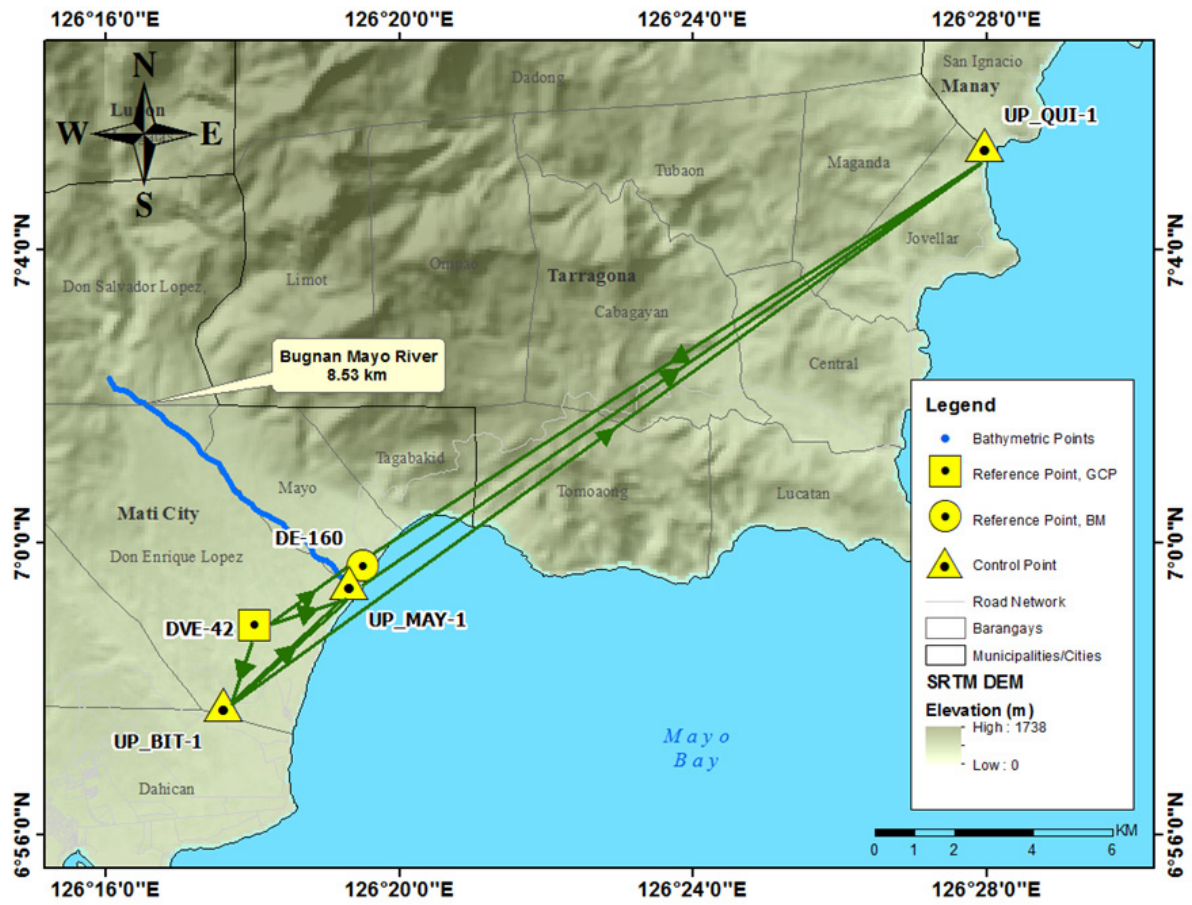


Figure 30. The GNSS Network established in the Mayo River Survey.

The GNSS set-ups on recovered reference points and established control points in Mayo River are shown from Figure 31 to Figure 35.

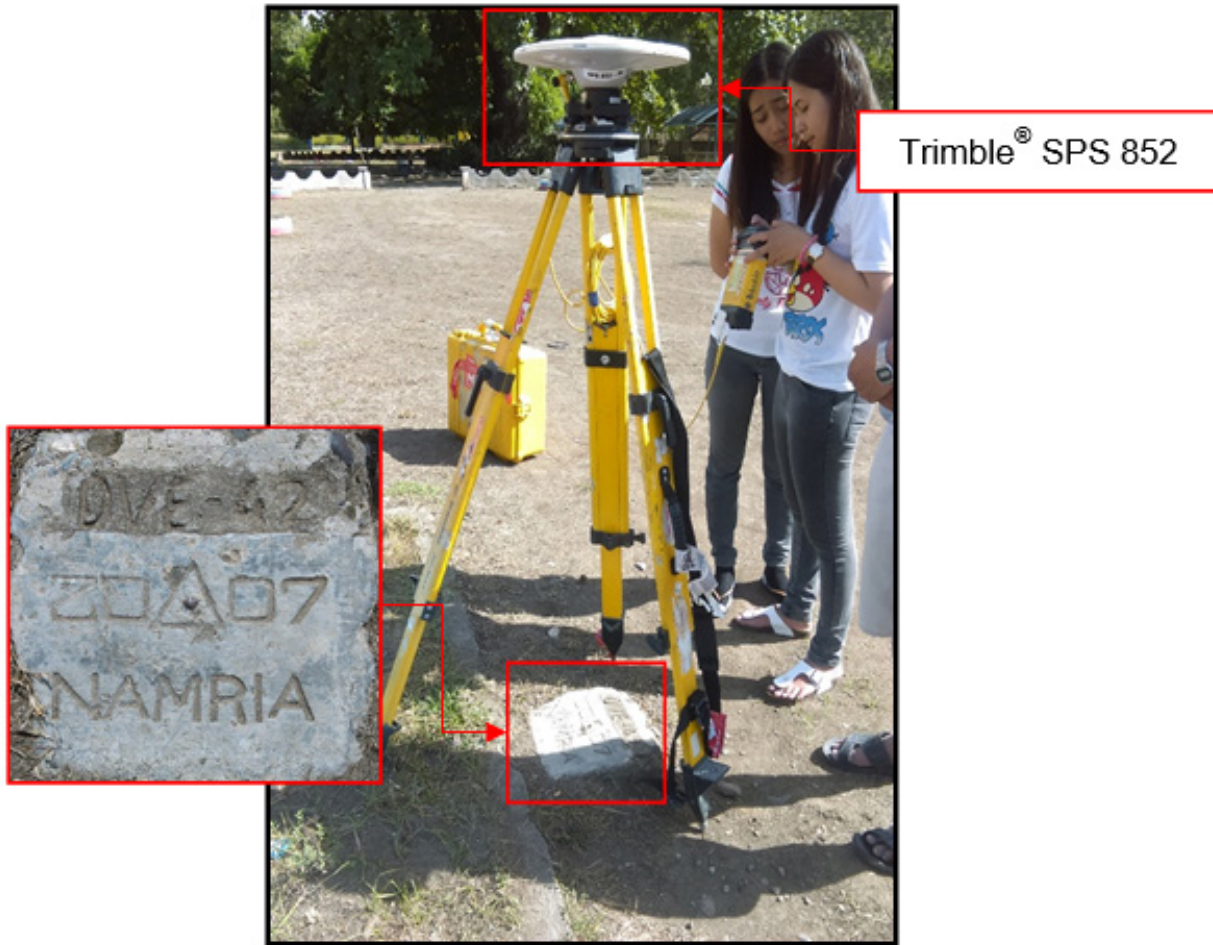


Figure 31. GNSS base set up, Trimble® SPS 852, at DVE-42, located in front of the flagpole inside Don Enrique Lopez Elementary School in Brgy. Don Enrique Lopez, Mati City, Davao Oriental



Figure 32. GNSS receiver set up, Trimble® SPS 985, at DE-160, located at approach of Calinan Bridge in Brgy. Mayo, City of Mati, Davao Oriental



Figure 33. GNSS receiver set up, Trimble® SPS 852, at UP_BIT-1, located at the side of the railing near the approach of Bitanagan Bridge in Brgy. Don Enrique Lopez, City of Mati, Davao Oriental



Figure 34. GNSS receiver set up, Trimble® SPS 985, at UP_MAY-1, located beside the approach of Mayo Bridge in Brgy. Mayo, City of Mati, Province of Davao Oriental



Figure 35. GNSS receiver set up, Trimble® SPS 882, at UP QUI-1, located beside the approach of Quinonoan Bridge in Brgy. San Ignacio, Municipality of Manay, Province of Davao Oriental

4.3 Baseline Processing

GNSS baselines were processed simultaneously in TBC by observing that all baselines have fixed solutions with horizontal and vertical precisions within +/- 20 cm and +/- 10 cm requirement, respectively. In case where one or more baselines did not meet all of these criteria, masking is performed. Masking is done by removing/masking portions of these baseline data using the same processing software. It is repeatedly processed until all baseline requirements are met. If the reiteration yields out of the required accuracy, resurvey is initiated. Baseline processing result of control points in Mayo River Basin is summarized in Table 22 generated by TBC software.

Table 22. Baseline Processing Summary Report for Mayo River Survey

| Observation | Date of Observation | Solution Type | H. Prec. (Meter) | V. Prec. (Meter) | Geodetic Az. | Ellipsoid Dist. (Meter) | ΔHeight (Meter) |
|------------------------|---------------------|---------------|------------------|------------------|--------------|-------------------------|-----------------|
| DVE-42 --- DE-160 | 5-522-2016 | Fixed | 0.005 | 0.026 | 60°47'28" | 3110.595 | -8.798 |
| UP_MAY-1 -- DE-160 | 5-522-2016 | Fixed | 0.003 | 0.004 | 38°23'28" | 559.167 | -1.723 |
| DVE-42 --- | 12-7-2015 | Fixed | 0.006 | 0.028 | 305°11'33" | 6328.249 | -229.449 |
| UP_MAY-1 | 5-522-2016 | Fixed | 0.003 | 0.014 | 65°29'18" | 2602.368 | -7.064 |
| UP_BIT-1 --- | 12-7-2015 | Fixed | 0.004 | 0.021 | 13°03'37" | 19960.518 | -55.135 |
| UP_MAY-1 | 5-522-2016 | Fixed | 0.004 | 0.018 | 45°34'22" | 4416.378 | -7.047 |
| UP_BIT-1 --- DE-160 | 5-522-2016 | Fixed | 0.005 | 0.025 | 44°46'00" | 4971.649 | -8.805 |
| UP_BIT-1 --- DVE-42 | 5-522-2016 | Fixed | 0.003 | 0.015 | 201°20'38" | 2159.894 | 0.009 |
| UP_BIT-1 --- | 12-7-2015 | Fixed | 0.004 | 0.019 | 320°20'42" | 10551.869 | -275.506 |
| UP_QUI-1 | 5-522-2016 | Fixed | 0.007 | 0.024 | 53°30'19" | 23747.730 | -9.665 |

As shown Table 22 a total of ten (10) baselines were processed with coordinates of DVE-42 and elevation of DE-160 held fixed. All of them passed the required accuracy.

4.4 Network Adjustment

After the baseline processing procedure, network adjustment is performed using TBC. Looking at the Adjusted Grid Coordinates table of the TBC generated Network Adjustment Report, it is observed that the square root of the squares of x and y must be less than 20 cm and z less than 10 cm in equation form:

$$\sqrt{((x_e)^2 + (y_e)^2)} < 20cm \text{ and } z_e < 10 \text{ cm}$$

Where:

- x_e is the Easting Error,
- y_e is the Northing Error, and
- z_e is the Elevation Error

for each control point. See the Network Adjustment Report shown from Table C- 3Table 23 to Table C- 5 Table 25 for the complete details.

The five (5) control points, DVE-42, DE-160, UP-BIT-1, UP_MAY-1, and UP-QUI-1 were occupied and observed simultaneously to form a GNSS loop. The coordinate values of DVE-42 and elevation of DE-160 were held fixed during the processing of the control points as presented in Table C- 323. Through these reference points, the coordinates and elevation of the unknown control points will be computed.

Table 23. Constraints applied to the adjustment of the control points.

| Point ID | Type | East σ (Meter) | North σ (Meter) | Height σ (Meter) | Elevation σ (Meter) |
|--------------------------|--------|----------------|-----------------|------------------|---------------------|
| DE-160 | Grid | | | | Fixed |
| DVE-42 | Global | Fixed | Fixed | | |
| Fixed = 0.000001 (Meter) | | | | | |

The list of adjusted grid coordinates, i.e. Northing, Easting, Elevation and computed standard errors of the control points in the network is indicated in Table 24. All fixed control points have no values for grid errors and elevation error.

Table 24. Adjusted grid coordinates for the control points used in the Mayo River Floodplain survey.

| Point ID | Easting (Meter) | Easting Error (Meter) | Northing (Meter) | Northing Error (Meter) | Elevation (Meter) | Elevation Error (Meter) | Constraint |
|----------|-----------------|-----------------------|------------------|------------------------|-------------------|-------------------------|------------|
| DE-160 | 774012.369 | 0.003 | 204436.373 | 0.005 | 6.419 | ? | e |
| DVE-42 | 772508.970 | ? | 201710.753 | ? | 15.122 | 0.023 | LL |
| UP_BIT-1 | 770500.332 | 0.003 | 200912.560 | 0.004 | 15.210 | 0.025 | |
| UP_MAY-1 | 773575.785 | 0.003 | 204086.387 | 0.004 | 8.152 | 0.009 | |
| UP_QUI-1 | 784522.580 | 0.004 | 220097.240 | 0.007 | 6.305 | 0.034 | |

With the mentioned equation, $\sqrt{((x_e)^2 + (y_e)^2)} < 20\text{cm}$ and $z_e < 10\text{ cm}$ for horizontal and $z_e < 10\text{ cm}$ for the vertical; the computation for the accuracy are as follows:

- a. DE-160
 - horizontal accuracy = $\sqrt{((0.3)^2 + (0.5)^2)}$
 - = $\sqrt{0.09 + 0.25}$
 - = $0.34 < 20\text{ cm}$
 - vertical accuracy = Fixed
- b. DVE-42
 - horizontal accuracy = Fixed
 - vertical accuracy = $2.3 < 10\text{ cm}$
- c. UP_BIT-1
 - horizontal accuracy = $\sqrt{((0.3)^2 + (0.4)^2)}$
 - = $\sqrt{0.09 + 0.16}$
 - = $0.25 < 20\text{ cm}$
 - vertical accuracy = $2.5 < 10\text{ cm}$
- d. UP_MAY-1
 - horizontal accuracy = $\sqrt{((0.3)^2 + (0.4)^2)}$
 - = $\sqrt{0.09 + 0.16}$
 - = $0.25 < 20\text{ cm}$
 - vertical accuracy = $0.9 < 10\text{ cm}$
- e. UP QUI-1
 - horizontal accuracy = $\sqrt{((0.4)^2 + (0.7)^2)}$
 - = $\sqrt{0.16 + 0.49}$
 - = $0.65 < 20\text{ cm}$
 - vertical accuracy = $3.4 < 10\text{ cm}$

Following the given formula, the horizontal and vertical accuracy result of the five (5) occupied control points are within the required precision.

Table 25. Adjusted geodetic coordinates for control points used in the Mayo River Floodplain validation.

| Point ID | Latitude | Longitude | Ellipsoid | Height | Constraint |
|----------|-----------------|-------------------|-----------|--------|------------|
| DE-160 | N6°59'41.20398" | E126°19'30.03464" | 71.754 | ? | e |
| DVE-42 | N6°58'51.79295" | E126°18'01.57690" | 80.539 | 0.023 | LL |
| UP_BIT-1 | N6°57'46.30507" | E126°17'35.96635" | 80.537 | 0.025 | |
| UP_MAY-1 | N6°59'26.93722" | E126°19'18.72092" | 73.478 | 0.009 | |
| UP QUI-1 | N7°05'25.95862" | E126°27'58.08622" | 70.854 | 0.034 | |

The corresponding geodetic coordinates of the observed points are within the required accuracy as shown in Table 25. Based on the result of the computation, the equation is satisfied; hence, the required accuracy for the program was met.

The summary of reference control points used is indicated in Table 26.

Table 26. The reference and control points utilized in the Balamban River Static Survey, with their corresponding locations (Source: NAMRIA, UP-TCAGP)

| Control Point | Order of Accuracy | Geographic Coordinates (WGS 84) | | | UTM ZONE 51 N | | | BM Ortho (m) |
|---------------|-------------------|---------------------------------|-------------------|------------------------|---------------|-------------|---------------|--------------|
| | | Latitude | Longitude | Ellipsoidal Height (m) | Northing (m) | Easting (m) | EGM Ortho (m) | |
| DVE-42 | 2nd order, GCP | 6°58'51.79295"N | 126°18'01.57690"E | 80.539 | 772508.97 | 201710.753 | 15.122 | 287.844 |
| DE-160 | 1st order, BM | 6°59'41.20398"N | 126°19'30.03464"E | 71.754 | 774012.369 | 204436.373 | 6.419 | 58.767 |
| UP_BIT-1 | Established | 6°57'46.30507"N | 126°17'35.96635"E | 80.537 | 770500.332 | 200912.56 | 15.21 | 3.317 |
| UP_MAY-1 | Established | 6°59'26.93722"N | 126°19'18.72092"E | 73.478 | 773575.785 | 204086.387 | 8.152 | 4.332 |
| UP_QUI-1 | Established | 7°05'25.95862"N | 126°27'58.08622"E | 70.854 | 784522.58 | 220097.24 | 6.305 | 13.001 |

4.5 Cross-section and Bridge As-Built survey and Water Level Marking

Cross-section and as-built surveys were conducted on March 20, 2016 at the downstream side of Mayo Bridge in Brgy. Mayo, City of Mati as shown in Figure 36. Horizon® Total Station was utilized for this survey as shown in Figure 37.



Figure 36. Mayo Bridge facing downstream

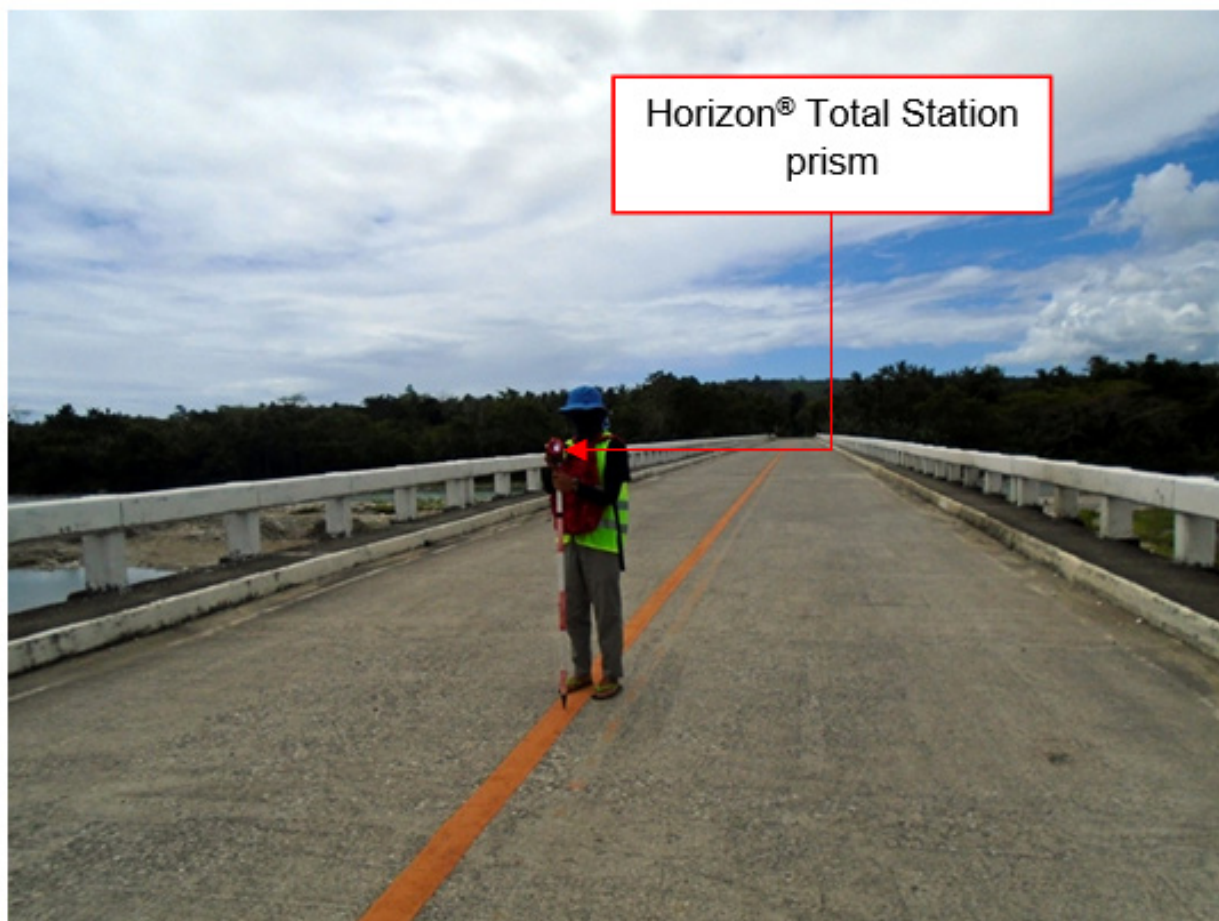


Figure 37. As-built survey of Mayo Bridge

The cross-sectional line of Mayo Bridge is about 151 m with two hundred fourteen (214) cross-sectional points using the control points UP_MAY-1 and UP_MAY-2 as the GNSS base stations. The cross-section diagram and the bridge data form are shown in Figure 38 and Figure 39. Gathering of random points for the checking of ABSD's bridge cross-section and bridge points data was performed by DVBC on May 16, 2016 using a survey grade GNSS Rover receiver attached to a 2-m pole.

Linear square correlation (R2) and RMSE analysis were performed on the two (2) datasets. The linear square coefficient range is determined to ensure that the submitted data of the contractor is within the accuracy standard of the project which is ± 20 cm and ± 10 cm for horizontal and vertical, respectively. The R2 value must be within 0.85 to 1. An R2 approaching 1 signifies a strong correlation between the vertical (elevation values) of the two datasets. A computed R2 value of 0.96 was obtained by comparing the data of the contractor and DVBC; signifying a strong correlation between the two (2) datasets.

In addition to the Linear Square correlation, Root Mean Square (RMSE) analysis is also performed in order to assess the difference in elevation between the DVBC checking points and the contractor's. The RMSE value should only have a maximum radial distance of 5 m and the difference in elevation within the radius of 5 meters should not be beyond 0.50 m. For the bridge cross-section data, a computed value of 0.429 was acquired. The computed R2 and RMSE values are within the accuracy requirement of the program.

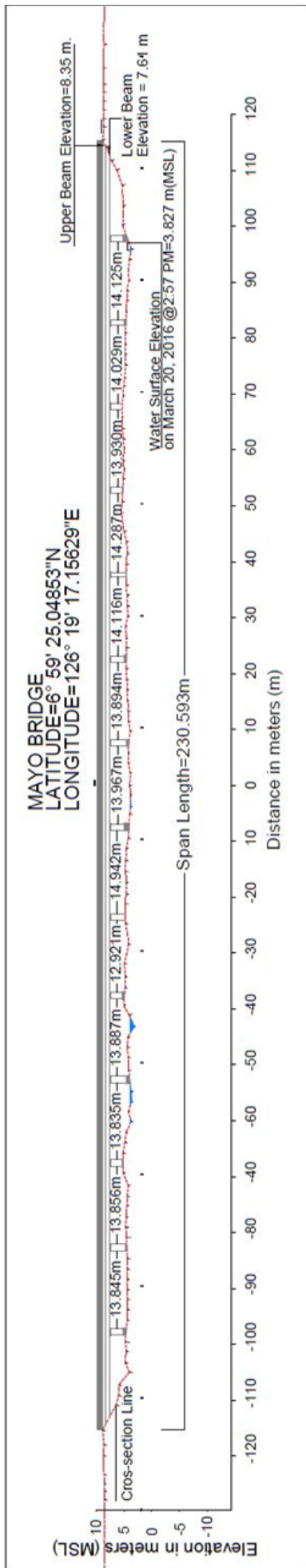


Figure 38. Mayo Bridge cross-section diagram

Figure 39. As-built survey of Mayo Bridge

Water surface elevation of Bugnan Mayo River was determined by a Horizon® Total Station on March 20, 2016 at 2:57 PM at Mayo Bridge area with a value of 3.827 m in MSL as shown in Figure 38. This was translated into marking on the bridge's pier as shown in Figure 40. The marking will serve as reference for flow data gathering and depth gauge deployment of the partner HEI responsible for Bugnan Mayo River, UP Mindanao.



Figure 40. Water level markings on Mayo Bridge

4.6 Validation Points Acquisition Survey

Validation points acquisition survey was conducted by DVBC on May 16, 2016 using a survey grade GNSS Rover receiver, Trimble® SPS 985, mounted on a range pole which was attached on the front of the vehicle as shown in Figure 41. It was secured with cable ties and ropes to ensure that it was horizontally and vertically balanced. The antenna height was 2.476 m and measured from the ground up to the bottom of the quick release of the GNSS Rover receiver. The PPK technique utilized for the conduct of the survey was set to continuous topo mode with UP_MAY-1 occupied as the GNSS base station in the conduct of the survey.

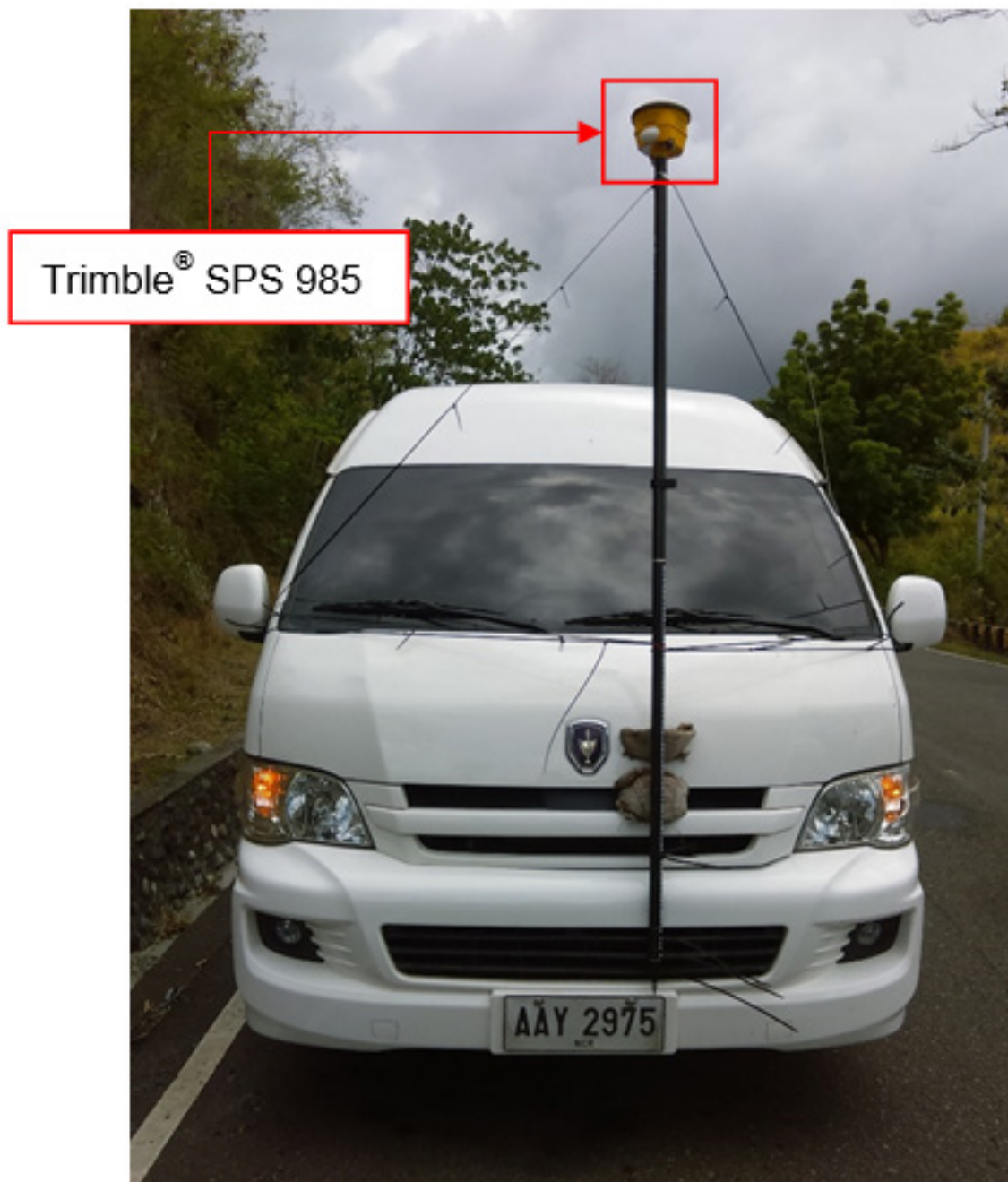


Figure 41. Validation points acquisition survey set-up for Mayo River

The survey started from Brgy. Dahican, Mati City, Davao Oriental going north east along national high way and ended in Brgy. Tagabakid, Mati City, Davao Oriental. The survey gathered a total of 1,365 points with approximate length of 15.1 km using UP_MAY-1 as GNSS base station for the entire extent of validation points acquisition survey as illustrated in the map in Figure 42. Due to the presence of heavy canopy in the survey area, around 20% of the surveyed area have no data.

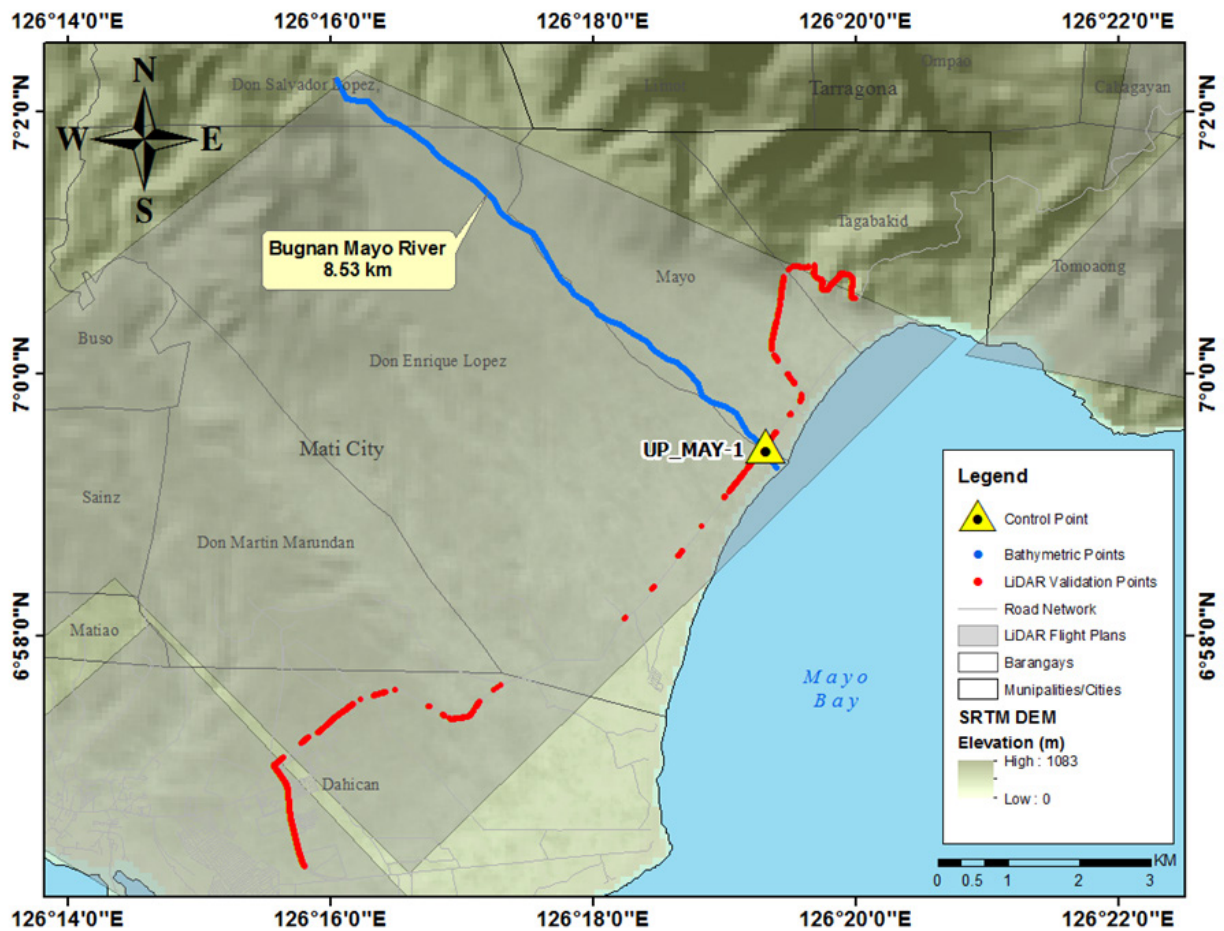


Figure 42. Validation point acquisition survey of Mayo River basin

4.7 River Bathymetric Survey

Bathymetric survey was executed manually on March 4 - 6, 2016 using a Horizon[®] Total Station as seen in Figure 43. The survey started in Brgy. Don Salvador Lopez, Sr., Mati City, Davao Oriental with coordinates 7° 2' 19.47587"N, 126° 16' 3.16644"E and ended at the mouth of the river in Brgy. Don Enrique Lopez, Mati City, Davao Oriental with coordinates 6° 59' 18.13026"N, 126° 19' 25.58137"E. The control points UP_MAY-1 and UP_MAY-2 served as the GNSS base stations all throughout the survey.



Figure 43. Manual bathymetric survey of ABSD at Bugnan Mayo River using Horizon[®] Total Station

Gathering of random points for the checking of ABSD's bathymetric data was performed by DVBC on May 16, 2016 using a GNSS Rover receiver, Trimble® SPS 985 attached to a 2-m pole, see Figure 44. A map showing the DVBC bathymetric checking points is shown in Figure 46.



Figure 44. Gathering of random bathymetric points along Bugnan Mayo River

Linear square correlation (R^2) and RMSE analysis were also performed on the two (2) datasets and a computed R^2 value of 0.99 is within the required range for R^2 , which is 0.85 to 1. Additionally, an RMSE value of 0.142 was obtained. Both the computed R^2 and RMSE values are within the accuracy required by the program.

The bathymetric survey for Bugnan Mayo River gathered a total of 4,150 points covering 8.53 km of the river traversing Barangays Don Salvador Lopez, Sr., Don Enrique Lopez, and Mayo in the City of Mati. A CAD drawing was also produced to illustrate the riverbed profile of Bugnan Mayo River. As shown in Figure 47, the highest and lowest elevation has a 135-m difference. The highest elevation observed was 135.324 m above MSL located in Brgy. Don Salvador Lopez, Sr., Mati City while the lowest was -0.628 m below MSL located in Brgy. Don Enrique Lopez, Mati City.

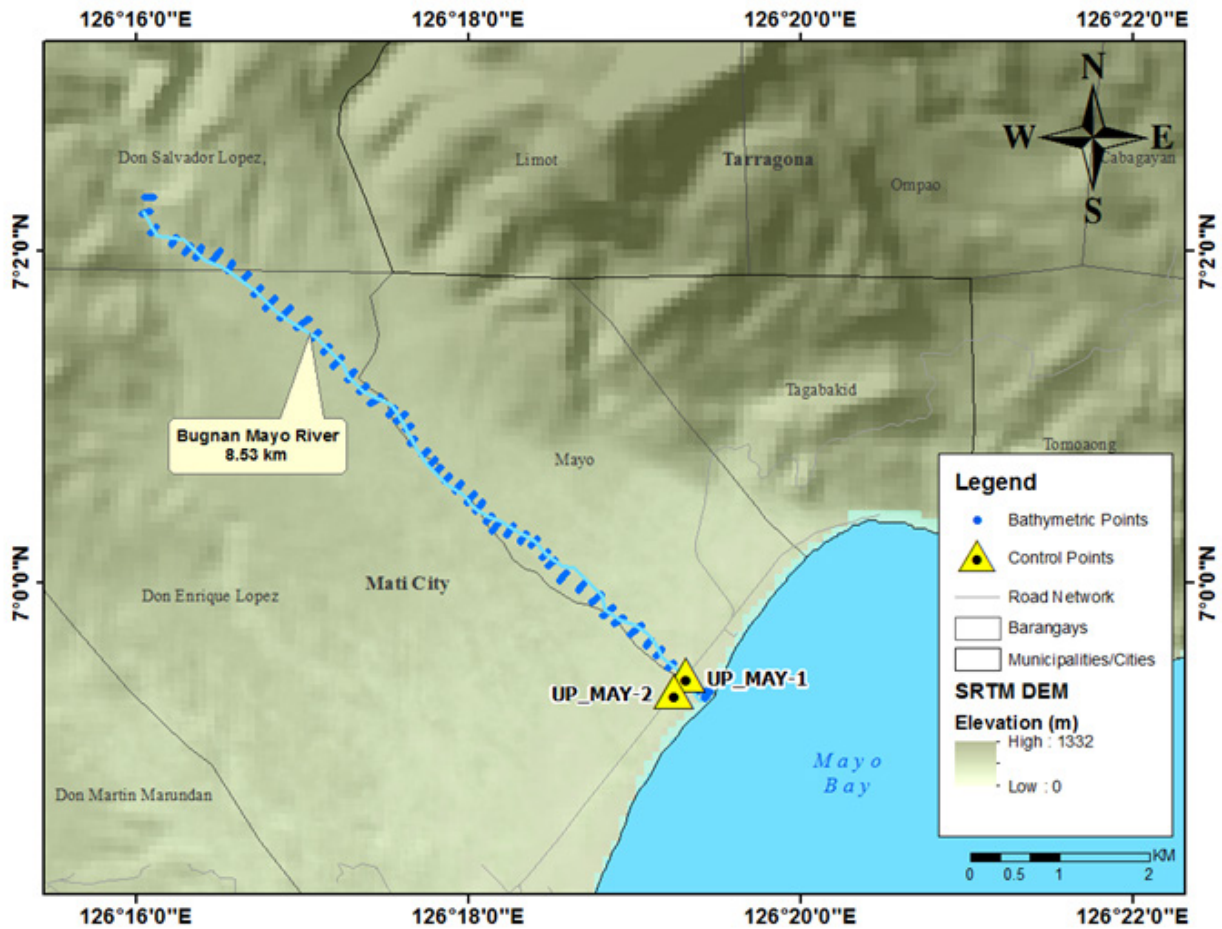


Figure 45. Extent of the Mayo River Bathymetry Survey

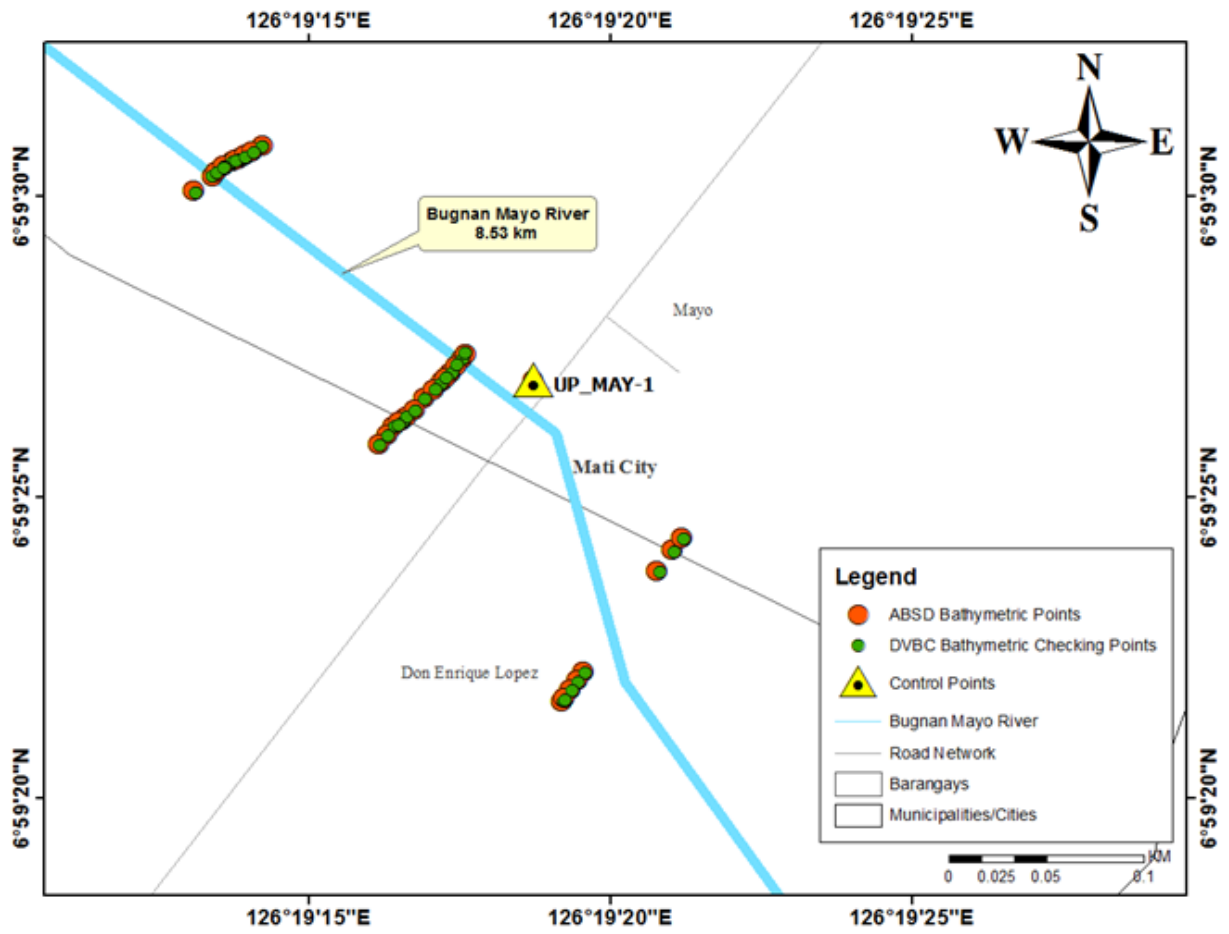


Figure 46. Quality checking points gathered along Mayo River by DVBC

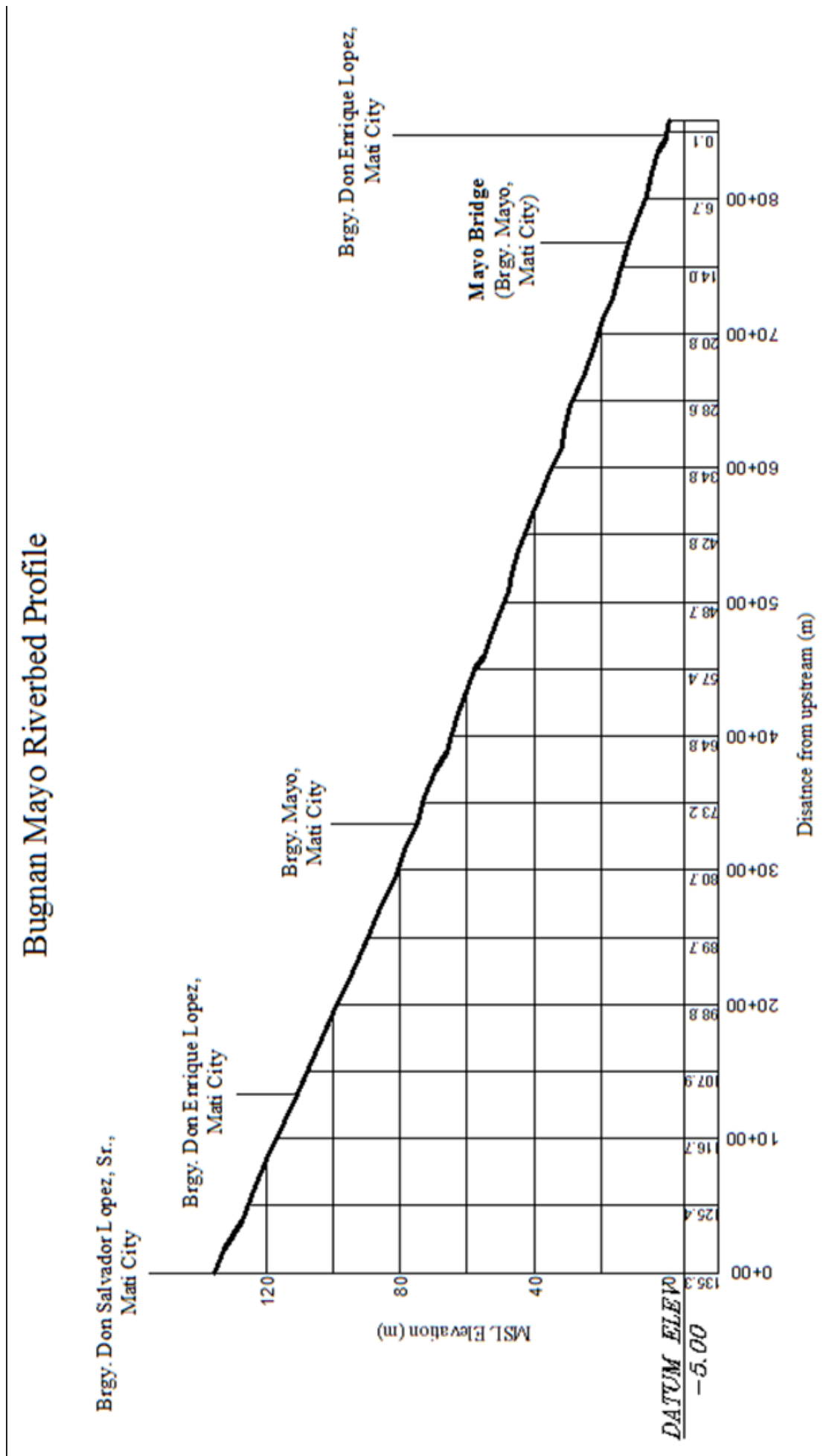


Figure 47. Mayo riverbed profile.

CHAPTER 5: FLOOD MODELING AND MAPPING

Alfredo Mahar Francisco A. Lagmay, Enrico C. Paringit, Dr. Eng., Christopher Noel L. Uichanco, Sylvia Sueno, Marc Moises, Hale Ines, Miguel del Rosario, Kenneth Punay, Neil R. Tingin, Narvin Clyd Tan, and Hannah Aventurado

The methods applied in this Chapter were based on the DREAM methods manual (Lagmay, et al., 2014) and further enhanced and updated in Paringit, et al. (2017)

5.1 Data Used for Hydrologic Modeling

5.1.1 Hydrometry and Rating Curves

All data that affect the hydrologic cycle of the Silaga River Basin were monitored, collected, and analyzed. Rainfall, water level, and flow in a certain period of time, which may affect the hydrologic cycle of the Silaga River Basin were monitored, collected, and analyzed.

5.1.2 Precipitation

Precipitation data was taken from the rain gauge installed by the University of the Philippines Mindanao Phil. LiDAR 1. This rain gauge is located in Barangay Limot, Tarragona, Davao Oriental with the following coordinates: 7° 4' 16.72" N, 126° 16' 43.61" E (Figure 1). The precipitation data collection started from October 9, 2016 at 7:00 PM to October 11, 2016 at 2:00 PM with a 10-minute recording interval.

The total precipitation for this event in the installed rain gauge was 75.2 mm. It has a peak rainfall of 15.4 mm. on October 10, 2016 at 1:00 PM. The lag time between the peak rainfall and discharge is 3 hours and 20 minutes.

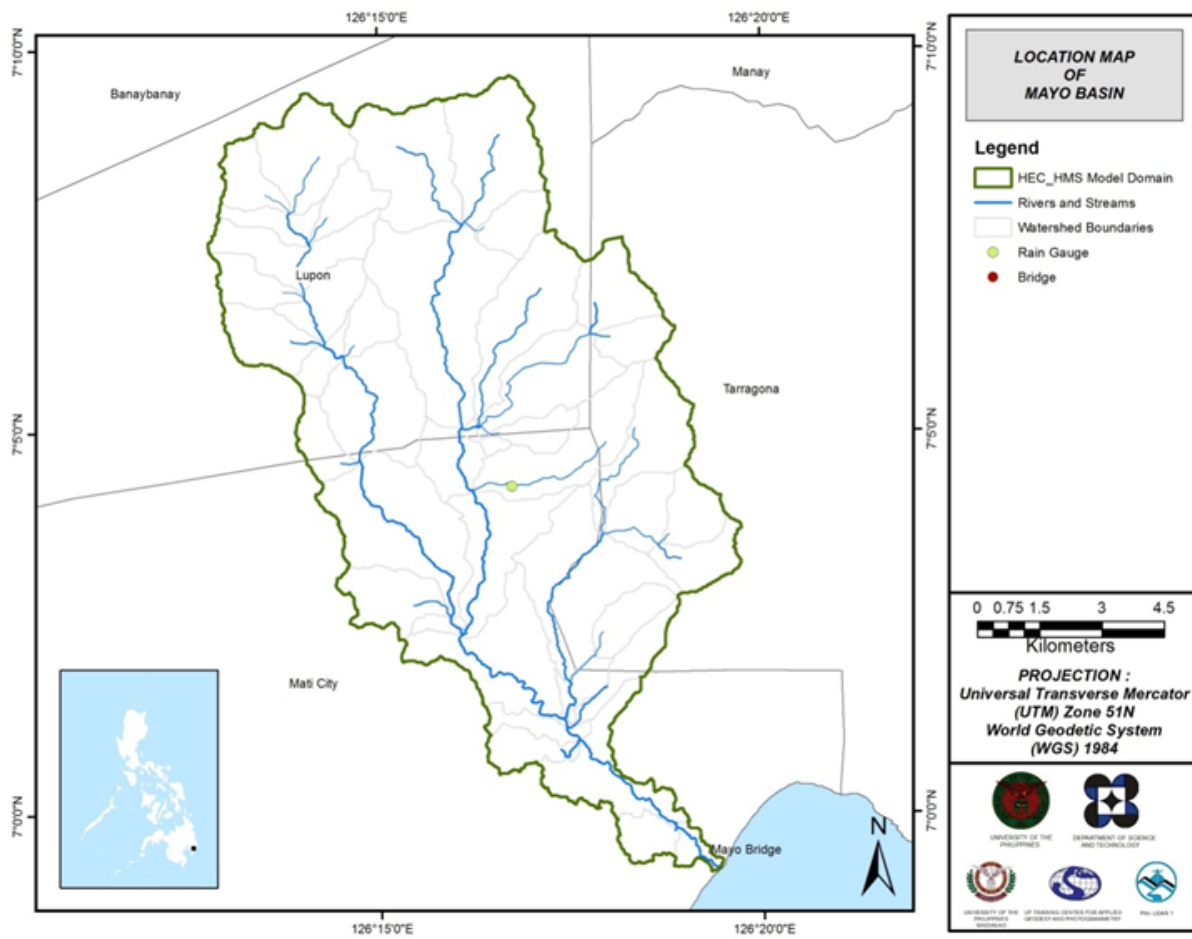


Figure 48. Location map of the Balamban HEC-HMS model used for calibration.

5.1.3 Rating Curves and River Outflow

A rating curve was developed at Mayo Bridge, Barangay Mayo, Tarragona, Davao Oriental (6° 59' 25.01" N, 126° 19' 17.76" E). It gives the relationship between the observed water level at the Mayo Bridge and outflow of the watershed at this location.

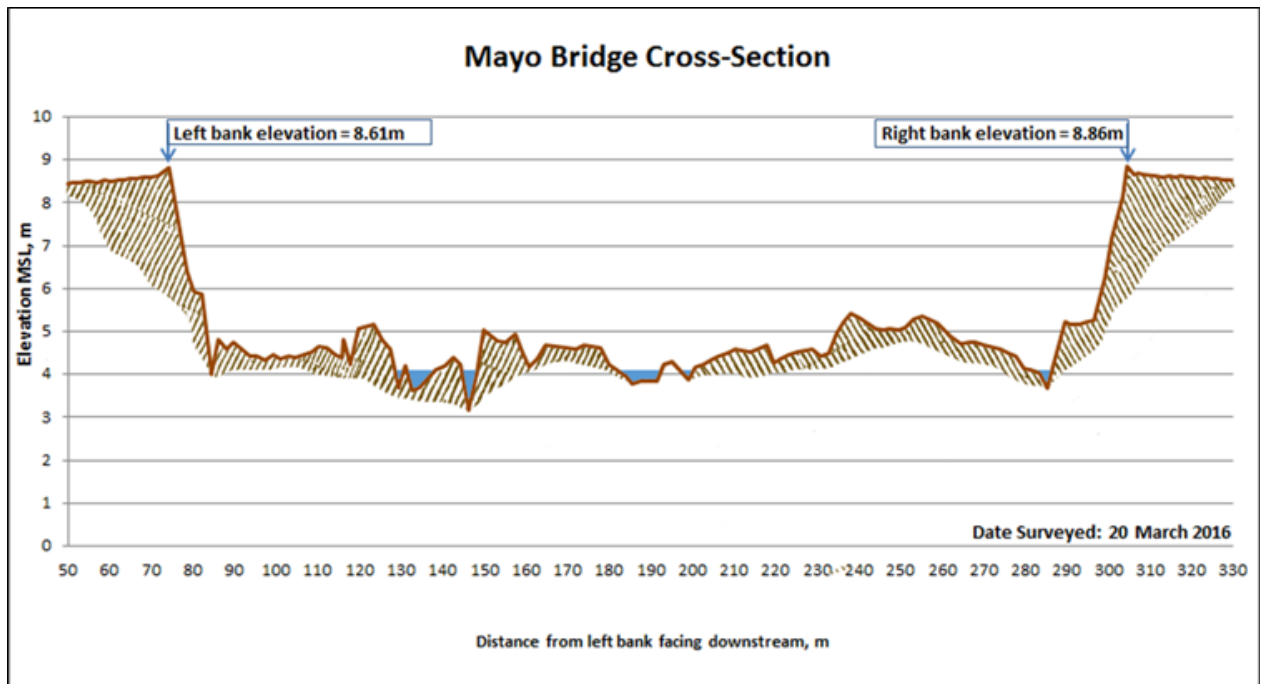


Figure 49. Cross-section plot of Mayo Bridge

For Mayo Bridge, the rating curve is expressed as $Q = 4.26E-07e4.05x$ as shown in Figure 50.

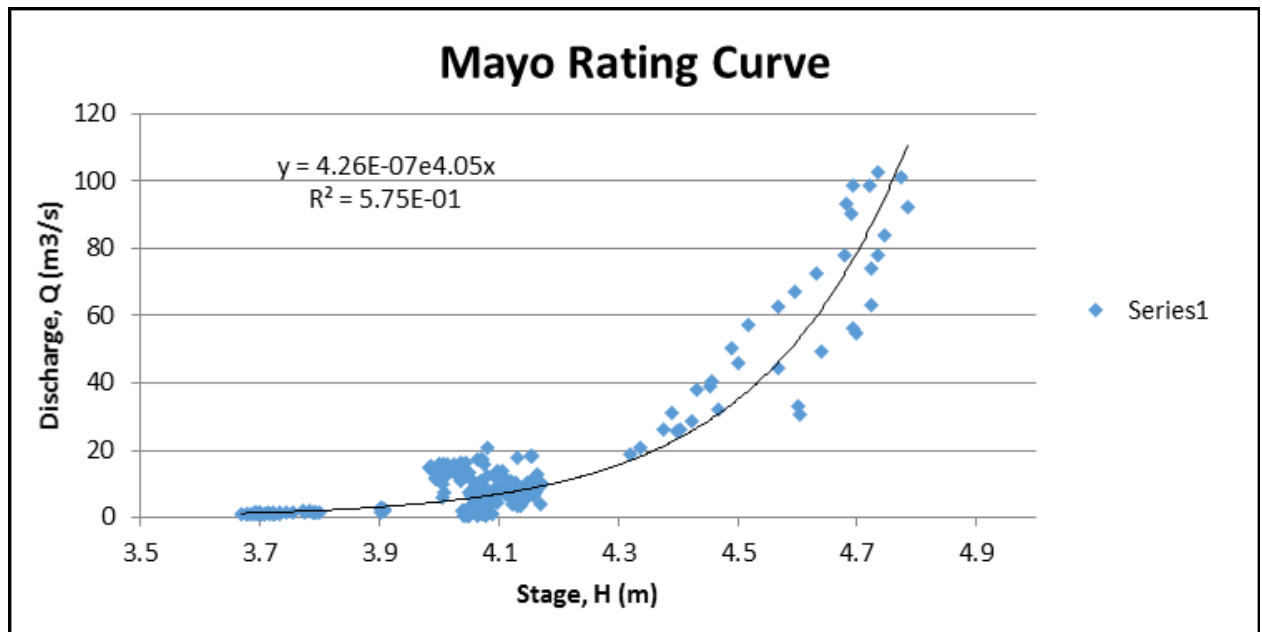


Figure 50. Rating curve at Mayo Bridge, Tarragona, Davao Oriental

The rating curve equation was used to compute for the river outflow at Mayo Bridge for the calibration of the HEC-HMS model for Mayo, as shown in Figure 51. The total rainfall for this event is 75.2 mm and the peak discharge is 102.5 m³/s at 4:20 PM of October 10, 2016.

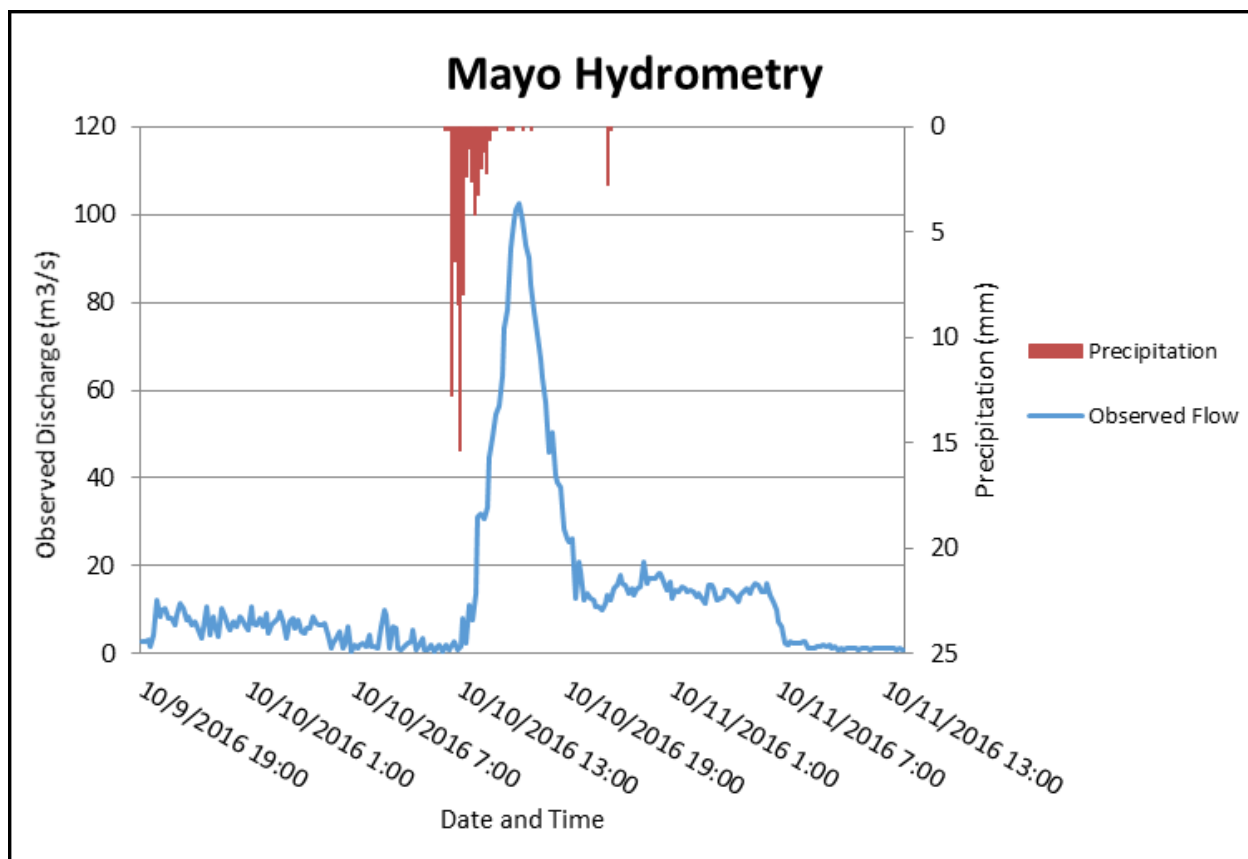


Figure 51. Rainfall and outflow data at Mayo Bridge used for modeling

5.2 RIDF Station

The Philippine Atmospheric Geophysical and Astronomical Services Administration (PAGASA) computed for Rainfall Intensity Duration Frequency (RIDF) values for the Davao Rain Gauge. The RIDF rainfall amount for 24 hours was converted to a synthetic storm by interpolating and re-arranging the values in such a way a certain peak value will be attained at a certain time. This station is chosen based on its proximity to the Mayo watershed. The extreme values for this watershed were computed based on a 59-year record.

Table 27. RIDF values for Davao Rain Gauge computed by PAGASA

| COMPUTED EXTREME VALUES (in mm) OF PRECIPITATION | | | | | | | | | |
|--|---------|---------|---------|-------|-------|-------|-------|--------|--------|
| T (yrs) | 10 mins | 20 mins | 30 mins | 1 hr | 2 hrs | 3 hrs | 6 hrs | 12 hrs | 24 hrs |
| 2 | 19.5 | 30 | 38.2 | 53.2 | 65.2 | 71.6 | 80.3 | 85.8 | 91.4 |
| 5 | 25.1 | 39.3 | 51 | 73.2 | 88.8 | 96.4 | 108.7 | 114.9 | 121.1 |
| 10 | 28.8 | 45.4 | 59.4 | 86.5 | 104.5 | 112.8 | 127.5 | 134.1 | 140.7 |
| 15 | 30.9 | 48.9 | 64.2 | 94 | 113.3 | 122.1 | 138.1 | 145 | 151.8 |
| 20 | 32.4 | 51.3 | 67.6 | 99.3 | 119.5 | 128.6 | 145.5 | 152.6 | 159.5 |
| 25 | 33.5 | 53.2 | 70.1 | 103.3 | 124.2 | 133.6 | 151.2 | 158.5 | 165.5 |
| 50 | 37 | 59 | 78.1 | 115.8 | 138.9 | 149 | 168.8 | 176.5 | 183.9 |
| 100 | 40.5 | 64.7 | 85.9 | 128.1 | 153.5 | 164.2 | 186.3 | 194.4 | 202.1 |

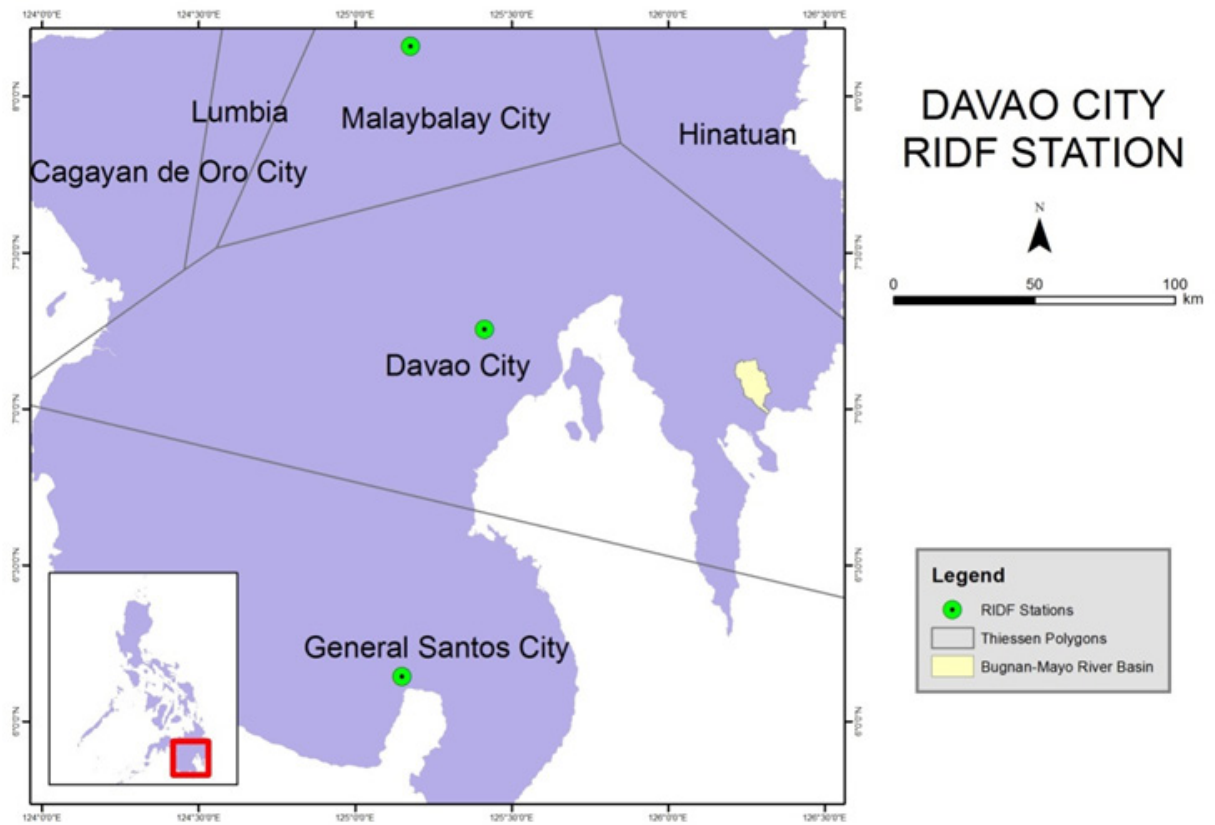


Figure 52. Location of Davao RIDF Station relative to Mayo River Basin

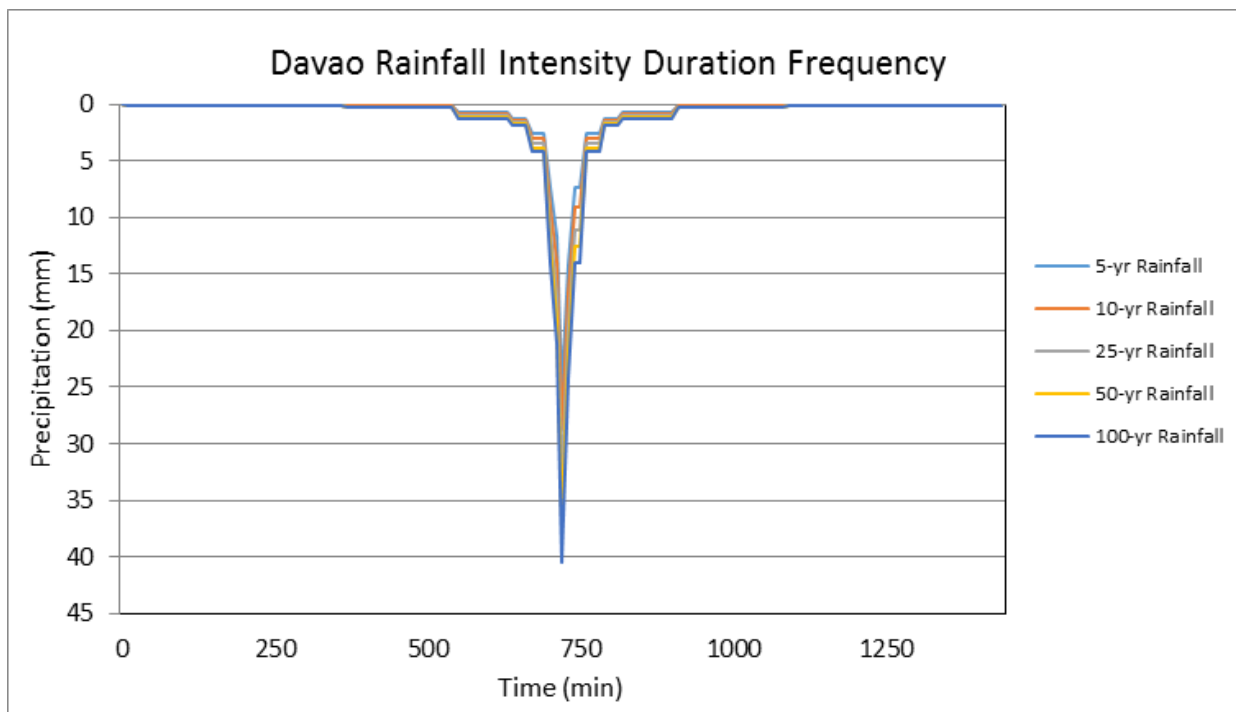


Figure 53. Synthetic storm generated for a 24-hr period rainfall for various return periods.

5.3 HMS Model

The soil dataset was generated before 2004 by the Bureau of Soils and Water Management under the Department of Agriculture (DA - BSWM). The land cover dataset is from the National Mapping and Resource information Authority (NAMRIA). The soil and land cover of the Mayo River Basin are shown in Figures 53 and Figure 54, respectively.

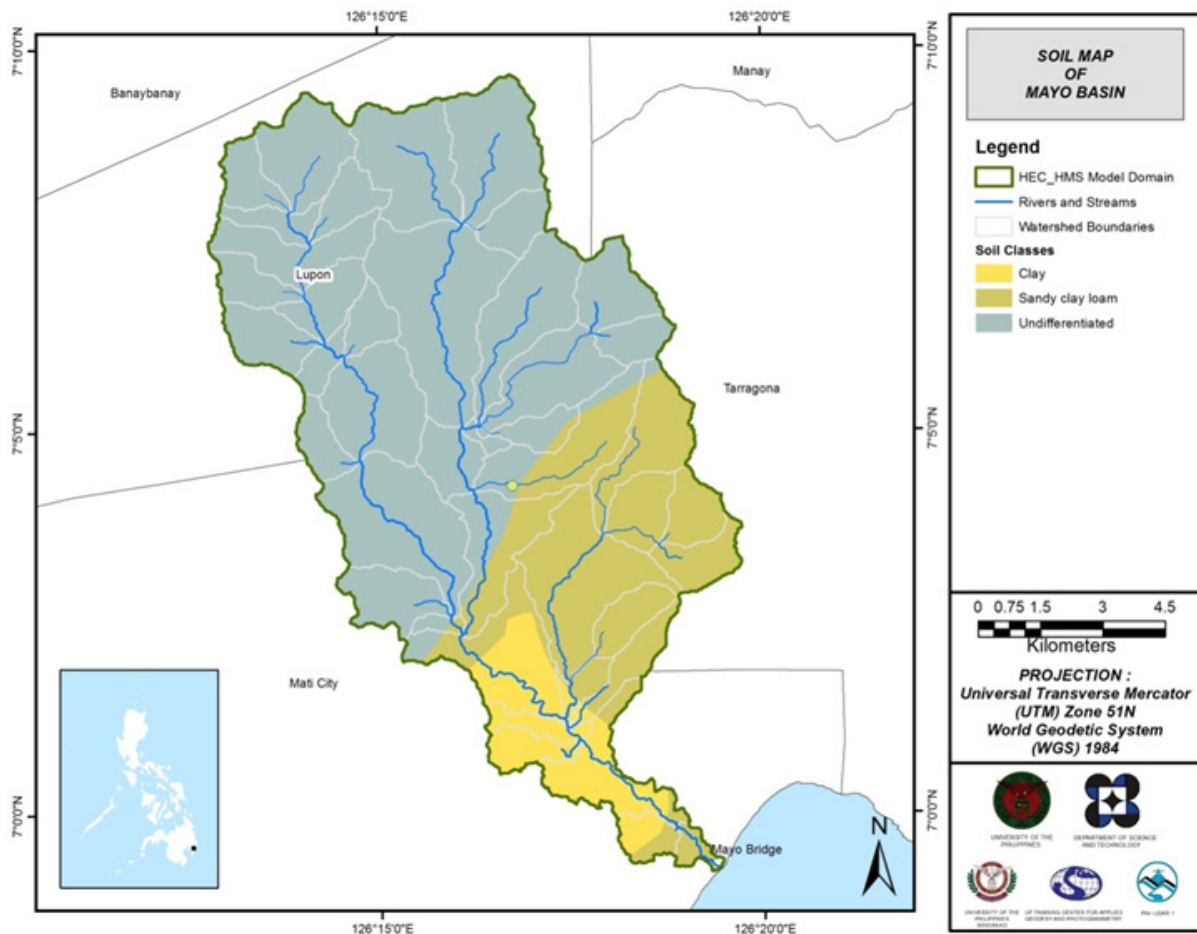


Figure 54. Soil Map of Mayo River Basin used for the estimation of the CN parameter.

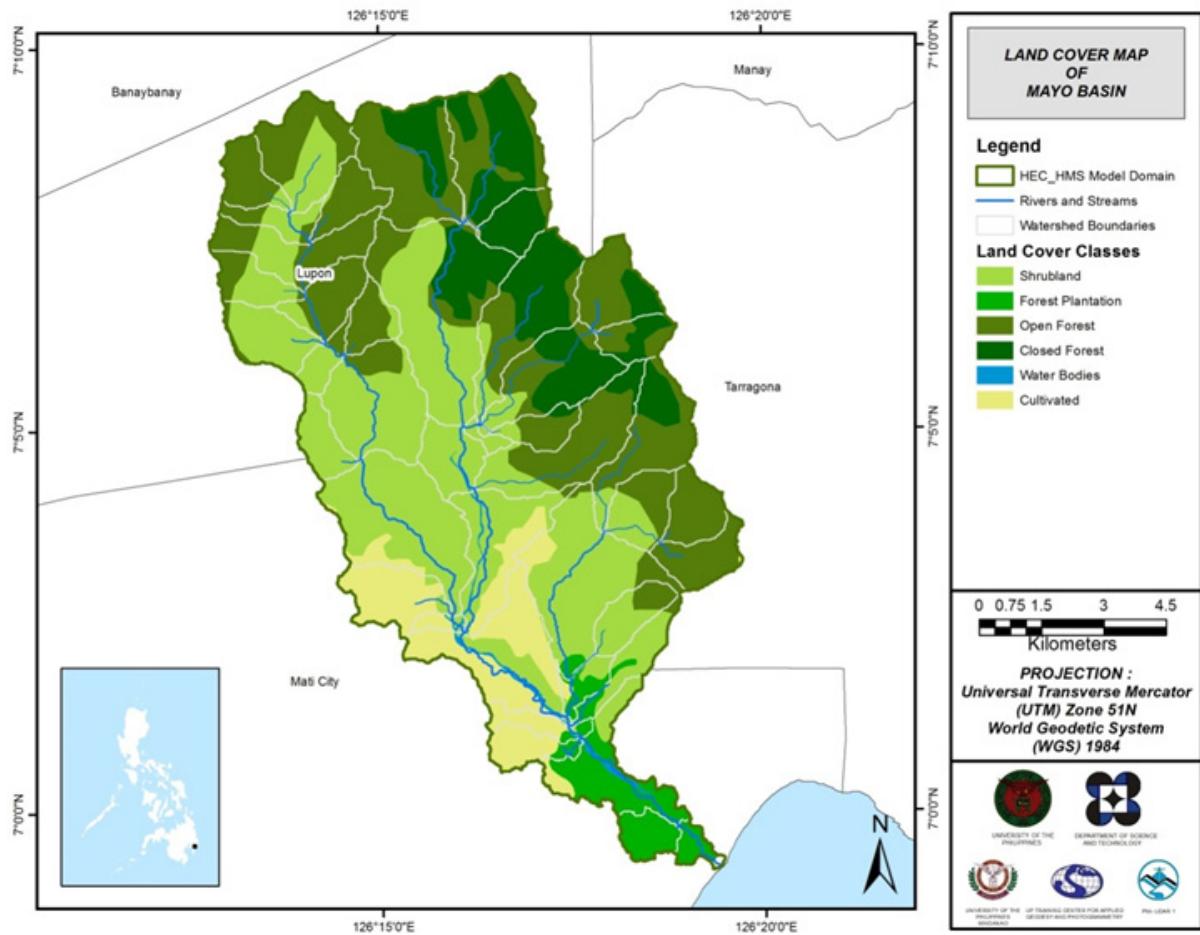


Figure 55. Land Cover Map of Mayo River Basin used for the estimation of the Curve Number (CN) and the watershed lag parameters of the rainfall-runoff model.

For Mayo, three soil classes were identified. These are clay, sandy clay loam, and undifferentiated land. Moreover, six land cover classes were identified. These are shrublands, forest plantations, open forests, closed forests, water bodies, and cultivated areas.

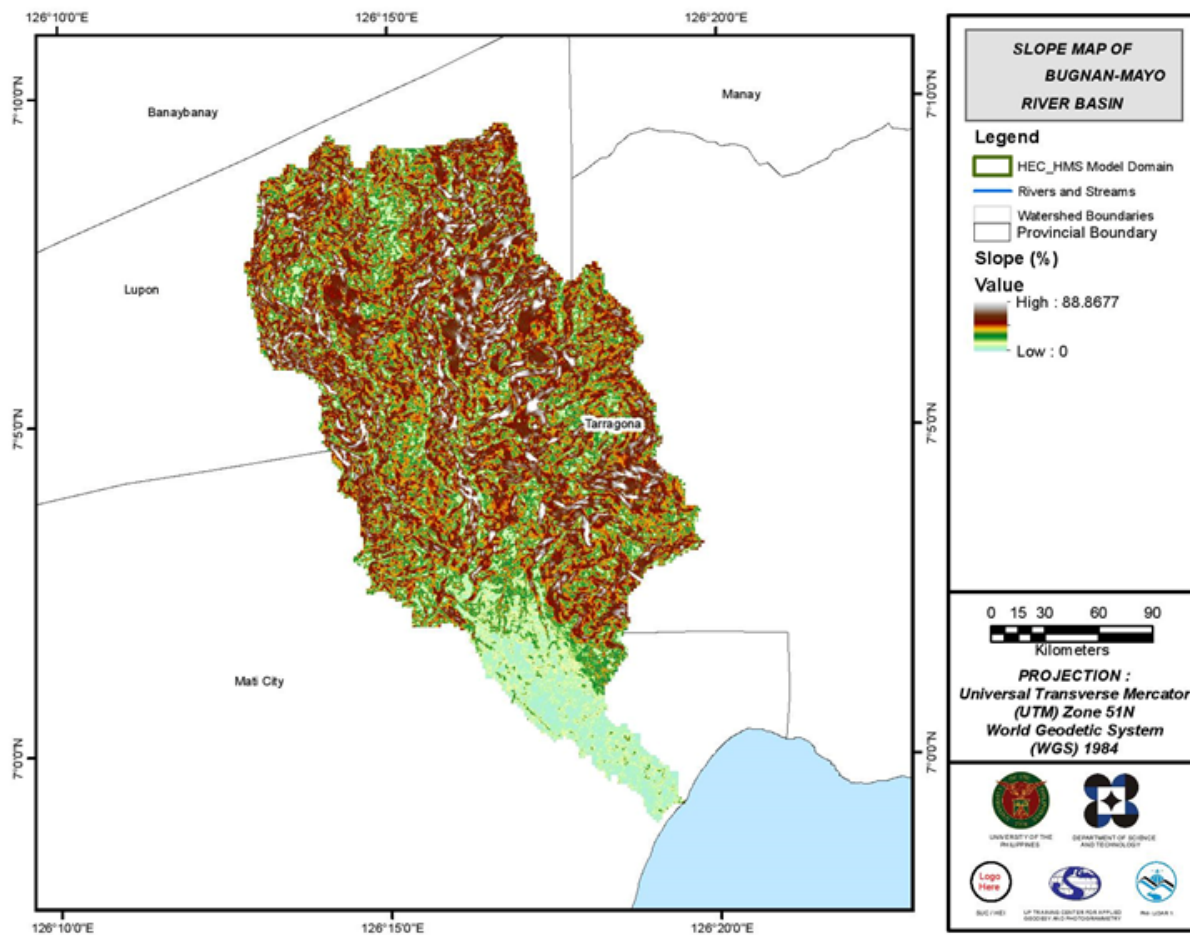


Figure 56. Slope Map of Mayo River Basin

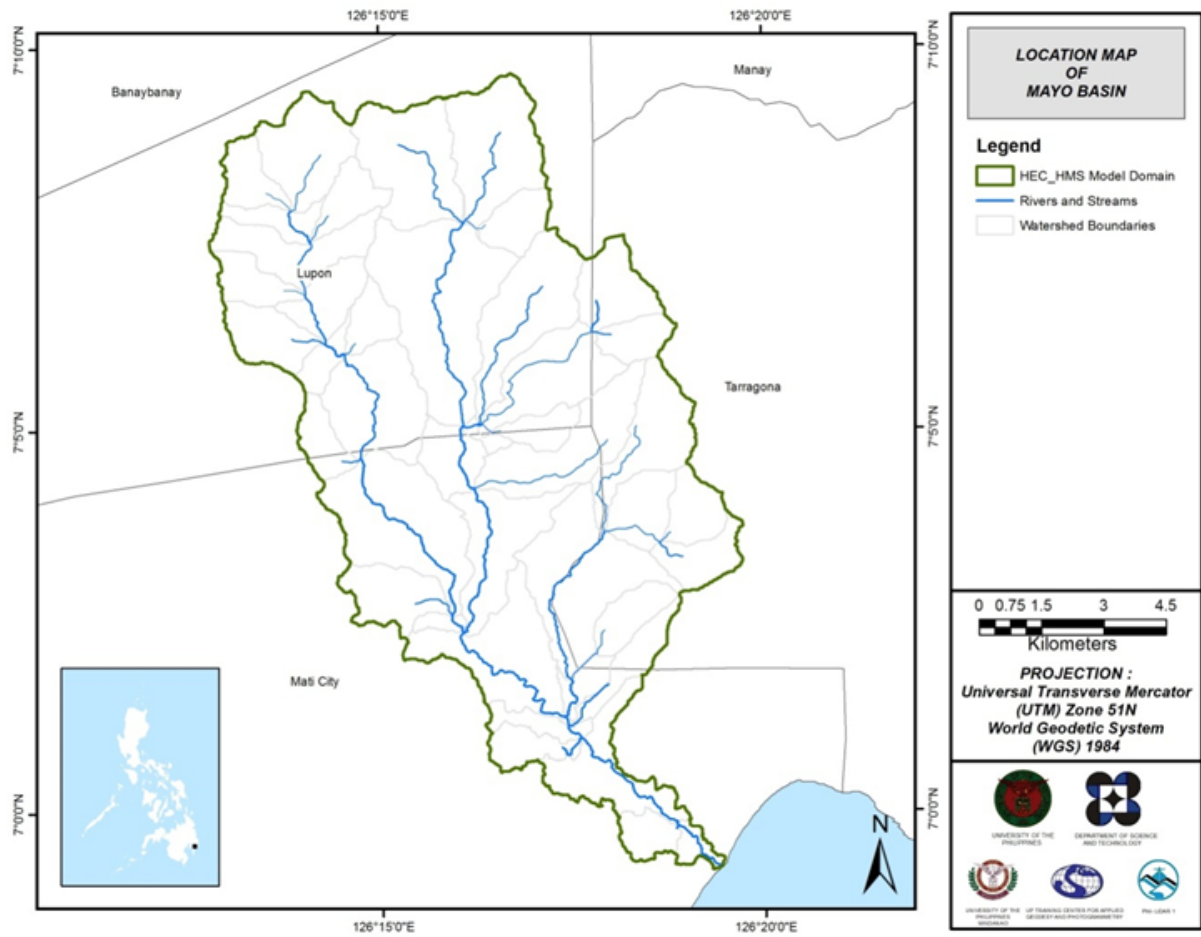


Figure 57. Stream Delineation Map of Mayo River Basin

Using the SAR-based DEM, the Mayo basin was delineated and further subdivided into subbasins. The model consists of 45 sub basins, 22 reaches, and 22 junctions, as shown in Figure 58. The main outlet is at Mayo Bridge.

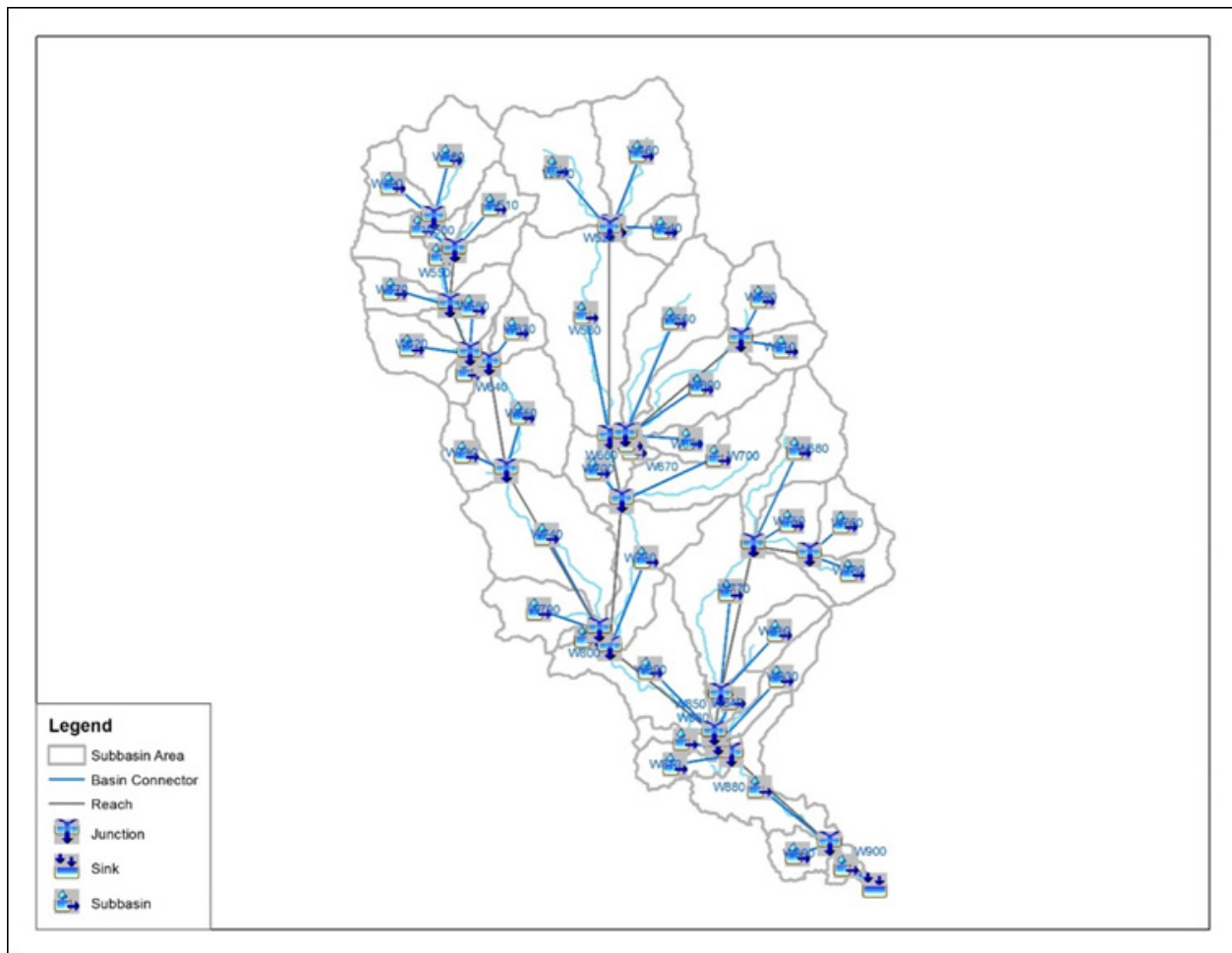


Figure 58. Mayo River Basin model generated in HEC-HMS

5.4 Cross-section Data

Riverbed cross-sections of the watershed are crucial in the HEC-RAS model setup. The cross-section data for the HEC-RAS model was derived using the LiDAR DEM data. It was defined using the Arc GeoRAS tool and was post-processed in ArcGIS.

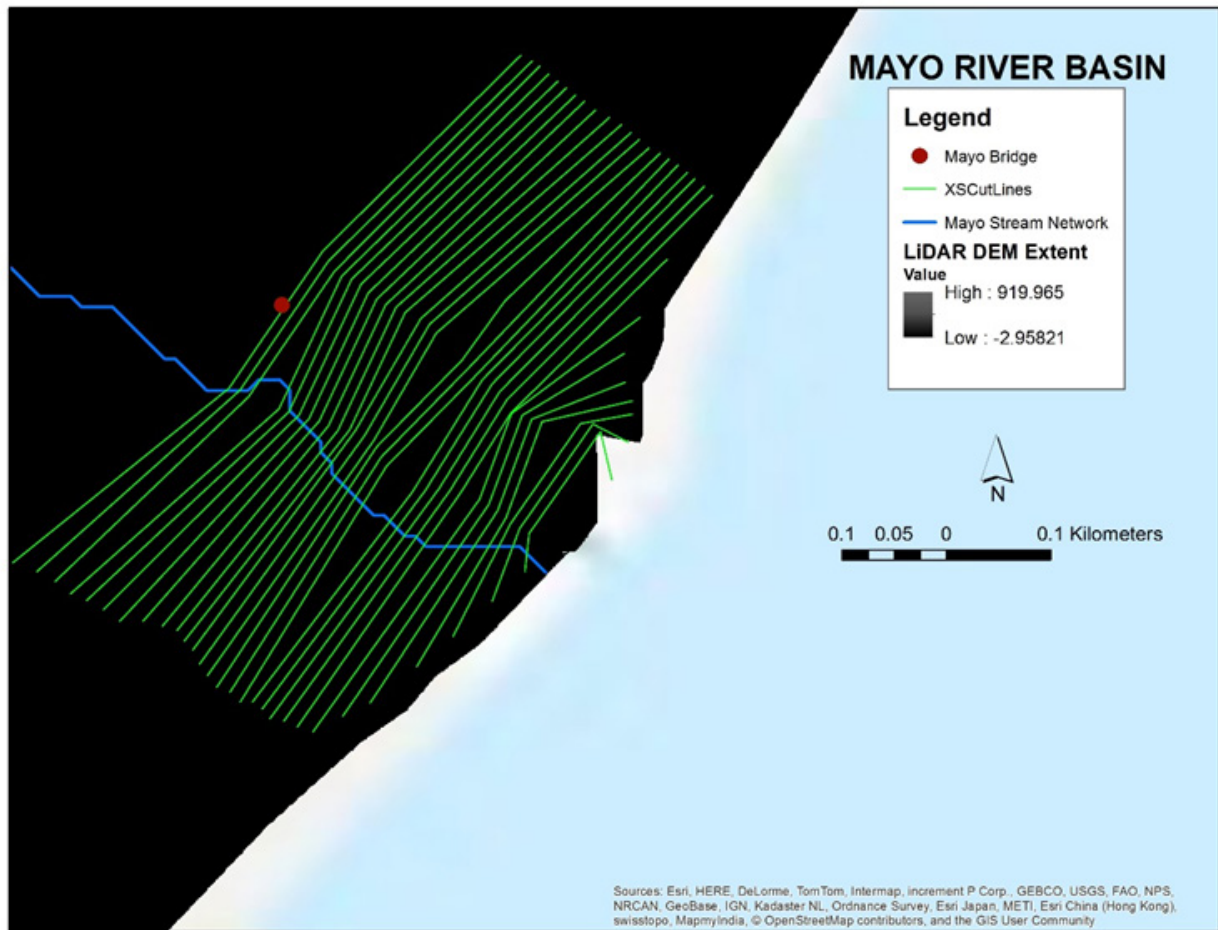


Figure 59. River cross-section of Mayo River generated through Arcmap HEC GeoRAS tool

5.5 Flo 2D Model

The automated modeling process allows for the creation of a model with boundaries that are almost exactly coincidental with that of the catchment area. As such, they have approximately the same land area and location. The entire area is divided into square grid elements, 10 meter by 10 meter in size. Each element is assigned a unique grid element number which serves as its identifier, then attributed with the parameters required for modelling such as x-and y-coordinate of centroid, names of adjacent grid elements, Manning coefficient of roughness, infiltration, and elevation value. The elements are arranged spatially to form the model, allowing the software to simulate the flow of water across the grid elements and in eight directions (north, south, east, west, northeast, northwest, southeast, southwest).

Based on the elevation and flow direction, it is seen that the water will generally flow from the northwest of the model to the southeast, following the main channel. As such, boundary elements northwest of the model are assigned as outflow elements.

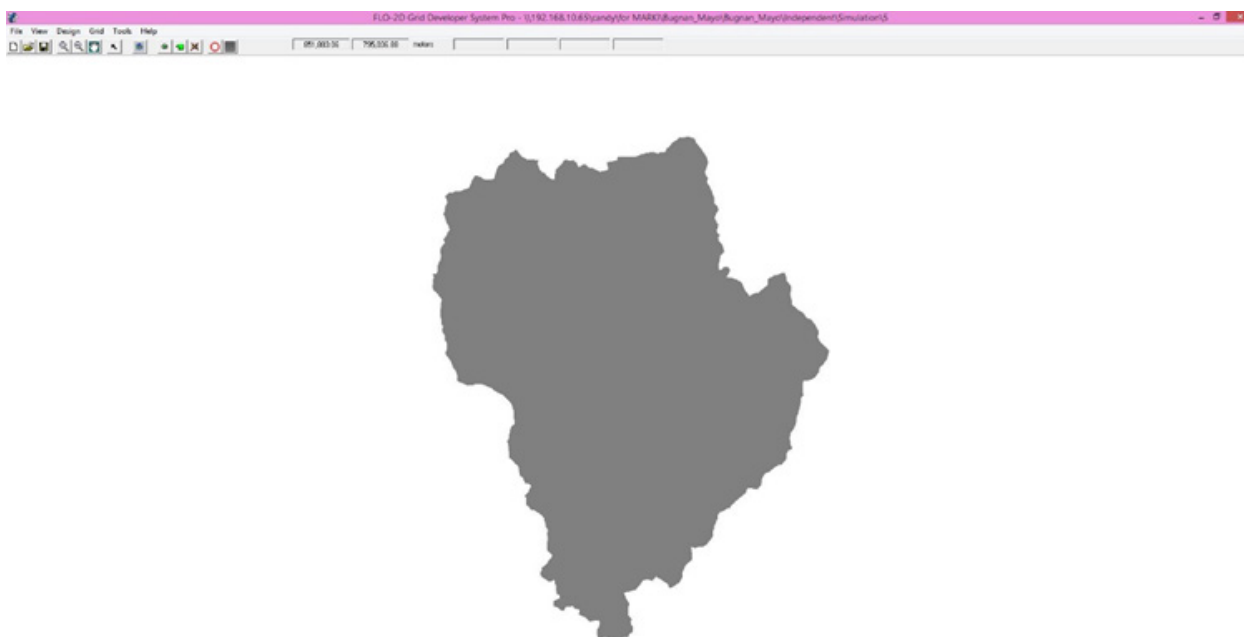


Figure 60. Screenshot of the river sub-catchment with the computational area to be modeled in FLO-2D Grid Developer System Pro (FLO-2D GDS Pro)

The simulation is then run through FLO-2D GDS Pro. This particular model had a computer run time of 23.81 hours. After the simulation, FLO-2D Mapper Pro is used to transform the simulation results into spatial data that shows flood hazard levels, as well as the extent and inundation of the flood. Assigning the appropriate flood depth and velocity values for Low, Medium, and High creates the following food hazard map. Most of the default values given by FLO-2D Mapper Pro are used, except for those in the Low hazard level. For this particular level, the minimum h (Maximum depth) is set at 0.2 m while the minimum vh (Product of maximum velocity (v) times maximum depth (h)) is set at 0 m²/s. The generated hazard maps for Mayo are in Figures 64, 66, and 68.

The creation of a flood hazard map from the model also automatically creates a flow depth map depicting the maximum amount of inundation for every grid element. The legend used by default in Flo-2D Mapper is not a good representation of the range of flood inundation values, so a different legend is used for the layout. In this particular model, the inundated parts cover a maximum land area of 63,728,800.00 m². The generated flood depth maps for Mayo are in Figures 65, 67, and 69.

There is a total of 61,013,245.56 m³ of water entering the model, of which 27,602,867.63 m³ is due to rainfall and 33,410,377.93 m³ is inflow from basins upstream. 3,929,004.00 m³ of this water is lost to infiltration and interception, while 1,941,097.02 m³ is stored by the flood plain. The rest, amounting up 55,143,145.00 m³, is outflow.

5.6 Results of HMS Calibration

After calibrating the Mayo HEC-HMS river basin model, its accuracy was measured against the observed values. Figure 61 shows the comparison between the two discharge data.

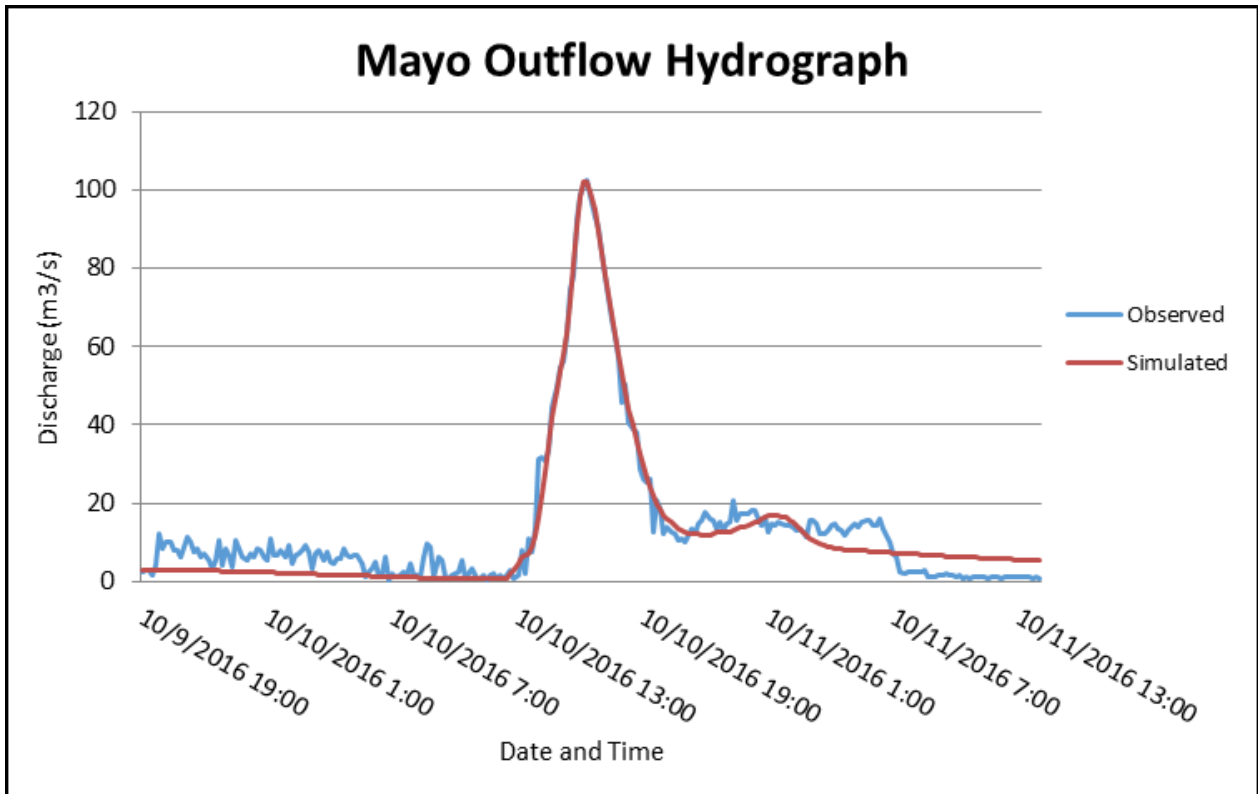


Figure 61. Outflow hydrograph of Balamban produced by the HEC-HMS model compared with observed outflow

Enumerated in Table 28 are the adjusted ranges of values of the parameters used in calibrating the model.

Table 28. Range of calibrated values for the Mayo River Basin.

| Hydrologic Element | Calculation Type | Method | Parameter | Range of Calibrated Values |
|--------------------|------------------|-----------------------|----------------------------|----------------------------|
| Basin | Loss | SCS Curve number | Initial Abstraction (mm) | 0.097 – 30.053 |
| | | | Curve Number | 35.285 – 99 |
| | Transform | Clark Unit Hydrograph | Time of Concentration (hr) | 0.0167 – 0.165 |
| | | | Storage Coefficient (hr) | 0.0167 – 96.127 |
| | Baseflow | Recession | Recession Constant | 0.00008 – 0.028 |
| Ratio to Peak | | | 0.00013 – 0.0645 | |
| Reach | Routing | Muskingum-Cunge | Manning's Coefficient | 0.053 |

Initial abstraction defines the amount of precipitation that must fall before surface runoff. The magnitude of the outflow hydrograph increases as initial abstraction decreases. The range of values from 0.097 mm to 30.053 mm means that there is a small initial fraction of the storm depth after which runoff begins, increasing the river outflow.

The curve number is the estimate of the precipitation excess of soil cover, land use, and antecedent moisture. The magnitude of the outflow hydrograph increases as curve number increases. The range of 65 to 90 for curve number is advisable for Philippine watersheds depending on the soil and land cover of the area (M. Horritt, personal communication, 2012). For Mayo, the basin consists mainly of shrublands and open forests and the soil consists of mostly undifferentiated land and sandy clay loam.

Time of concentration and storage coefficient are the travel time and index of temporary storage of runoff in a watershed. The range of calibrated values from 0.0167 hours to 96.127 hours determines the reaction time of the model with respect to the rainfall. The peak magnitude of the hydrograph also decreases when these parameters are increased.

Recession constant is the rate at which baseflow recedes between storm events and ratio to peak is the ratio of the baseflow discharge to the peak discharge. Recession constant values within the range of 0.00013 to 0.028 indicate that the basin is likely to quickly go back to its original discharge. Values of ratio to peak within the range of 0.00013 to 0.0645 indicate a much steeper receding limb of the outflow hydrograph.

Manning’s roughness coefficients correspond to the common roughness of Philippine watersheds. Mayo river basin reaches’ Manning’s coefficient is 0.053, showing that the catchment is mostly filled with floodplains with light brushlands (Brunner, 2010).

Table 29. Summary of the Efficiency Test of the Balamban HMS Model

| Accuracy measure | Value |
|------------------|-------|
| RMSE | 4.2 |
| r2 | 0.962 |
| NSE | 0.96 |
| PBIAS | 9.31 |
| RSR | 0.21 |

The Root Mean Square Error (RMSE) method aggregates the individual differences of these two measurements. It was computed as 4.2 m³/s.

The Pearson correlation coefficient (r²) assesses the strength of the linear relationship between the observations and the model. This value being close to 1 corresponds to an almost perfect match of the observed discharge and the resulting discharge from the HEC HMS model. Here, it measured 0.962.

The Nash-Sutcliffe (E) method was also used to assess the predictive power of the model. Here the optimal value is 1. The model attained an efficiency coefficient of 0.96.

A positive Percent Bias (PBIAS) indicates a model’s propensity towards under-prediction. Negative values indicate bias towards over-prediction. Again, the optimal value is 0. In the model, the PBIAS is 9.31.

The Observation Standard Deviation Ratio, RSR, is an error index. A perfect model attains a value of 0 when the error in the units of the valuable a quantified. The model has an RSR value of 0.21.

5.7 Calculated outflow hydrographs and discharge values for different rainfall return periods

5.7.1 Hydrograph using the Rainfall Runoff Model

The summary graph (Figure 62) shows the Mayo outflow using the Davao Rainfall Intensity-Duration-Frequency curves (RIDF) in 5 different return periods (5-year, 10-year, 25-year, 50-year, and 100-year rainfall time series) based on the Philippine Atmospheric Geophysical and Astronomical Services Administration (PAGASA) data. The simulation results reveal significant increase in outflow magnitude as the rainfall intensity increases for a range of durations and return periods.

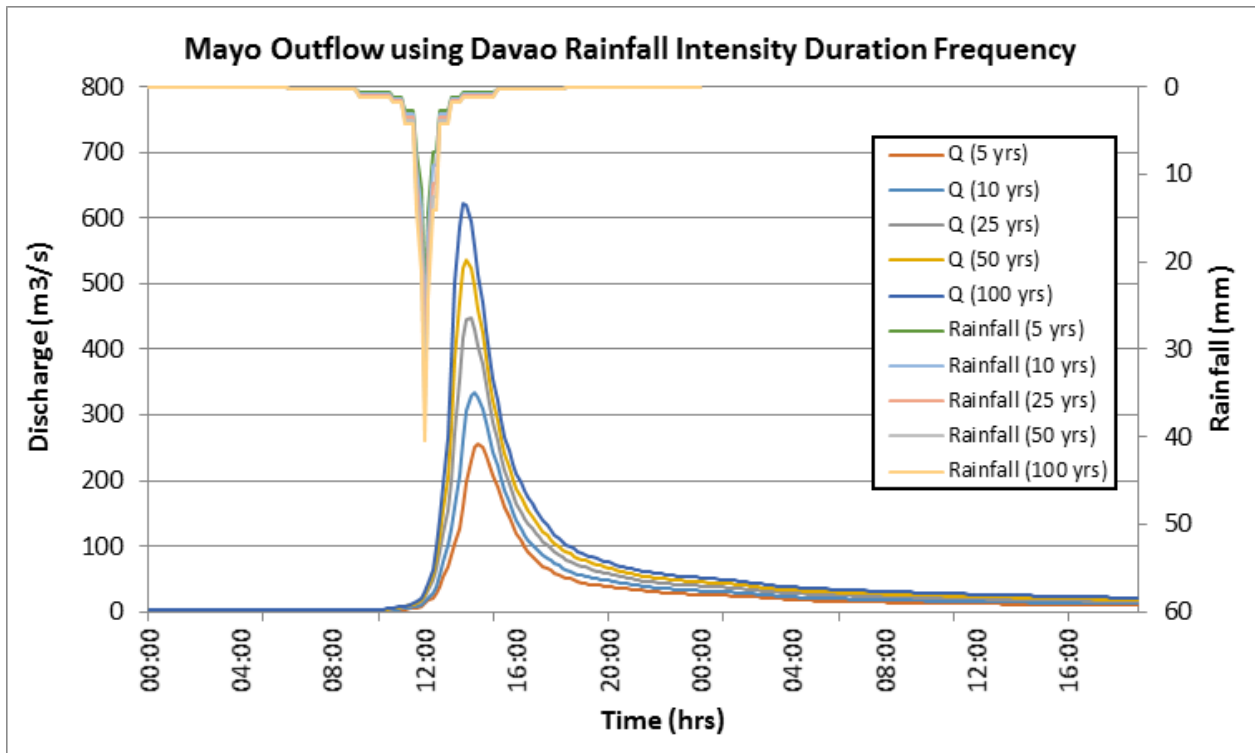


Figure 62. Outflow hydrograph at Mayo Station generated using the Davao RIDF simulated in HEC-HMS.

A summary of the total precipitation, peak rainfall, peak outflow and time to peak of the Mayo discharge using the Davao Rainfall Intensity-Duration-Frequency curves (RIDF) in five different return periods is shown in Table 30.

Table 30. Peak values of the Mayo HEC-HMS Model outflow using the Davao RIDF 24-hour values.

| RIDF Period | Total Precipitation (mm) | Peak rainfall (mm) | Peak outflow (m ³ /s) | Time to Peak |
|-------------|--------------------------|--------------------|----------------------------------|---------------------|
| 5-Year | 121.1 | 25.1 | 255.5 | 2 hours, 20 minutes |
| 10-Year | 140.7 | 28.8 | 335.3 | 2 hours, 10 minutes |
| 25-Year | 165.5 | 33.5 | 447.6 | 2 hours |
| 50-Year | 183.9 | 37 | 536.1 | 1 hour, 50 minutes |
| 100-Year | 202.1 | 40.5 | 623.3 | 1 hour, 40 minutes |

5.8 River Analysis (RAS) Model Simulation

The HEC-RAS Flood Model produced a simulated water level at every cross section for every time step for every flood simulation created. The resulting model will be used in determining the flooded areas within the model. The simulated model will be an integral part in determining real-time flood inundation extent of the river after it has been automated and uploaded on the DREAM website. For this publication, only a sample output map river was to be shown. The sample generated map of Balamban River using the calibrated HMS event flow is shown in Figure 60.

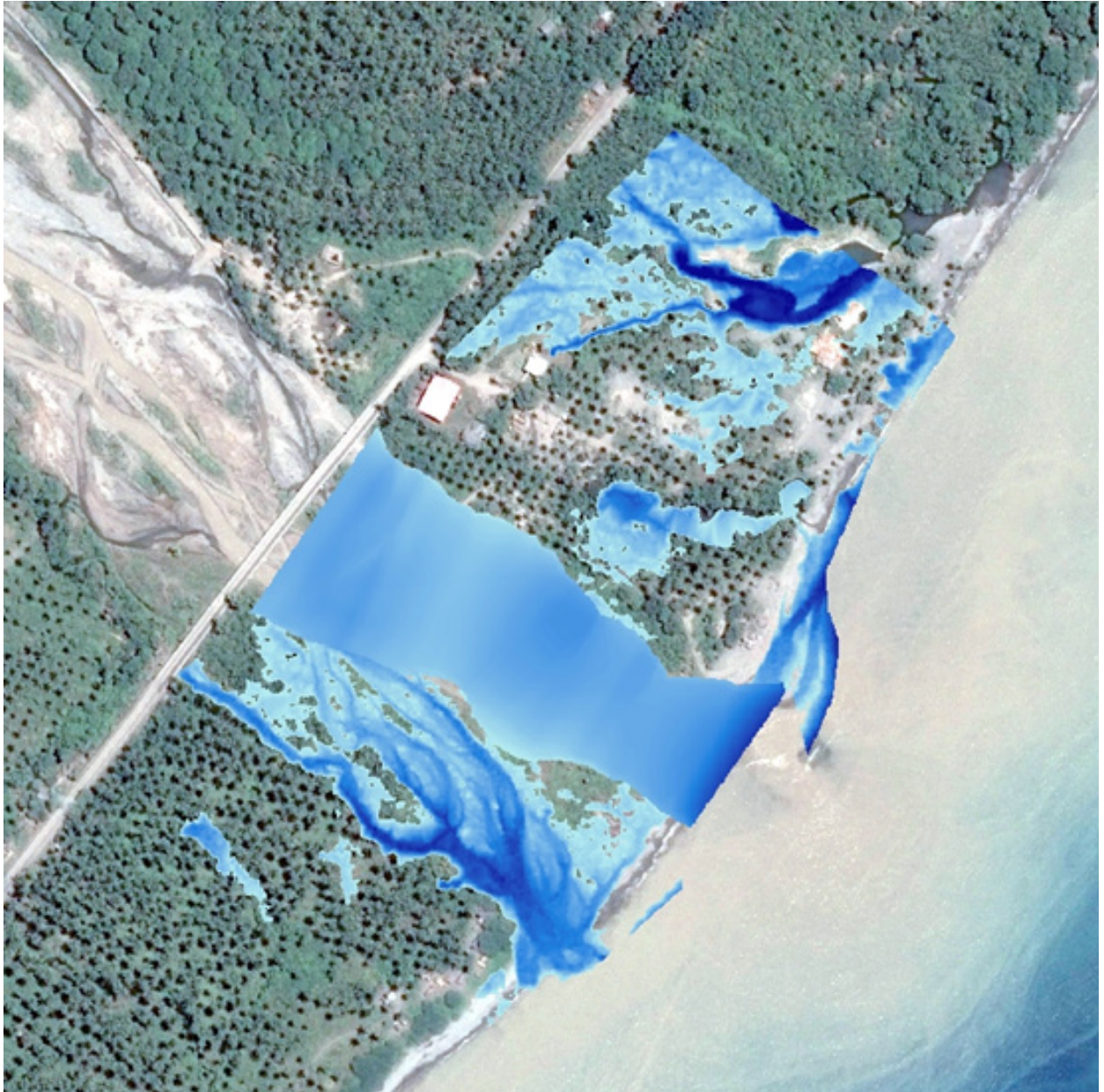


Figure 63. Sample output map of Mayo RAS Model

5.9 Flow Depth and Flood Hazard

The resulting hazard and flow depth maps have a 10m resolution. The 100-, 25-, and 5-year rain return scenarios of the Mayo floodplain are shown in Figures 15 to 20. The floodplain, with an area of 63.73 sq. km., covers two municipalities. Table 31 shows the percentage of area affected by flooding per municipality.

Table 31. Municipalities affected in Mayo Floodplain

| Province | Municipality | Total Area | Area Flooded | % Flooded |
|----------------|--------------|------------|--------------|-----------|
| Davao Oriental | Mati City | 797.382 | 40.2854 | 5.05% |
| Davao Oriental | Tarragona | 277.904 | 23.4413 | 8.44% |

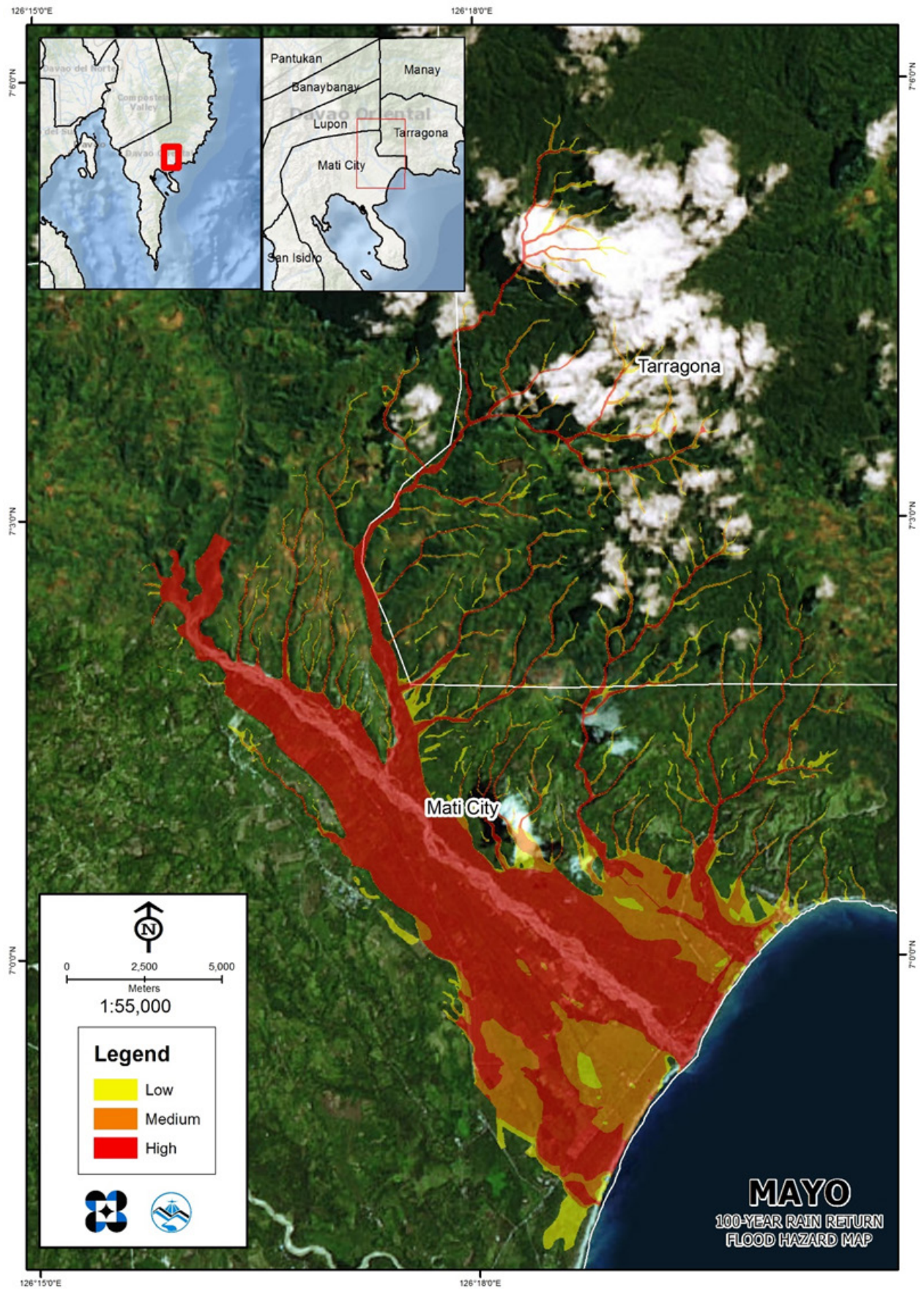


Figure 64. 100-year Flood Hazard Map for Mayo Floodplain overlaid on Google Earth imagery

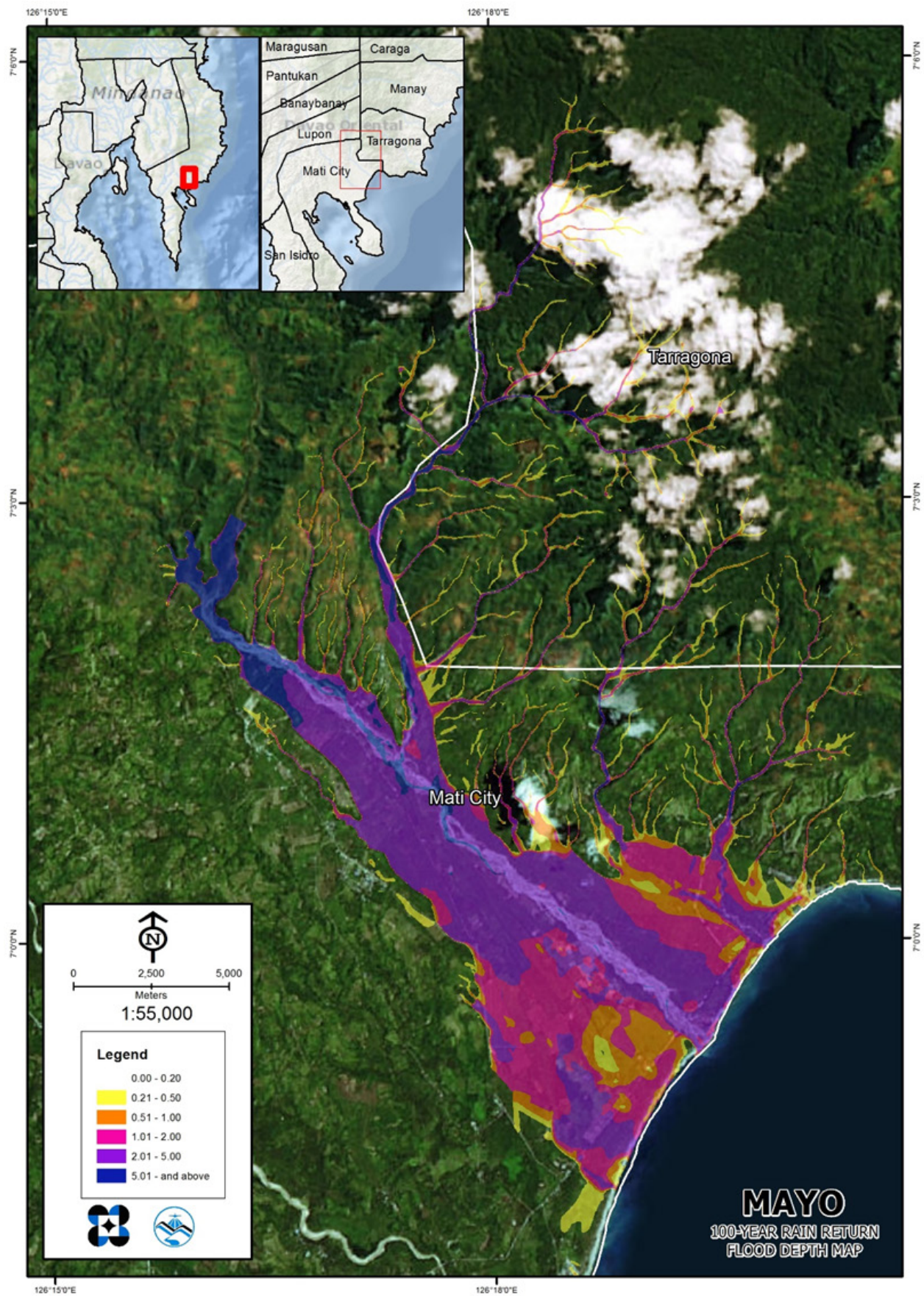


Figure 65. 100-year Flow Depth Map for Mayo Floodplain overlaid on Google Earth imagery

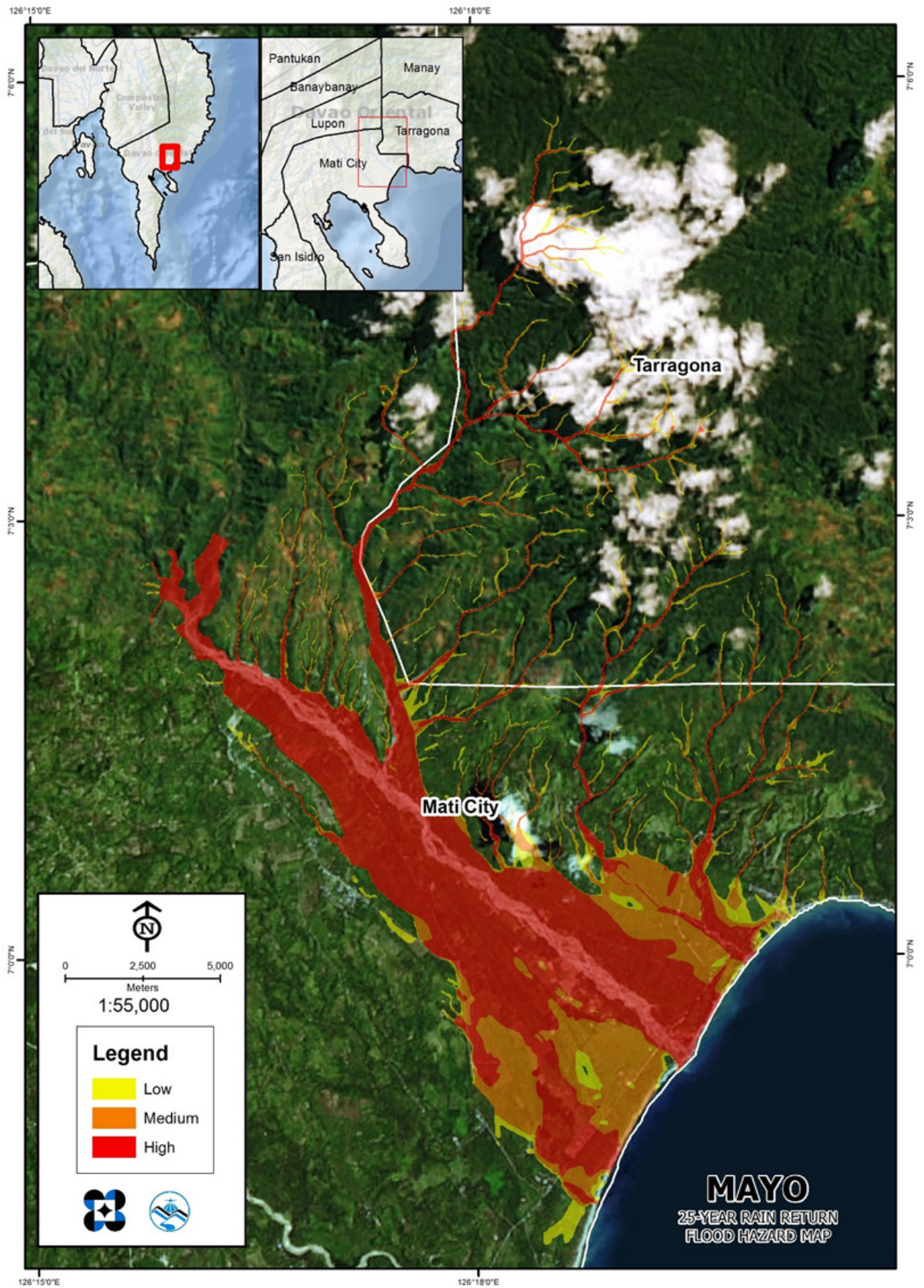


Figure 66. 25-year Flood Hazard Map for Mayo Floodplain overlaid on Google Earth imagery

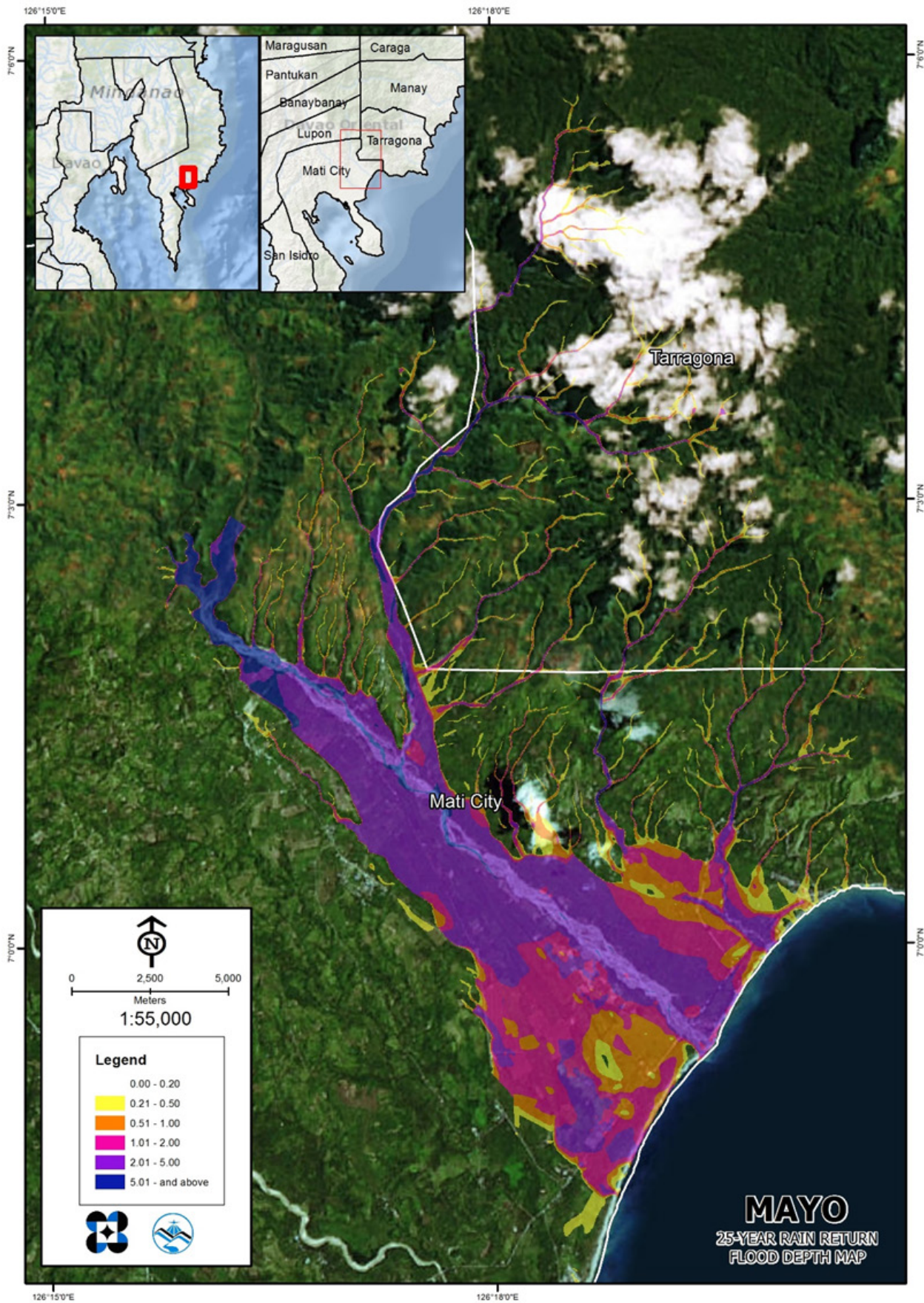


Figure 67. 25-year Flow Depth Map for Mayo Floodplain overlaid on Google Earth imagery

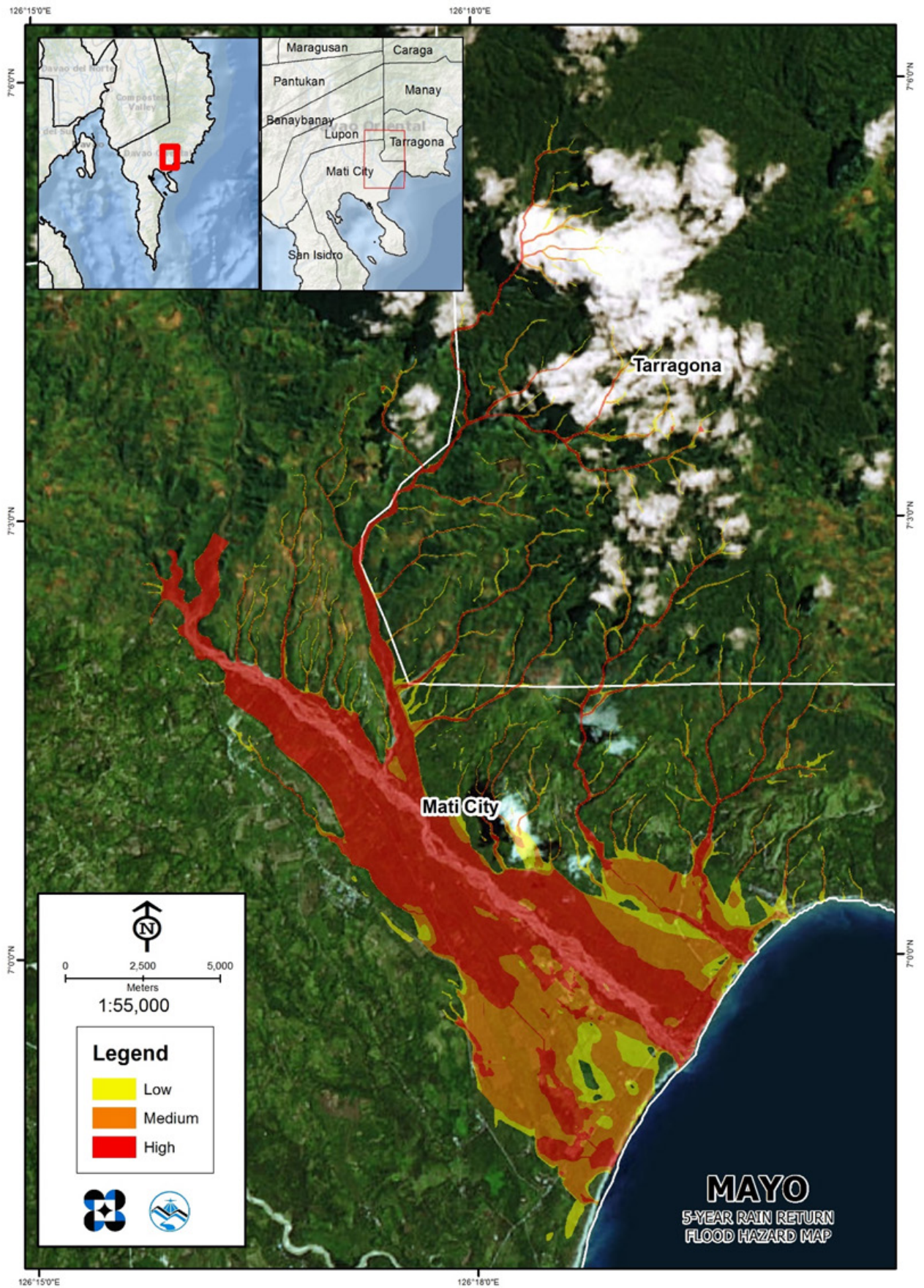


Figure 68. 5-year Flood Hazard Map for Mayo Floodplain overlaid on Google Earth imagery

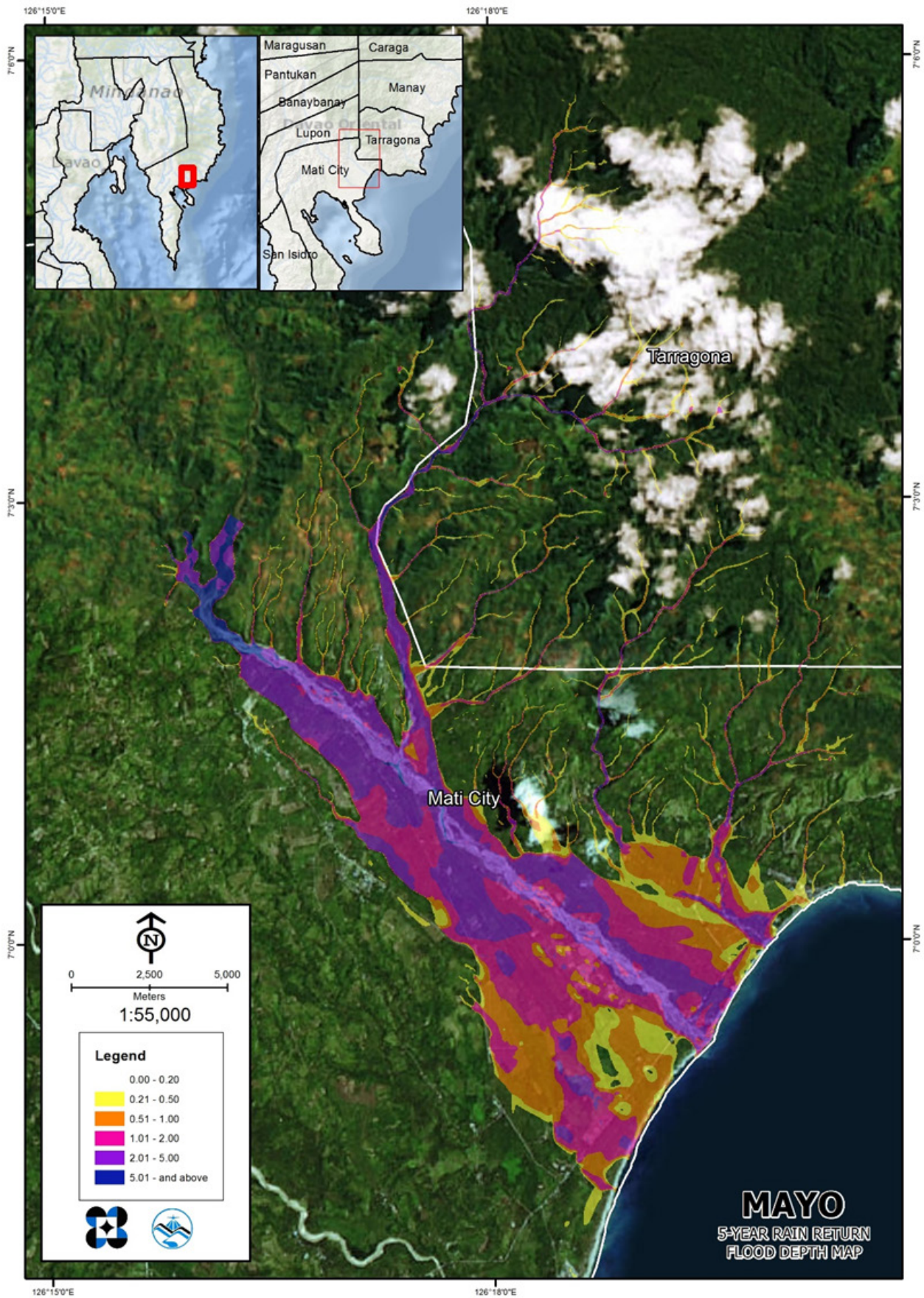


Figure 69. 5-year Flood Depth Map for Mayo Floodplain overlaid on Google Earth imagery

5.10 Inventory of Areas Exposed to Flooding

Affected barangays in Mayo river basin, grouped by municipality, are listed below. For the said basin, two municipalities consisting of seven barangays are expected to experience flooding when subjected to 5-yr rainfall return period.

For the 5-year return period, 2.82% of the municipality of Mati City with an area of 797.38 sq. km. will experience flood levels of less than 0.20 meters. 0.29% of the area will experience flood levels of 0.21 to 0.50 meters while 0.47%, 0.67%, 0.75%, and 0.06% of the area will experience flood depths of 0.51 to 1 meter, 1.01 to 2 meters, 2.01 to 5 meters, and more than 5 meters, respectively. Listed in Table 32 and shown in Figure 70 are the affected areas in square kilometers by flood depth per barangay.

Table 32. Affected areas in Mati City, Davao Oriental during a 5-Year Rainfall Return Period

| Affected area (sq. km.) by flood depth (in m.) | Area of affected barangays in Mati City (in sq. km.) | | | |
|--|--|--------------------|-------|-----------|
| | Don Enrique Lopez | Don Salvador Lopez | Mayo | Tagabakid |
| 0.03-0.20 | 3.66 | 7.12 | 5.45 | 6.25 |
| 0.21-0.50 | 0.87 | 0.22 | 0.88 | 0.35 |
| 0.51-1.00 | 2 | 0.15 | 1.43 | 0.16 |
| 1.01-2.00 | 3.29 | 0.16 | 1.79 | 0.097 |
| 2.01-5.00 | 3.22 | 0.53 | 2.17 | 0.041 |
| > 5.00 | 0.043 | 0.39 | 0.024 | 0.0017 |

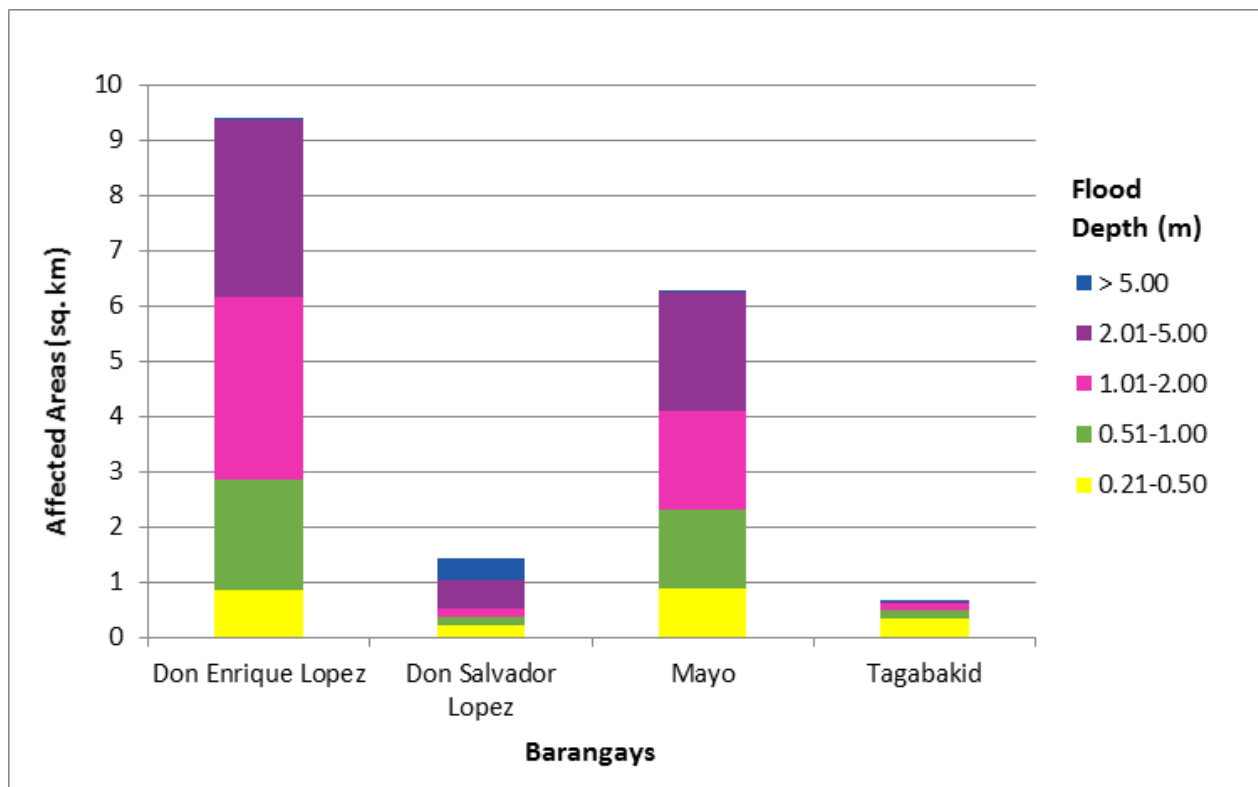


Figure 70. Affected Areas in Mati City, Davao Oriental during 5-Year Rainfall Return Period

For the 5-year return period, 7.83% of the municipality of Tarragona with an area of 277.904 sq. km. will experience flood levels of less than 0.20 meters. 0.33% of the area will experience flood levels of 0.21 to 0.50 meters while 0.12%, 0.07%, 0.06%, and 0.02% of the area will experience flood depths of 0.51 to 1 meter, 1.01 to 2 meters, 2.01 to 5 meters, and more than 5 meters, respectively. Listed in Table 33 and shown in Figure 71 are the affected areas in square kilometers by flood depth per barangay.

Table 33. Affected areas in Tarragona, Davao Oriental during a 5-Year Rainfall Return Period

| Affected area (sq. km.) by flood depth (in m.) | Area of affected barangays in Tarragona (in sq. km.) | | |
|--|--|-------|--------|
| | Dadong | Limot | Ompao |
| 0.03-0.20 | 0.38 | 19.19 | 2.18 |
| 0.21-0.50 | 0.0095 | 0.84 | 0.078 |
| 0.51-1.00 | 0.0016 | 0.31 | 0.025 |
| 1.01-2.00 | 0 | 0.19 | 0.01 |
| 2.01-5.00 | 0 | 0.17 | 0.0004 |
| > 5.00 | 0 | 0.047 | 0 |

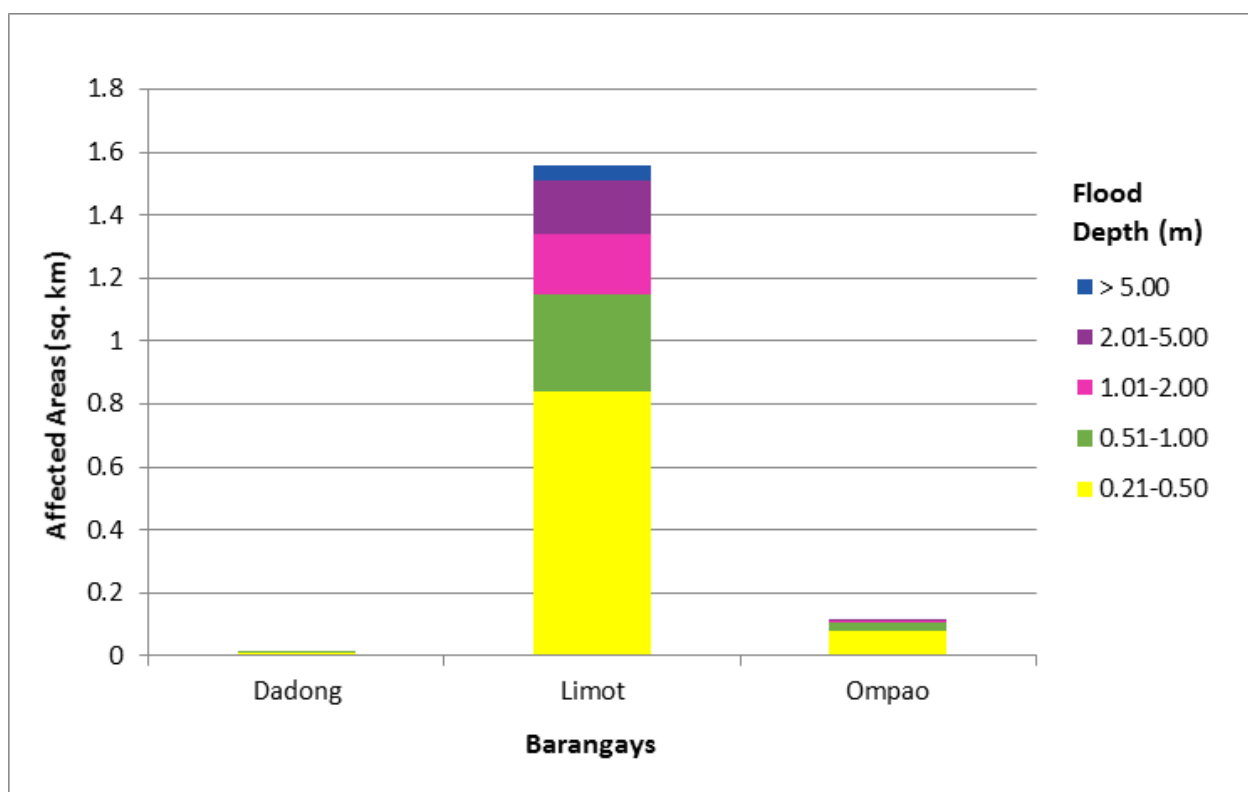


Figure 71. Affected Areas in Tarragona, Davao Oriental during 5-Year Rainfall Return Period

For the 25-year return period, 1.81% of the municipality of Mati City with an area of 797.38 sq. km. will experience flood levels of less than 0.20 meters. 0.19% of the area will experience flood levels of 0.21 to 0.50 meters while 0.31%, 0.57%, 1.04%, and 0.05% of the area will experience flood depths of 0.51 to 1 meter, 1.01 to 2 meters, 2.01 to 5 meters, and more than 5 meters, respectively. Listed in the Table 34 and shown in Figure 72 are the affected areas in square kilometers by flood depth per barangay.

Table 34. Affected areas in Mati City, Davao Oriental during a 25-Year Rainfall Return Period

| Affected area (sq. km.) by flood depth (in m.) | Area of affected barangays in Mati City (in sq. km.) | | | |
|--|--|--------------------|-------|-----------|
| | Don Enrique Lopez | Don Salvador Lopez | Mayo | Tagabakid |
| 0.03-0.20 | 3.24 | 0 | 5.13 | 6.1 |
| 0.21-0.50 | 0.52 | 0 | 0.63 | 0.4 |
| 0.51-1.00 | 1.22 | 0 | 1.04 | 0.18 |
| 1.01-2.00 | 2.87 | 0 | 1.57 | 0.13 |
| 2.01-5.00 | 4.91 | 0 | 3.29 | 0.081 |
| > 5.00 | 0.32 | 0 | 0.093 | 0.0083 |

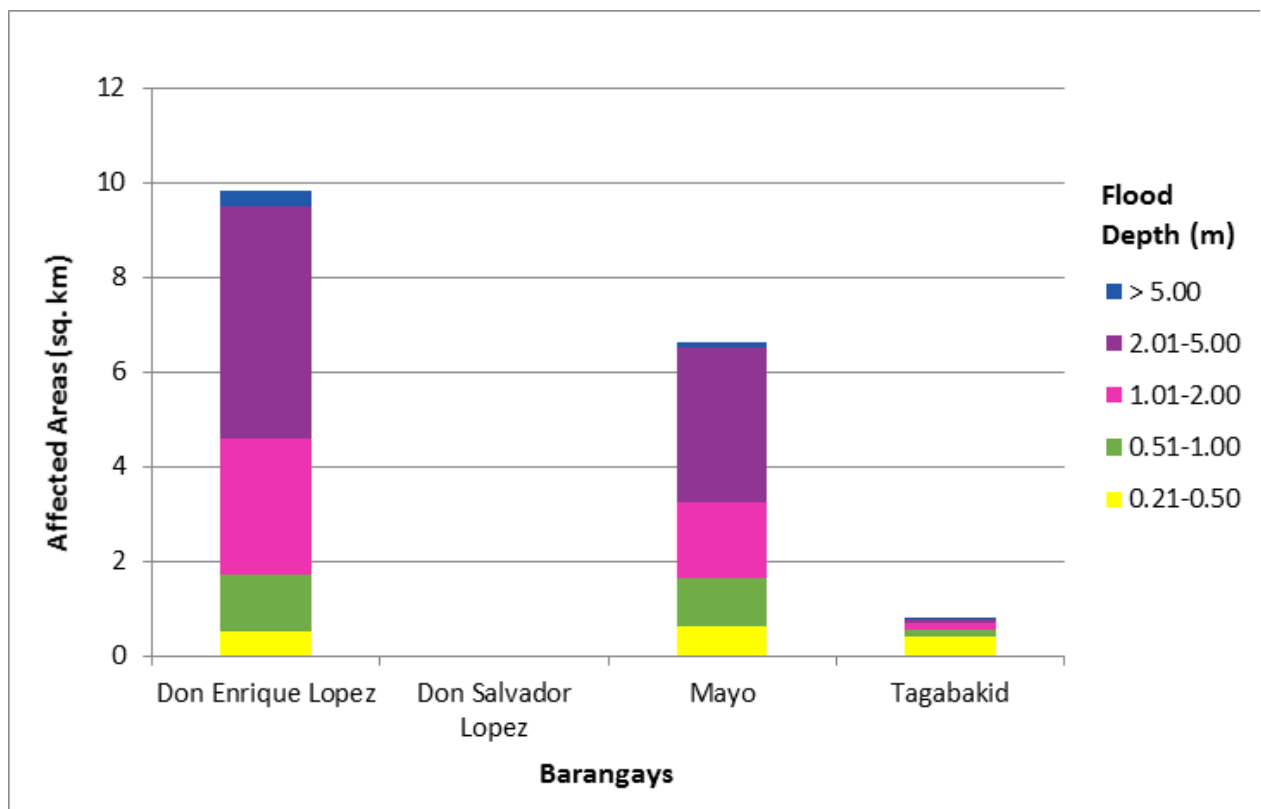


Figure 72. Affected Areas in Mati City, Davao Oriental during 25-Year Rainfall Return Period

For the 25-year return period, 7.67% of the municipality of Tarragona with an area of 277.904 sq. km. will experience flood levels of less than 0.20 meters. 0.40% of the area will experience flood levels of 0.21 to 0.50 meters while 0.15%, 0.09%, 0.08%, and 0.04% of the area will experience flood depths of 0.51 to 1 meter, 1.01 to 2 meters, 2.01 to 5 meters, and more than 5 meters, respectively. Listed in Table 35 and shown in Figure 73 are the affected areas in square kilometers by flood depth per barangay.

Table 35. Affected areas in Tarragona, Davao Oriental during a 25-Year Rainfall Return Period

| Affected area (sq. km.) by flood depth (in m.) | Area of affected barangays in Tarragona (in sq. km.) | | |
|--|--|-------|-------|
| | Dadong | Limot | Ompao |
| 0.03-0.20 | 0.37 | 18.81 | 2.14 |
| 0.21-0.50 | 0.014 | 1 | 0.095 |
| 0.51-1.00 | 0.0023 | 0.38 | 0.034 |
| 1.01-2.00 | 0 | 0.24 | 0.013 |
| 2.01-5.00 | 0 | 0.23 | 0.005 |
| > 5.00 | 0 | 0.099 | 0 |

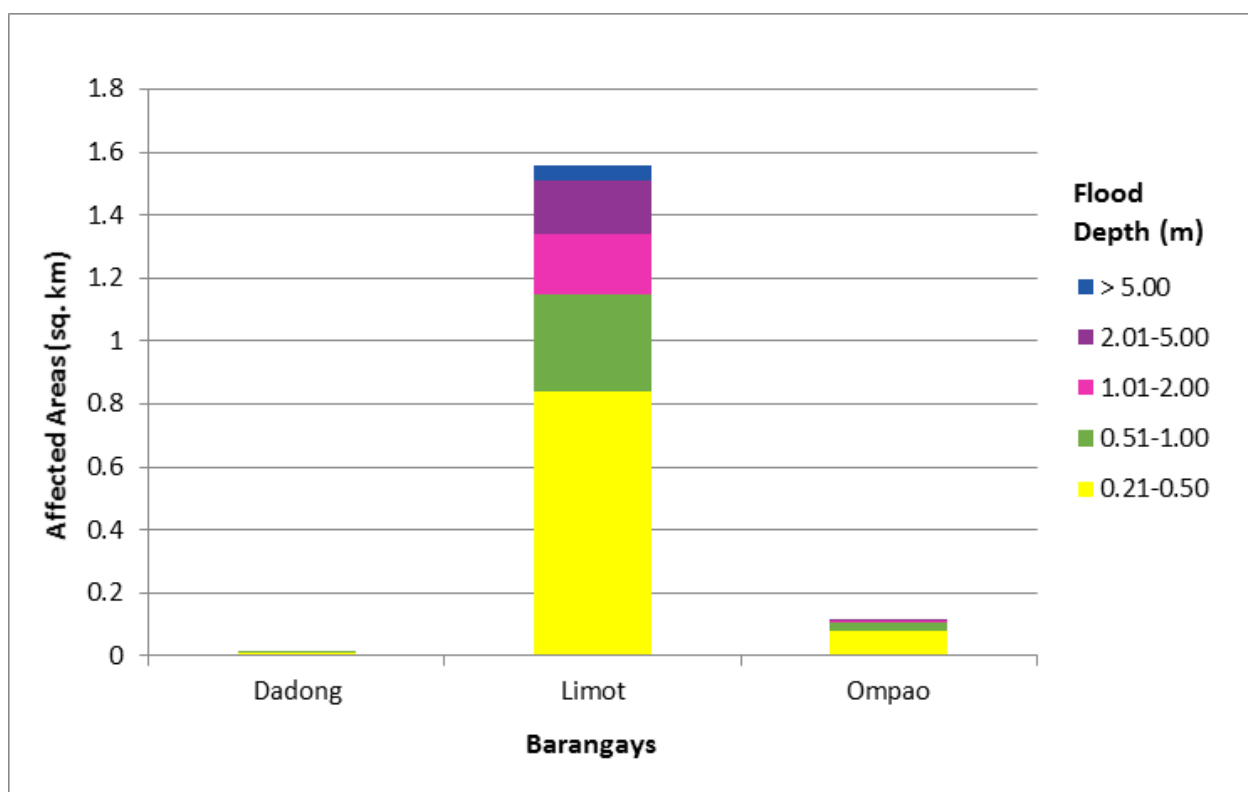


Figure 73. Affected Areas in Tarragona, Davao Oriental during 25-Year Rainfall Return Period

For the 100-year return period, 1.76% of the municipality of Mati City with an area of 797.38 sq. km. will experience flood levels of less than 0.20 meters. 0.21% of the area will experience flood levels of 0.21 to 0.50 meters while 0.26%, 0.59%, 1.07%, and 0.08% of the area will experience flood depths of 0.51 to 1 meter, 1.01 to 2 meters, 2.01 to 5 meters, and more than 5 meters, respectively. Listed in Table 36 and shown in Figure 74 are the affected areas in square kilometers by flood depth per barangay.

Table 36. Affected areas in Mati City, Davao Oriental during a 100-Year Rainfall Return Period

| Affected area (sq. km.) by flood depth (in m.) | Area of affected barangays in Mati City (in sq. km.) | | | |
|--|--|--------------------|------|-----------|
| | Don Enrique Lopez | Don Salvador Lopez | Mayo | Tagabakid |
| 0.03-0.20 | 3.06 | 0 | 4.98 | 6.01 |
| 0.21-0.50 | 0.6 | 0 | 0.62 | 0.44 |
| 0.51-1.00 | 1.03 | 0 | 0.87 | 0.2 |
| 1.01-2.00 | 2.87 | 0 | 1.71 | 0.13 |
| 2.01-5.00 | 5.01 | 0 | 3.43 | 0.098 |
| > 5.00 | 0.5 | 0 | 0.14 | 0.013 |

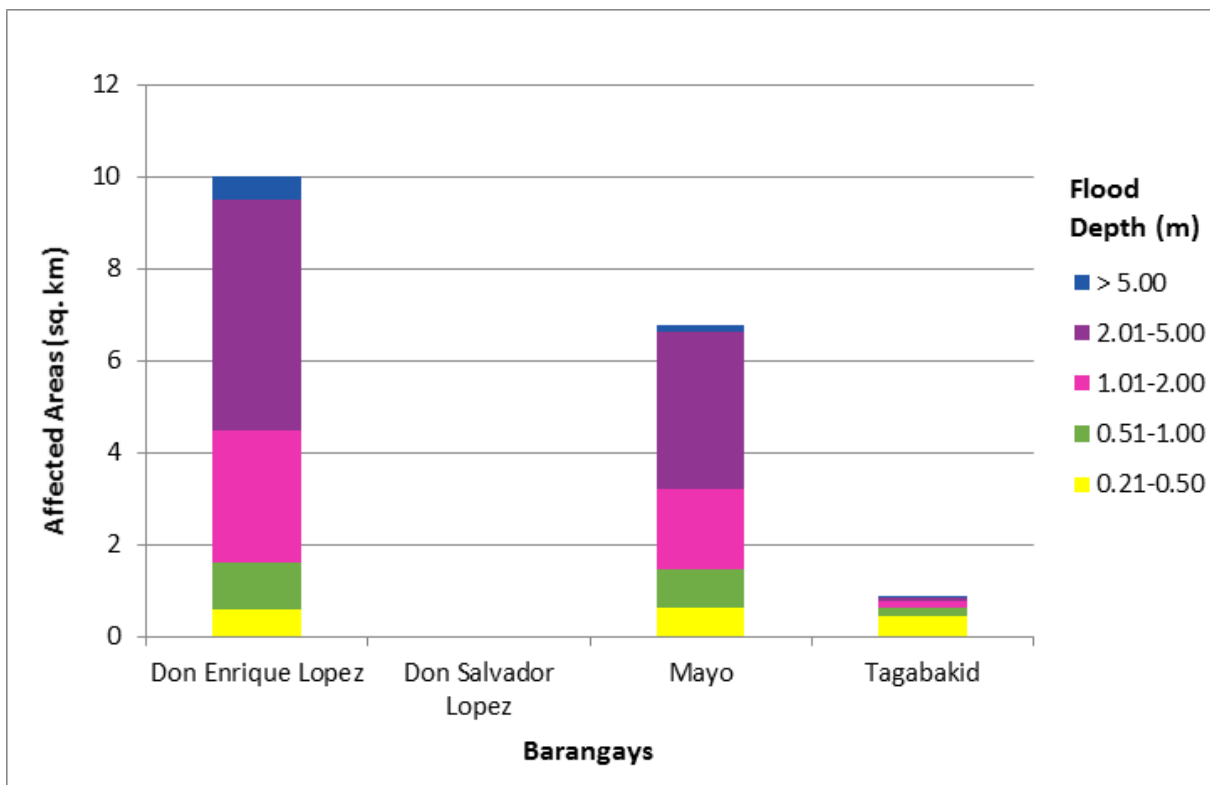


Figure 74. Affected Areas in Mati City, Davao Oriental during 100-Year Rainfall Return Period

For the 100-year return period, 7.58% of the municipality of Tarragona with an area of 277.904 sq. km. will experience flood levels of less than 0.20 meters. 0.45% of the area will experience flood levels of 0.21 to 0.50 meters while 0.17%, 0.10%, 0.09%, and 0.05% of the area will experience flood depths of 0.51 to 1 meter, 1.01 to 2 meters, 2.01 to 5 meters, and more than 5 meters, respectively. Listed in Table 37 and shown in Figure 75 are the affected areas in square kilometers by flood depth per barangay.

Table 37. Affected areas in Tarragona, Davao Oriental during a 100-Year Rainfall Return Period

| Affected area (sq. km.) by flood depth (in m.) | Area of affected barangays in Tarragona (in sq. km.) | | |
|--|--|-------|--------|
| | Dadong | Limot | Ompao |
| 0.03-0.20 | 0.37 | 18.57 | 2.12 |
| 0.21-0.50 | 0.017 | 1.13 | 0.11 |
| 0.51-1.00 | 0.0022 | 0.43 | 0.038 |
| 1.01-2.00 | 0.0003 | 0.26 | 0.016 |
| 2.01-5.00 | 0 | 0.25 | 0.0068 |
| > 5.00 | 0 | 0.13 | 0 |

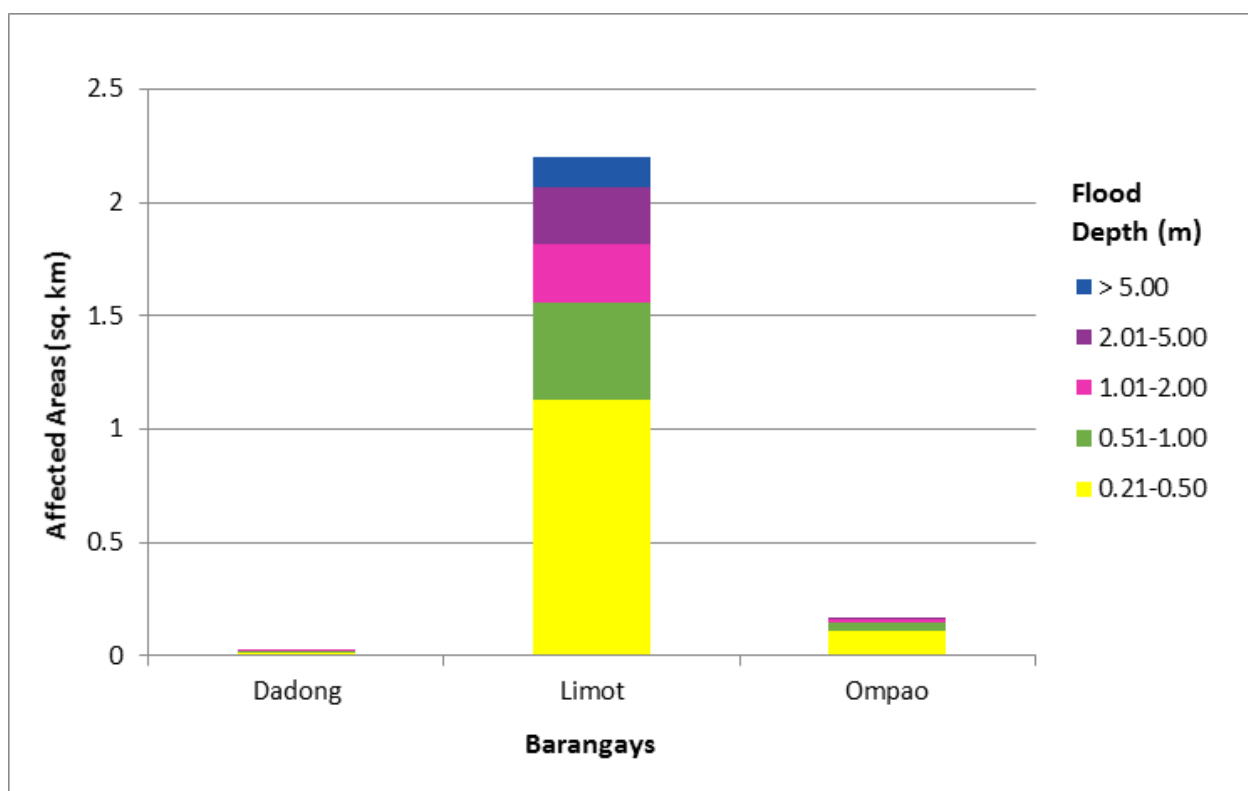


Figure 75. Affected Areas in Tarragona, Davao Oriental during 100-Year Rainfall Return Period

Among the barangays in the municipality of Mati City in Davao Oriental, Don Enrique Lopez is projected to have the highest percentage of area that will experience flood levels at 1.64%. Meanwhile, Mayo posted the second highest percentage of area that may be affected by flood depths at 1.47%.

Among the barangays in the municipality of Tarragona in Davao Oriental, Limot is projected to have the highest percentage of area that will experience flood levels at 7.47%. Meanwhile, Ompao posted the second highest percentage of area that may be affected by flood depths at 0.83%.

Moreover, the generated flood hazard maps for the Mayo Floodplain were used to assess the vulnerability of the educational and medical institutions in the floodplain. Using the flood depth units of PAGASA for hazard maps - "Low", "Medium", and "High" - the affected institutions were given their individual assessment for each Flood Hazard Scenario (5 yr, 25 yr, and 100 yr).

Table 38. Areas covered by each warning level with respect to the rainfall scenarios

| Warning Level | Area Covered in sq. km. | | |
|---------------|-------------------------|-------------|-------------|
| | 5 year | 25 year | 100 year |
| Low | 2.95 | 2.59 | 2.79 |
| Medium | 6.19 | 5.29 | 5.14 |
| High | 10.50 | 13.22 | 13.97 |
| TOTAL | 19.64 | 21.1 | 21.9 |

Of the six identified educational institutions in the Mayo Floodplain, one school was assessed to be highly prone to flooding as it is exposed to the High level flooding for all three rainfall scenarios. This is the Limot Elementary School in Brgy. Don Enrique Lopez. Another institution was found to be also relatively susceptible to flooding, experiencing Low level flooding in the 5- and 25-year return periods, and Medium level flooding in the 100-year rainfall scenario. The educational institutions exposed to flooding are shown in Annex 12.

Only one medical institution was identified in the Mayo Floodplain. The Barangay Mayo Health Center in Brgy. Tagabukid was found to be relatively prone to flooding, having Medium level flooding in all three rainfall scenarios. The medical institutions exposed to flooding are found in Annex 13.

5.11 Flood Validation

In order to check and validate the extent of flooding in different river systems, there is a need to perform validation survey work. Field personnel gather secondary data regarding flood occurrence in the area within the major river system in the Philippines.

From the Flood Depth Maps produced by Phil-LiDAR 1 Program, multiple points representing the different flood depths for different scenarios are identified for validation.

The validation personnel will then go to the specified points identified in a river basin and will gather data regarding the actual flood level in each location. Data gathering can be done through a local DRRM office to obtain maps or situation reports about the past flooding events or interview some residents with knowledge of or have had experienced flooding in a particular area.

After which, the actual data from the field will be compared to the simulated data to assess the accuracy of the Flood Depth Maps produced and to improve on what is needed.

The flood validation survey was conducted on October 11-13, 2016. The flood validation consists of 180 points randomly selected all over the Mayo Floodplain. It has an RMSE value of 1.35.

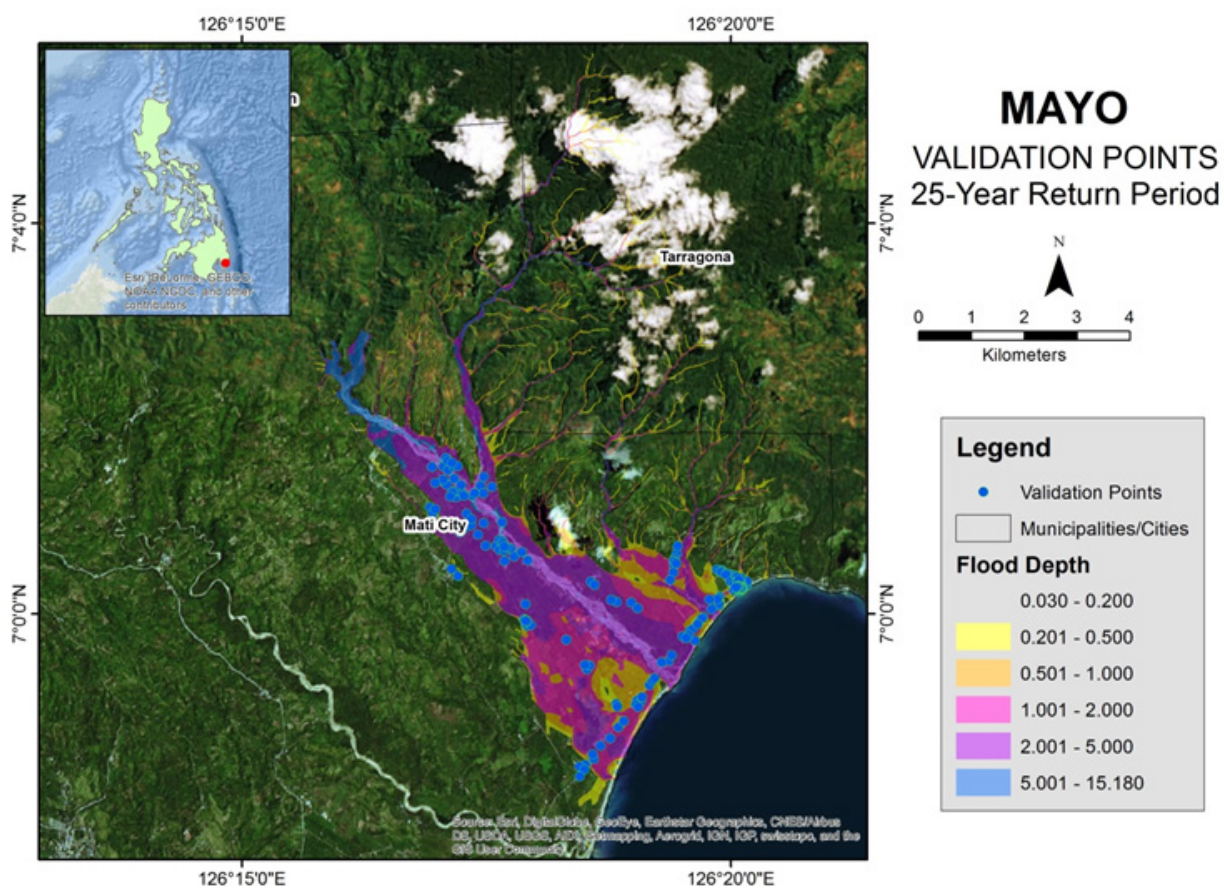


Figure 76. Mayo Flood Validation Points

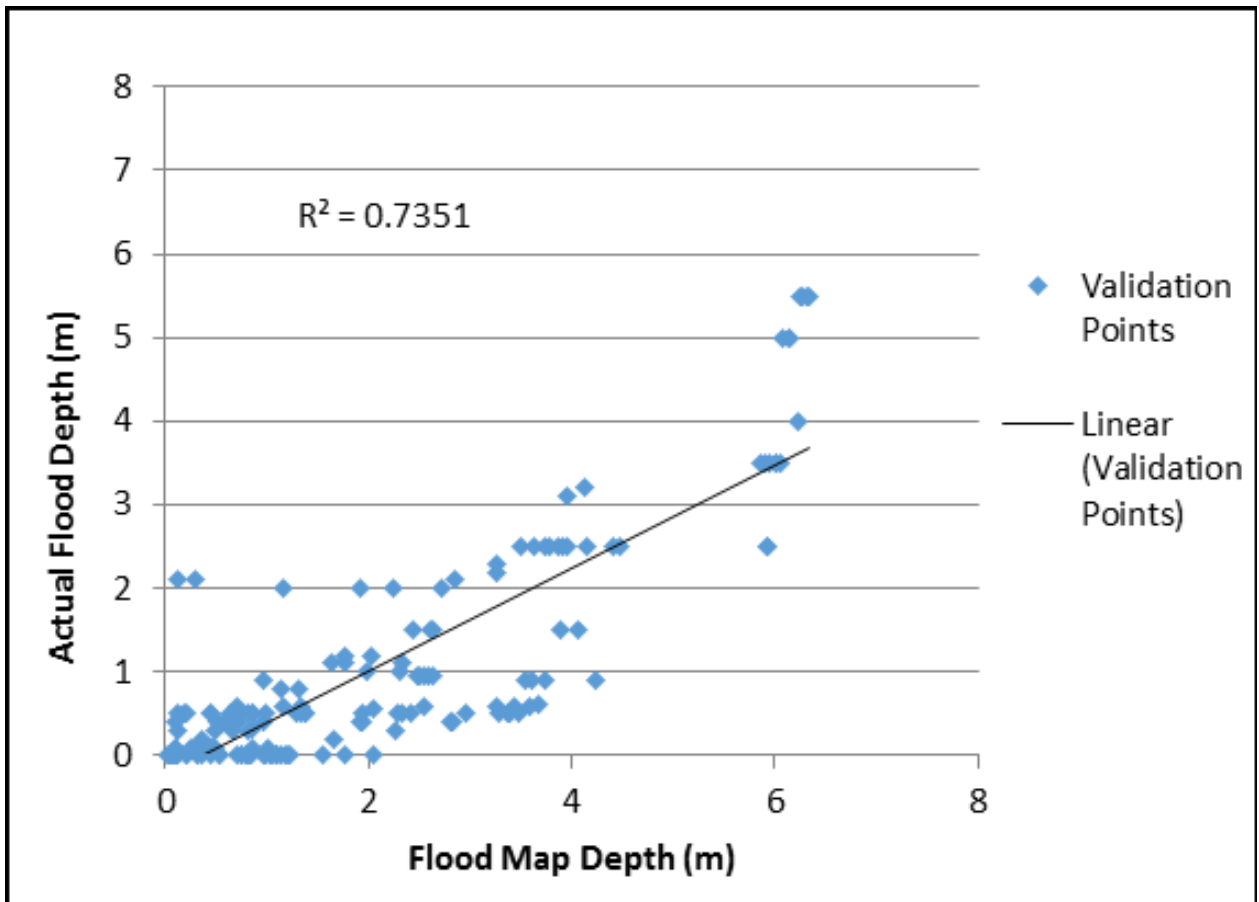


Figure 77. Flood map depth vs. actual flood depth

Table 39. Actual flood vs simulated flood depth at different levels in the Mayo River Basin.

| Actual Flood Depth (m) | Modeled Flood Depth (m) | | | | | | Total |
|------------------------|-------------------------|-----------|-----------|-----------|-----------|--------|-------|
| | 0-0.20 | 0.21-0.50 | 0.51-1.00 | 1.01-2.00 | 2.01-5.00 | > 5.00 | |
| 0-0.20 | 22 | 18 | 13 | 13 | 1 | 0 | 67 |
| 0.21-0.50 | 2 | 3 | 17 | 7 | 11 | 0 | 40 |
| 0.51-1.00 | 2 | 1 | 2 | 5 | 16 | 0 | 26 |
| 1.01-2.00 | 0 | 0 | 0 | 5 | 9 | 0 | 14 |
| 2.01-5.00 | 1 | 1 | 0 | 0 | 15 | 12 | 29 |
| > 5.00 | 0 | 0 | 0 | 0 | 0 | 4 | 4 |
| Total | 27 | 23 | 32 | 30 | 52 | 16 | 180 |

The overall accuracy generated by the flood model is estimated at 28.33%, with 51 points correctly matching the actual flood depths. In addition, there were 64 points estimated one level above and below the correct flood depths while there were 38 points and 27 points estimated two levels above and below, and three or more levels above and below the correct flood depth. A total of 122 points were overestimated while a total of 7 points were underestimated in the modelled flood depths of Mayo.

Table 40. Summary of the Accuracy Assessment in the Mayo River Basin Survey

| | No. of Points | % |
|----------------|----------------------|----------|
| Correct | 51 | 28.33 |
| Overestimated | 122 | 67.78 |
| Underestimated | 7 | 3.89 |
| Total | 180 | 100 |

REFERENCES

Ang M.C., Paringit E.C., et al. 2014. DREAM Data Processing Component Manual. Quezon City, Philippines: UP Training Center for Applied Geodesy and Photogrammetry

Balicanta L.P, Paringit E.C., et al. 2014. DREAM Data Validation Component Manual. Quezon City, Philippines: UP Training Center for Applied Geodesy and Photogrammetry

Lagmay A.F., Paringit E.C., et al. 2014. DREAM Flood Modeling Component Manual. Quezon City, Philippines: UP Training Center for Applied Geodesy and Photogrammetry

Paringit, E.C., Balicanta, L.P., Ang, M.C., Lagmay, A.F., Sarmiento, C. 2017, Flood Mapping of Rivers in the Philippines Using Airborne LiDAR: Methods. Quezon City, Philippines: UP Training Center for Applied Geodesy and Photogrammetry

Sarmiento C.J.S., Paringit E.C., et al. 2014. DREAM Data Aquisition Component Manual. Quezon City, Philippines: UP Training Center for Applied Geodesy and Photogrammetry

UP TCAGP 2016. Acceptance and Evaluation of Synthetic Aperture Radar Digital Surface Model (SAR DSM) and Ground Control Points (GCP). Quezon City, Philippines: UP Training Center for Applied Geodesy and Photogrammetry

ANNEXES

Annex 1. Optech Technical Specification of the Gemini Sensor

Table A-1.1. Parameters and Specification of the Gemini Sensor

| Parameter | Specification |
|---|---|
| Operational envelope (1,2,3,4) | 150-4000 m AGL, nominal |
| Laser wavelength | 1064 nm |
| Horizontal accuracy (2) | 1/5,500 x altitude, (m AGL) |
| Elevation accuracy (2) | <5-35 cm, 1 σ |
| Effective laser repetition rate | Programmable, 33-167 kHz |
| Position and orientation system | POS AV™ AP50 (OEM); |
| 220-channel dual frequency GPS/GNSS/ Galileo/L-Band receiver | Programmable, 0-75 ° |
| Scan width (WOV) | Programmable, 0-50° |
| Scan frequency (5) | Programmable, 0-70 Hz (effective) |
| Sensor scan product | 1000 maximum |
| Beam divergence | Dual divergence: 0.25 mrad (1/e) and 0.8 mrad (1/e), nominal |
| Roll compensation | Programmable, $\pm 5^\circ$ (FOV dependent) |
| Range capture | Up to 4 range measurements, including 1st, 2nd, 3rd, and last returns |
| Intensity capture | Up to 4 intensity returns for each pulse, including last (12 bit) |
| Video Camera | Internal video camera (NTSC or PAL) |
| Image capture | Compatible with full Optech camera line (optional) |
| Full waveform capture | 12-bit Optech IWD-2 Intelligent Waveform Digitizer (optional) |
| Data storage | Removable solid state disk SSD (SATA II) |
| Power requirements | 28 V; 900 W; 35 A (peak) |
| Dimensions and weight | Sensor: 260 mm (w) x 190 mm (l) x 570 mm (h); 23 kg |
| Control rack: 650 mm (w) x 590 mm (l) x 530 mm (h); 53 kg | -10°C to +35°C |
| Operating temperature | -10°C to +35°C (with insulating jacket) |
| Relative humidity | 0-95% no-condensing |

1 Target reflectivity $\geq 20\%$

2 Dependent on selected operational parameters using nominal FOV of up to 40° in standard atmospheric conditions with 24-km visibility

3 Angle of incidence $\leq 20^\circ$

4 Target size \geq laser footprint 5 Dependent on system configuration

Annex 2. NAMRIA Certification of Reference Points Used in the LIDAR Survey

1. DVE-42



Republic of the Philippines
Department of Environment and Natural Resources
NATIONAL MAPPING AND RESOURCE INFORMATION AUTHORITY

June 24, 2014

CERTIFICATION

To whom it may concern:

This is to certify that according to the records on file in this office, the requested survey information is as follows -

| | | |
|-------------------------------------|--------------------------------------|-------------------------------------|
| Province: DAVAO ORIENTAL | | |
| Station Name: DVE-42 | | |
| Order: 2nd | | |
| Island: MINDANAO | | Barangay: DON ENRIQUE LOPEZ |
| Municipality: MATI (CAPITAL) | PRS92 Coordinates | |
| Latitude: 6° 58' 54.82726" | Longitude: 126° 17' 56.05259" | Ellipsoidal Hgt: 6.39500 m. |
| WGS84 Coordinates | | |
| Latitude: 6° 58' 51.79295" | Longitude: 126° 18' 1.57690" | Ellipsoidal Hgt: 81.02500 m. |
| PTM Coordinates | | |
| Northing: 772166.69 m. | Easting: 643534.636 m. | Zone: 5 |
| UTM Coordinates | | |
| Northing: 772,554.34 | Easting: 201,538.20 | Zone: 52 |

Location Description

DVE-42
"DVE-42" is in Barangay Don Enrique Lopez, Mati City, Davao Oriental. From Mati Proper, travel south for about 12 km. then turn left and continue travel for about 2.3 km. towards the Don Enrique Elem. School. Station is located at the Don Enrique Elem. School, 5 cm "SW" of the flagpole. Mark is the head of 4" copper nail embedded in a .30x0.30x1.0 m. concrete monument with inscription "DVE-42 2007 NAMRIA".

Requesting Party: **Engr. Cruz**
Pupose: **Reference**
OR Number: **8796376 A**
T.N.: **2014-1446**



RUEL DM. BELEN, MNSA
Director, Mapping And Geodesy Branch



9 9 0 6 2 4 2 0 1 4 1 1 8 4 2



NAMRIA OFFICES:
Main : Lawton Avenue, Fort Bonifacio, 1634 Taguig City, Philippines Tel. No. : (632) 810-4831 to 41
Branch : 421 Barraca St. San Nicolas, 1010 Manila, Philippines, Tel. No. (632) 241-3494 to 98
www.namria.gov.ph
ISO 9001: 2008 CERTIFIED FOR MAPPING AND GEOSPATIAL INFORMATION MANAGEMENT

Figure A-2.1. DVE-42

2. DVE-61



Republic of the Philippines
Department of Environment and Natural Resources
NATIONAL MAPPING AND RESOURCE INFORMATION AUTHORITY

July 11, 2014

CERTIFICATION

To whom it may concern:

This is to certify that according to the records on file in this office, the requested survey information is as follows -

| | | |
|-------------------------------------|--------------------------------------|--------------------------------------|
| Province: DAVAO ORIENTAL | | |
| Station Name: DVE-61 | | |
| Order: 2nd | | |
| Island: MINDANAO | | Barangay: UPPER BLISS |
| Municipality: MATI (CAPITAL) | | MSL Elevation: |
| PRS92 Coordinates | | |
| Latitude: 6° 57' 39.37336" | Longitude: 126° 13' 22.44550" | Ellipsoidal Hgt: 48.47400 m. |
| WGS84 Coordinates | | |
| Latitude: 6° 57' 36.33777" | Longitude: 126° 13' 27.97256" | Ellipsoidal Hgt: 122.95300 m. |
| PTM / PRS92 Coordinates | | |
| Northing: 769826.046 m. | Easting: 635140.8 m. | Zone: 5 |
| UTM / PRS92 Coordinates | | |
| Northing: 770,283.71 | Easting: 193,120.25 | Zone: 52 |

Location Description

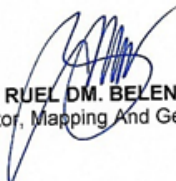
DVE-61
"DVE-61" is in Barangay Upper Bliss, Gov. Mati City, Davao Oriental. To reach the station travel for about 2.5 kms. from City Hall of mati, going east towards brgy. Zign, Mati City. Station is located at the center of the playground of Zign Elem. School, about 10 m "W" of school flagpole. Mark is the head of 4" copper nail embedded in a 0.30x0.30x1.0 m. concrete monument with inscription "DVE-61 2007 NAMRIA".

Requesting Party: **UP TCAGP / Engr. Christopher Cruz**

Purpose: **Reference**

OR Number: **8796507 A**

T.N.: **2014-1586**



RUEL M. BELEN, MNSA
Director, Mapping And Geodesy Branch



9 9 0 7 1 1 2 0 1 4 1 4 5 5 4 7



NAMRIA OFFICES:
Main : Lawton Avenue, Fort Bonifacio, 1634 Taguig City, Philippines Tel. No.: (632) 810-4831 to 41
Branch : 421 Barraca St. San Nicolas, 1010 Manila, Philippines, Tel. No. (632) 241-5494 to 98
www.namria.gov.ph

ISO 9001: 2008 CERTIFIED FOR MAPPING AND GEOSPATIAL INFORMATION MANAGEMENT

Figure A-2.2. DVE-61

Annex 3. Baseline Processing Reports of Control Points used in the LIDAR Survey

1. DVE-3088

Table A-3.1. DVE-3088

Processing Summary

| Observation | From | To | Solution Type | H. Prec. (Meter) | V. Prec. (Meter) | Geodetic Az. | Ellipsoid Dist. (Meter) | ΔHeight (Meter) |
|--------------------------|--------|----------|---------------|------------------|------------------|--------------|-------------------------|-----------------|
| DVE-3088 --- DVE-42 (B1) | DVE-42 | DVE-3088 | Fixed | 0.001 | 0.002 | 160°37'05" | 8.200 | -0.026 |
| DVE-3088 --- DVE-42 (B2) | DVE-42 | DVE-3088 | Fixed | 0.001 | 0.002 | 160°36'36" | 8.199 | -0.029 |
| DVE-3088 --- DVE-42 (B3) | DVE-42 | DVE-3088 | Fixed | 0.001 | 0.002 | 160°40'50" | 8.200 | -0.031 |
| DVE-42 --- DVE-3088 (B4) | DVE-42 | DVE-3088 | Fixed | 0.001 | 0.001 | 160°40'53" | 8.203 | -0.034 |
| DVE-42 --- DVE-3088 (B5) | DVE-42 | DVE-3088 | Fixed | 0.001 | 0.002 | 160°41'28" | 8.204 | -0.032 |

Acceptance Summary

| Processed | Passed | Flag | Fail |
|-----------|--------|------|------|
| 5 | 5 | 0 | 0 |

Vector Components (Mark to Mark)

| From: DVE-42 | | | | | |
|--------------|--------------|-----------|-------------------|-----------|-------------------|
| Grid | | Local | | Global | |
| Easting | 864582.336 m | Latitude | N6°58'54.82726" | Latitude | N6°58'51.79294" |
| Northing | 772976.674 m | Longitude | E126°17'56.05259" | Longitude | E126°18'01.67690" |
| Elevation | 15.606 m | Height | 6.396 m | Height | 81.024 m |

| To: DVE-3088 | | | | | |
|--------------|--------------|-----------|-------------------|-----------|-------------------|
| Grid | | Local | | Global | |
| Easting | 864586.414 m | Latitude | N6°58'54.69466" | Latitude | N6°58'51.66036" |
| Northing | 772968.449 m | Longitude | E126°17'56.18366" | Longitude | E126°18'01.70798" |
| Elevation | 15.681 m | Height | 6.369 m | Height | 80.998 m |

| Vector | | | | | |
|------------|----------|-----------------|------------|----|----------|
| ΔEasting | 4.078 m | NS Fwd Azimuth | 160°37'05" | ΔX | -3.741 m |
| ΔNorthing | -7.126 m | Ellipsoid Dist. | 8.200 m | ΔY | -1.703 m |
| ΔElevation | -0.026 m | ΔHeight | -0.026 m | ΔZ | -7.096 m |

Standard Errors

| Vector errors: | | | | | |
|----------------|---------|-------------------|----------|------|---------|
| σ ΔEasting | 0.001 m | σ NS fwd Azimuth | 0°00'12" | σ ΔX | 0.001 m |
| σ ΔNorthing | 0.000 m | σ Ellipsoid Dist. | 0.000 m | σ ΔY | 0.001 m |
| σ ΔElevation | 0.001 m | σ ΔHeight | 0.001 m | σ ΔZ | 0.000 m |

2. DVE-3118

Table A-3.2. DVE-3118

Processing Summary

| Observation | From | To | Solution Type | H. Prec. (Meter) | V. Prec. (Meter) | Geodetic Az. | Ellipsoid Dist. (Meter) | ΔHeight (Meter) |
|--------------------------|--------|----------|---------------|------------------|------------------|--------------|-------------------------|-----------------|
| DVE-61 --- DVE-3118 (B1) | DVE-61 | DVE-3118 | Fixed | 0.017 | 0.050 | 222°57'30" | 8321.258 | 81.505 |
| DVE-61 --- DVE-3118 (B2) | DVE-61 | DVE-3118 | Fixed | 0.013 | 0.040 | 222°57'30" | 8321.247 | 81.572 |
| DVE-61 --- DVE-3118 (B3) | DVE-61 | DVE-3118 | Fixed | 0.017 | 0.043 | 222°57'29" | 8321.266 | 81.487 |

Acceptance Summary

| Processed | Passed | Flag | Fail |
|-----------|--------|------|------|
| 3 | 3 | 0 | 0 |

Vector Components (Mark to Mark)

| From: DVE-61 | | | | | |
|--------------|--------------|-----------|-------------------|-----------|-------------------|
| Grid | | Local | | Global | |
| Easting | 856189.978 m | Latitude | N6°57'39.37336" | Latitude | N6°57'36.33777" |
| Northing | 770596.911 m | Longitude | E126°13'22.44550" | Longitude | E126°13'27.97255" |
| Elevation | 57.159 m | Height | 48.474 m | Height | 122.954 m |

| To: DVE-3118 | | | | | |
|--------------|--------------|-----------|-------------------|-----------|-------------------|
| Grid | | Local | | Global | |
| Easting | 850554.409 m | Latitude | N6°54'21.10869" | Latitude | N6°54'18.08333" |
| Northing | 764461.564 m | Longitude | E126°10'17.73141" | Longitude | E126°10'23.26402" |
| Elevation | 138.504 m | Height | 129.979 m | Height | 204.434 m |

| Vector | | | | | |
|------------|-------------|-----------------|------------|----|-------------|
| ΔEasting | -5635.570 m | NS Fwd Azimuth | 222°57'30" | ΔX | 4093.802 m |
| ΔNorthing | -6135.347 m | Ellipsoid Dist. | 8321.258 m | ΔY | 4007.271 m |
| ΔElevation | 81.345 m | ΔHeight | 81.505 m | ΔZ | -6036.086 m |

Standard Errors

| Vector errors: | | | | | |
|----------------|---------|-------------------|----------|------|---------|
| σ ΔEasting | 0.007 m | σ NS fwd Azimuth | 0°00'00" | σ ΔX | 0.015 m |
| σ ΔNorthing | 0.005 m | σ Ellipsoid Dist. | 0.006 m | σ ΔY | 0.021 m |
| σ ΔElevation | 0.025 m | σ ΔHeight | 0.025 m | σ ΔZ | 0.006 m |

Aposteriori Covariance Matrix (Meter²)

| | X | Y | Z |
|---|---------------|--------------|--------------|
| X | 0.0002242317 | | |
| Y | -0.0002729544 | 0.0004576374 | |
| Z | -0.0000517483 | 0.0000689019 | 0.0000341757 |

Annex 4. The LIDAR Survey Team Composition

Table A-4.1. The LiDAR Survey Team Composition

| Data Acquisition Component Sub-Team | Designation | Name | Agency/ Affiliation |
|-------------------------------------|---|-------------------------------|---------------------|
| PHIL-LIDAR 1 | Program Leader | ENRICO C. PARINGIT, DR.ENG | UP-TCAGP |
| Data Acquisition Component Leader | Data Component Project Leader - I | ENGR. CZAR JAKIRI SARMIENTO | UP-TCAGP |
| Survey Supervisor | Chief Science Research Specialist (CSRS) | ENGR. CHRISTOPHER CRUZ | UP-TCAGP |
| | Supervising Science Research Specialist (Supervising SRS) | LOVELY GRACIA ACUÑA | UP-TCAGP |
| | | LOVELYN ASUNCION | UP-TCAGP |

FIELD TEAM

| | | | |
|---|---|-------------------------------|-----------------------------------|
| LiDAR Operation | Senior Science Research Specialist (SSRS) | JULIE PEARL MARS | UP-TCAGP |
| | Research Associate (RA) | FOR. MA. VERLINA TONGA | UP-TCAGP |
| | RA | ENGR. LARAH KRISSELLE PARAGAS | UP-TCAGP |
| Ground Survey, Data Download and Transfer | RA | ENGR. KENNETH QUISADO | UP-TCAGP |
| LiDAR Operation | Airborne Security | TSG. MIKE DIAPANA | PHILIPPINE AIR FORCE (PAF) |
| | Pilot | CAPT. RAUL CZ SAMAR II | ASIAN AEROSPACE CORPORATION (AAC) |
| | | CAPT. BRYAN JOHN DONGUINES | AAC |

Annex 5. Data Transfer Sheet for Mayo Floodplain

DATA TRANSFER SHEET
07/08/2014 (Davao Oriental - ready)

| DATE | FLIGHT NO. | MISSION NAME | SENSOR | RAW LAS | | LOGS(MB) | POB | RAW IMAGES/CSA/ SI | MISSION LOG FILES/CSA/ LOGS | RANGE | DIGITIZER | BASE STATION(S) | | OPERATOR LOGS (OP/LOG) | FLIGHT PLAN | | SERVER LOCATION |
|-----------|------------|---------------|--------|------------|-------------|----------|------|--------------------|-----------------------------|-------|-----------|-----------------|-----------------|------------------------|-------------|--------|------------------------|
| | | | | Output LAS | KML (swath) | | | | | | | BASE STATION(S) | Base Info (lat) | | Actual | KML | |
| 6/27/2014 | 7337GC | 2BLK86A178A | Gemini | NA | 209/70 | 366 | 163 | NA | NA | 16.9 | NA | 7.59 | 1KB | 1KB | 4/4/5/5/4 | 24 | Z:\Airborne_Raw\7337GC |
| 6/28/2014 | 7339GC | 2BLK79C179A | Gemini | NA | 179/11 | 367 | 74.8 | NA | NA | 14.3 | NA | 5.08 | 1KB | 1KB | 5 | 179/11 | Z:\Airborne_Raw\7339GC |
| 6/29/2014 | 7340GC | 2BLK79B180A | Gemini | NA | 119 | 580 | 265 | NA | NA | 28.2 | NA | 4.68 | 1KB | 1KB | 5 | 119 | Z:\Airborne_Raw\7340GC |
| 7/1/2014 | 7344GC | 2BLK84B182A | Gemini | NA | 158/22 | 188 | 174 | NA | NA | 69 | NA | 6.95 | 1KB | 1KB | 9 | 158/22 | Z:\Airborne_Raw\7344GC |
| 7/2/2014 | 7346GC | 2BLK798SA183A | Gemini | NA | 376 | 612 | 279 | NA | NA | 29.7 | NA | 5.32 | 1KB | 1KB | 9 | 376 | Z:\Airborne_Raw\7346GC |
| 7/3/2014 | 7348GC | 2BLK79V184A | Gemini | NA | 597 | 200 | 212 | NA | NA | 6.58 | NA | 6.49 | 1KB | 1KB | 14 | 597 | Z:\Airborne_Raw\7348GC |
| 7/4/2014 | 7350GC | 2BLK85B185A | Gemini | NA | 300 | 499 | 258 | NA | NA | 23.8 | NA | 7.05 | 1KB | 1KB | 8 | 300 | Z:\Airborne_Raw\7350GC |

Received from

Name Kristine Andaya
Position B.A.
Signature 

Received by

Name CIDA F. PRIETO
Position SSS
Signature  7/17/14

Figure A-5.1. Transfer Sheet for Mayo Floodplain - A

DATA TRANSFER SHEET
07/08/2014(Davao Oriental - ready)

| DATE | FLIGHT NO. | MISSION NAME | SENSOR | RAW LAS | | LOGS(MB) | POS | RAW IMAGES/CASI LOGS | MISSION LOG FILES/CASI LOGS | RANGE | DIGITIZER | BASE STATION(S) | | OPERATOR LOGS (PLOG) | FLIGHT PLAN | | SERVER LOCATION |
|-----------|------------|-----------------|--------|------------|-------------|----------|------|----------------------|-----------------------------|-------|-----------|-----------------|------------------|----------------------|-------------|----------|-----------------|
| | | | | Output LAS | KML (swath) | | | | | | | BASE STATION(S) | Base Info (.txt) | | Actual | KML | |
| 7/7/2014 | 7356GC | 2BLK80AS188A | Gemini | NA | 347/11 | 589 | 265 | NA | NA | 27.7 | NA | 9.58 | 1KB | 1KB | 4 | 374/11 | Z:\Airborne_Raw |
| 7/7/2014 | 7357GC | 2BLK80BS188B | Gemini | NA | 406 | 111 | 79.8 | NA | NA | 5.05 | NA | 7.68 | 1KB | 1KB | 4 | 406 | Z:\Airborne_Raw |
| 7/8/2014 | 7358GC | 2BLK80BS189A | Gemini | NA | 165/7/14 | 318 | 196 | NA | NA | 20.1 | | 4.83 | 1KB | 1KB | 7/3 | 165/7/14 | Z:\Airborne_Raw |
| 7/10/2014 | 7362GC | 2BLK85CS191A | Gemini | NA | 138 | 244 | 188 | NA | NA | 7.95 | NA | 4.7 | 1KB | 1KB | 8/5/4 | 138 | Z:\Airborne_Raw |
| 7/11/2014 | 7364GC | 2BLK85V192A | Gemini | NA | 234/9/12 | 488 | 207 | NA | NA | 27.3 | NA | 5.8 | 1KB | 1KB | 4/9 | 234/9/12 | Z:\Airborne_Raw |
| 7/12/2014 | 7366GC | 2BLK79D08BV193A | Gemini | NA | 60 | 409 | 241 | NA | NA | 12.2 | NA | 4.89 | 1KB | 1KB | 5/7 | 14/17 | Z:\Airborne_Raw |
| 7/15/2014 | 7372GC | 2BLK79E196A | Gemini | NA | 30/6 | 68.7 | 158 | NA | NA | 3.47 | NA | 4.56 | 1KB | 1KB | 3 | 30/6 | Z:\Airborne_Raw |
| 7/16/2014 | 7374GC | 2BLK79ES197A | Gemini | NA | 139 | 239 | 156 | NA | NA | 9.01 | NA | 3.42 | 1KB | 1KB | 3/4 | 139 | Z:\Airborne_Raw |

Received from

Name: TIN ANASTASIA
Position: [Signature]
Signature: [Signature]

Received by

Name: JOIDA F. PRIETO
Position: SRS
Signature: [Signature] 7/28/14

Figure A-5.2. Transfer Sheet for Mayo Floodplain - B

Annex 6. Flight Logs for the Flight Missions

1. Flight Log for Mission 7320GC

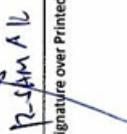
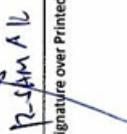
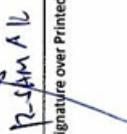
| DREAM Data Acquisition Flight Log | | | | Flight Log No.: 7320 | | | | | |
|--|---|---|--|-------------------------------------|--|---|---|---|--|
| 1 LIDAR Operator: <u>Lk Paragas</u> | 2 ALTM Model: <u>60m FCSB</u> | Mission Name: <u>BLK 83A & B</u> | 4 Type: VFR | 5 Aircraft Type: <u>Cesna T206H</u> | 6 Aircraft Identification: <u>R-1932</u> | | | | |
| 7 Pilot: <u>R. Samal</u> | 8 Co-Pilot: <u>B. Dominguez</u> | 9 Route: <u>19DA</u> | 12 Airport of Arrival (Airport, City/Province): | | | | | | |
| 10 Date: <u>6-19-14</u> | 11 Airport of Departure (Airport, City/Province): <u>KPMQ</u> | 12 Airport of Arrival (Airport, City/Province): <u>RPMQ</u> | 16 Take off: | 17 Landing: | 18 Total Flight Time: | | | | |
| 13 Engine On: <u>8:45</u> | 14 Engine Off: <u>12:42</u> | 15 Total Engine Time: <u>3:47</u> | | | | | | | |
| 19 Weather: | | | | | | | | | |
| 20 Remarks: <p style="text-align: center;"><i>Surveyed 9 lines in BLK 83A & 6 lines in BLK 84B Conducted CASI test</i></p> | | | | | | | | | |
| 21 Problems and Solutions: | | | | | | | | | |
| <table border="0" style="width: 100%;"> <tr> <td style="width: 25%;">Acquisition Flight Approved by  Signature over Printed Name (End User Representative)</td> <td style="width: 25%;">Acquisition Flight Certified by  Signature over Printed Name (PAF Representative)</td> <td style="width: 25%;">Pilot-in-Command  Signature over Printed Name</td> <td style="width: 25%;">Lidar Operator  Signature over Printed Name</td> </tr> </table> | | | | | | Acquisition Flight Approved by  Signature over Printed Name (End User Representative) | Acquisition Flight Certified by  Signature over Printed Name (PAF Representative) | Pilot-in-Command  Signature over Printed Name | Lidar Operator  Signature over Printed Name |
| Acquisition Flight Approved by  Signature over Printed Name (End User Representative) | Acquisition Flight Certified by  Signature over Printed Name (PAF Representative) | Pilot-in-Command  Signature over Printed Name | Lidar Operator  Signature over Printed Name | | | | | | |

Figure A-6.1. Flight Log for Mission 7320GC

2. Flight Log for 7344GC Mission

Flight Log No.: **7344**

DREAM Data Acquisition Flight Log

| | | | | | |
|---|--|---|---|--------------------------------------|---------------------------------------|
| 1 LiDAR Operator: MVE TONSA | 2 ALTM Model: SENT ANS | 3 Mission Name: BK79C | 4 Type: VFR | 5 Aircraft Type: Cessna T206H | 6 Aircraft Identification: 922 |
| 7 Pilot: R. SANDER | 8 Co-Pilot: B. DONSUMES | 9 Route: MTT | 12 Airport of Arrival (Airport, City/Province): | | |
| 10 Date: JUNY 07, 2014 | 11 Airport of Departure (Airport, City/Province): MTT | 12 Airport of Arrival (Airport, City/Province): | 16 Take off: | 17 Landing: | 18 Total Flight Time: |
| 13 Engine On: 9:23 | 14 Engine Off: 12:34 | 15 Total Engine Time: 3711 | | | |
| 19 Weather: cloudy | | | | | |
| 20 Remarks: Survey B line of BK79C (without ANS) | | | | | |
| 21 Problems and Solutions: | | | | | |

Acquisition Flight Approved by



Signature over Printed Name
(End User Representative)

Acquisition Flight Certified by



Signature over Printed Name
(PIF Representative)

Pilot-in-Command



Signature over Printed Name

Lidar Operator



Signature over Printed Name

Figure A-6.2. Flight Log for Mission 7344GC

3. Flight Log for 7362GC Mission

Flight Log No.: **7362**

| | | | |
|--------------------------------------|--|---|---|
| DREAM Data Acquisition Flight Log | | Flight Log No.: 7362 | |
| 1 LIDAR Operator: LK Pargos | 2 ALTM Model: GM+CS | 3 Mission Name: 2BLK85-CAHA | 4 Type: VFR |
| 5 Aircraft Type: Cessna T206H | 6 Aircraft Identification: 9372 | 7 Pilot: X-SANAK | 8 Co-Pilot: B-Dangwa |
| 9 Route: MFTI | 10 Date: July 10, 2014 | 11 Airport of Departure (Airport, City/Province): MFTI | 12 Airport of Arrival (Airport, City/Province): |
| 13 Engine On: 7:37 | 14 Engine Off: 10:48 | 15 Total Engine Time: 3:11 | 16 Take off: 17 Landing: |
| 17 Total Flight Time: 18 | 19 Weather: Fair | 20 Remarks: Completa BLK84C (without CASI) | |
| 21 Problems and Solutions: | | | |

Acquisition Flight Approved by



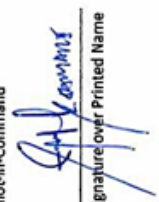
Signature over Printed Name
(End User Representative)

Acquisition Flight Certified by



Signature over Printed Name
(PA Representative)

Pilot-in-Command



Signature over Printed Name

Lidar Operator



Signature over Printed Name

Figure A-6.3. Flight Log for Mission 7362GC

4. Flight Log for 7364GC Mission

Flight Log No.: 7364

DREAM Data Acquisition Flight Log

| | | | | | |
|--|--|---|---|-------------------------------------|--|
| 1 LIDAR Operator: <i>MVF TONER</i> | 2 ALTM Model: <i>SENT ASI</i> | 3 Mission Name: <i>BLK85A + CP 1924</i> | 4 Type: <i>VFR</i> | 5 Aircraft Type: <i>Cesna T206H</i> | 6 Aircraft Identification: <i>9822</i> |
| 7 Pilot: <i>C. TAMAR</i> | 8 Co-Pilot: <i>B. DEXTER</i> | 9 Route: <i>MAF</i> | 12 Airport of Arrival (Airport, City/Province): | | |
| 10 Date: <i>July 11, 2014</i> | 12 Airport of Departure (Airport, City/Province): <i>MAF</i> | 15 Total Engine Time: <i>07:35</i> | 16 Take off: | 17 Landing: | 18 Total Flight Time: |
| 13 Engine On: <i>0:10</i> | 14 Engine Off: <i>0:45</i> | 19 Weather: <i>Fair</i> | | | |
| 20 Remarks: <i>Completed BLK85A and voids in BLK 84C (without CASI)</i> | | | | | |

21 Problems and Solutions:

Acquisition Flight Approved by

[Signature]
Signature over Printed Name
(End User Representative)

Acquisition Flight Certified by

[Signature]
Signature over Printed Name
(PAF Representative)

Pilot-in-Command

[Signature]
Signature over Printed Name

Lidar Operator

[Signature]
Signature over Printed Name

Figure A-6.4. Flight Log for Mission 7364GC

Annex 7. Flight Status Reports

DAVAO ORIENTAL
June 16 - July 16, 2014

Table A-7.1. Flight Status Report

| FLIGHT NO. | AREA | MISSION | OPERATOR | DATE FLOWN | REMARKS |
|------------|-----------------------|----------------|------------|---------------|--|
| 7320GC | BLK84B | 2BLK83A84B170A | LK PARAGAS | June 19, 2014 | Started with 86B. Moved to 84B due to high terrain (6 lines). Moved to 83A due to clouds (9 lines). *CASI testing at the end of the mission flight |
| 7344GC | BLK84C | 2BLK84BCR182A | MV TONGA | July 01, 2014 | Encountered abnormal POS behavior. Completed 14 lines. Lines cut due to clouds. |
| 7362GC | BLK85B_ additional | 2BLK85CS191A | LK PARAGAS | July 10, 2014 | Covered BLK85B at 1200m. Experienced strong head wind. |
| 7364GC | BLK85B_ additional | 2BLK85V192A | MV TONGA | July 11, 2014 | Covered BLK 86A at 1300m. with voids area in BLK 85B |

LAS BOUNDARIED PER FLIGHT

Flight No. : 7320GC
Area: BLK84B
Mission name: 2BLK83A84B170A
Parameters: Altitude: 1000 m; Scan Frequency: 50Hz;
Scan Angle: 20deg; Overlap: 40 %
Area covered: 105.391 sq.km.



Figure A-7.1. Swath for Flight No. 7320GC

Flight No. : 7344GC
Area: BLK84C
Mission name: 2BLK84BCR182A
Parameters: Altitude: 1200m; Scan Frequency: 60Hz;
Scan Angle: 12 deg; Overlap: 45 %
Area covered: 194.96 sq.km



Figure A-7.2. Swath for Flight No. 7344GC

Flight No. : 7362GC
Area: BLK85B_additional
Mission name: 2BLK85CS191A
Parameters: Altitude: 1200m; Scan Frequency: 60Hz;
Scan Angle: 13 deg; Overlap: 40 %
Area covered: 60.6 sq.km



Figure A-7.3. Swath for Flight No. 7362GC

Flight No. : 7364GC
Area: BLK85B_additional
Mission name: 2BLK85V192A
Parameters: Altitude: 1200m; Scan Frequency: 60Hz;
Scan Angle: 12 deg/ 20 deg; Overlap: 40 %
Area covered: 80.6 sq.km

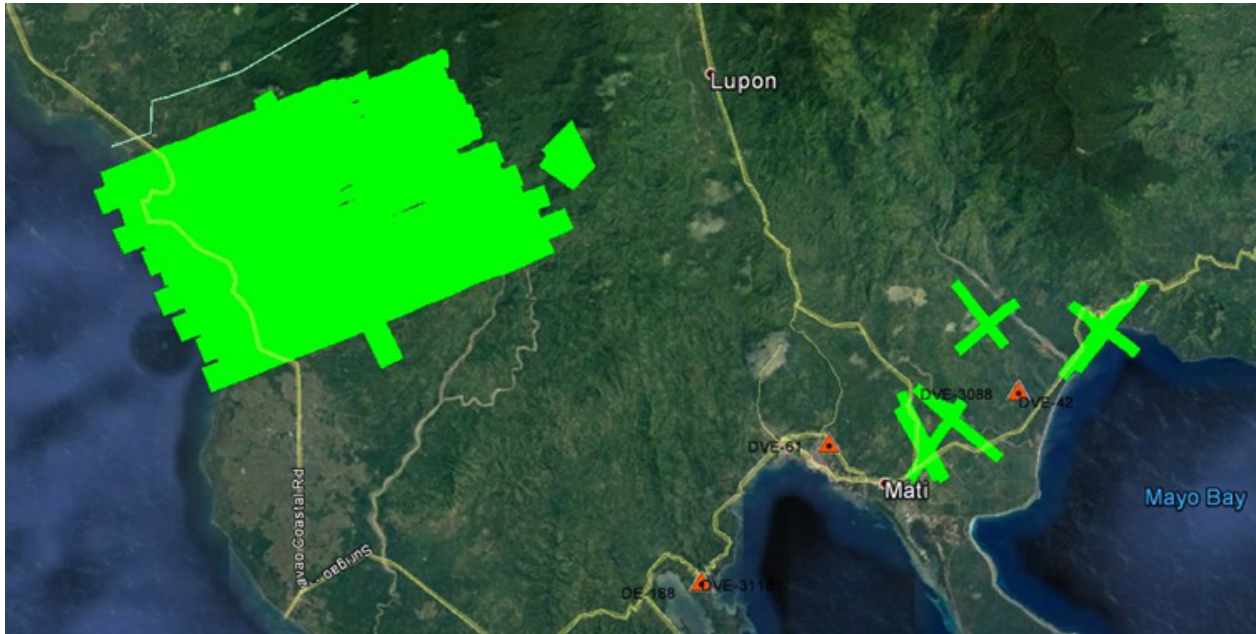


Figure A-7.4. Swath for Flight No. 7364GC

Annex 8. Mission Summary Reports

Table A-8.1. Mission Summary Report for Mission Blk85B_Additional

| Flight Area | Davao Oriental |
|--|---|
| Mission Name | Blk85B_Additional |
| Inclusive Flights | 7362G,7364G |
| Range data size | 43.2 GB |
| POS | 395 MB |
| Image | na |
| Transfer date | July 28, 2014 |
| | |
| Solution Status | |
| Number of Satellites (>6) | Yes |
| PDOP (<3) | Yes |
| Baseline Length (<30km) | Yes |
| Processing Mode (<=1) | Yes |
| | |
| Smoothed Performance Metrics(in cm) | |
| RMSE for North Position (<4.0 cm) | 0.085 |
| RMSE for East Position (<4.0 cm) | 1.0 |
| RMSE for Down Position (<8.0 cm) | 2.4 |
| | |
| Boresight correction stdev (<0.001deg) | 0.000237 |
| IMU attitude correction stdev (<0.001deg) | 0.0074 |
| GPS position stdev (<0.01m) | 0.000612 |
| | |
| Minimum % overlap (>25) | 42.20% |
| Ave point cloud density per sq.m. (>2.0) | 3.63 |
| Elevation difference between strips (<0.20m) | Yes |
| | |
| Number of 1km x 1km blocks | 100 |
| Maximum Height | 473.31 m |
| Minimum Height | 64.36 m |
| | |
| Classification (# of points) | |
| Ground | 32762250 |
| Low vegetation | 26062179 |
| Medium vegetation | 36538890 |
| High vegetation | 103876886 |
| Building | 2730384 |
| | |
| Orthophoto | No |
| Processed by | Engr. Kenneth Solidum, Engr. AnalynNaldo, Engr. Melanie Hingpit |

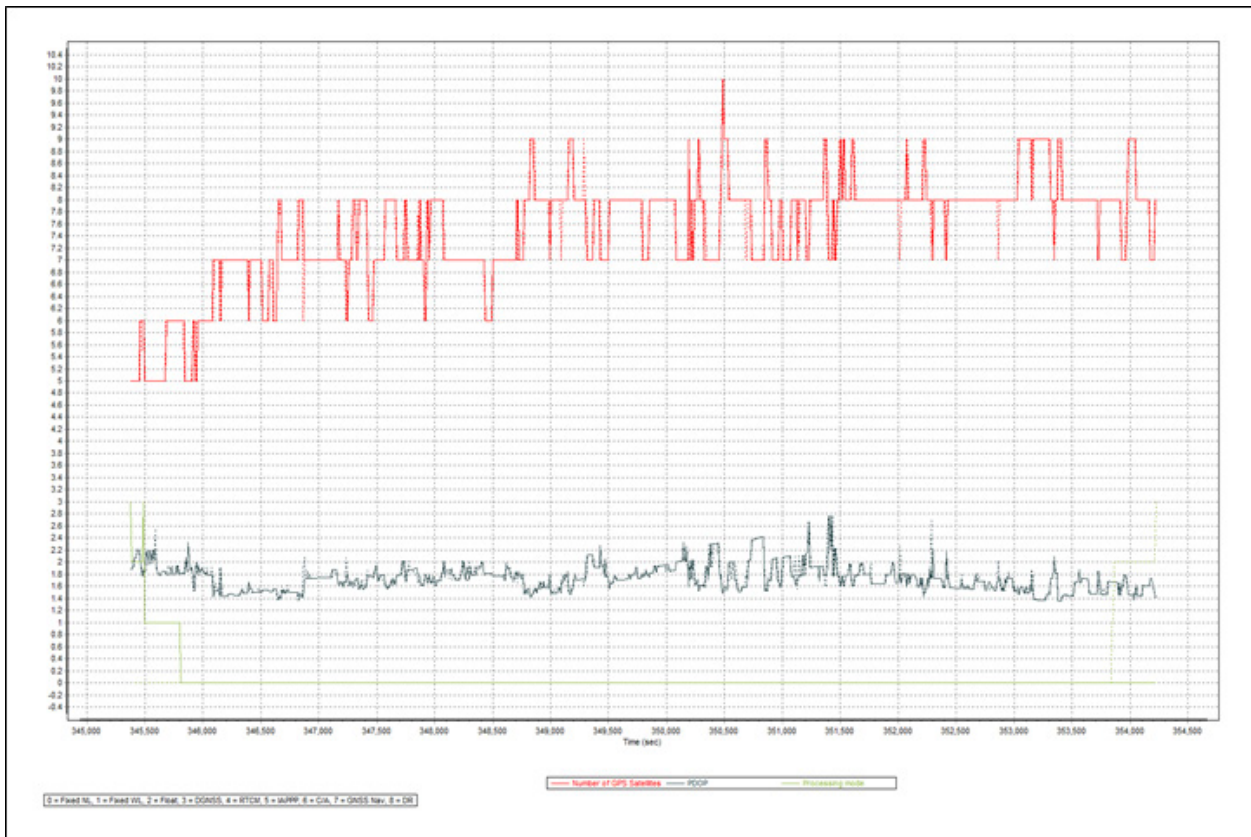


Figure A-8.1. Solution Status

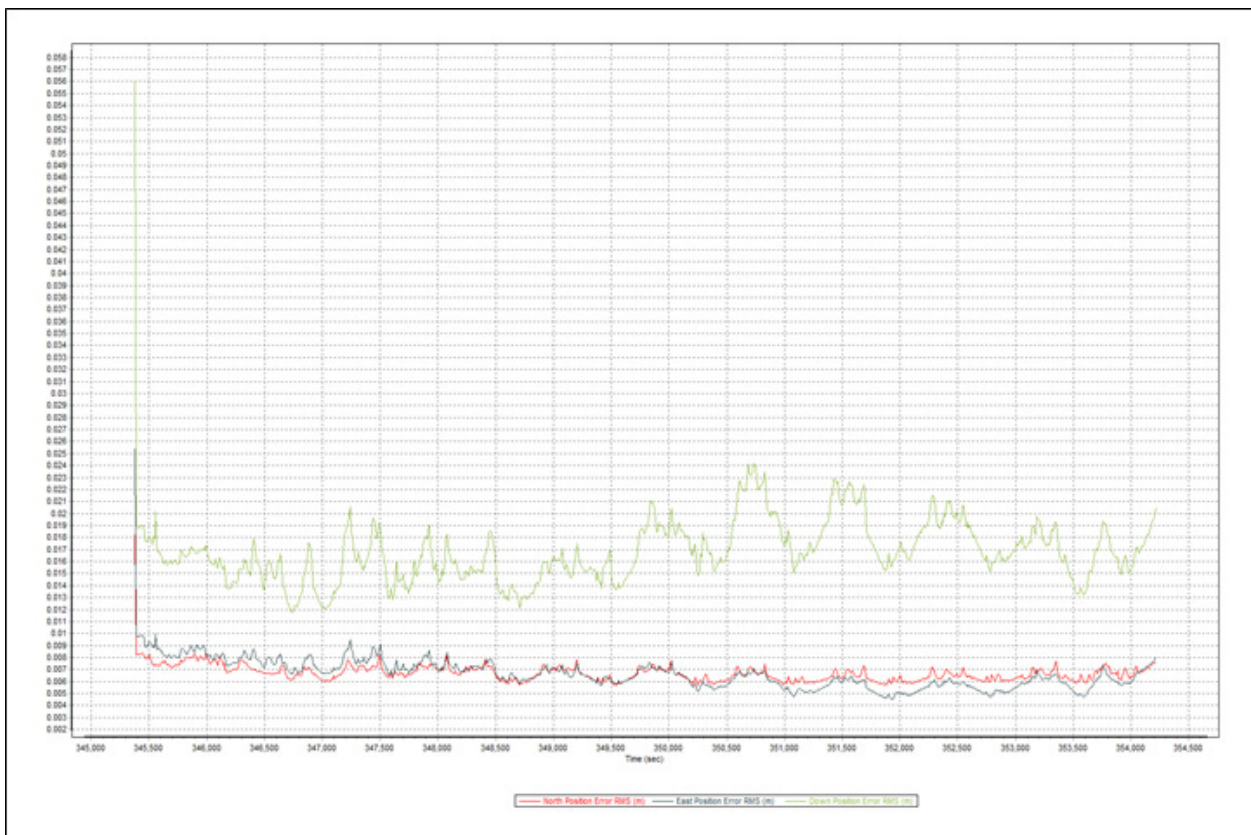


Figure A-8.2. Smoothed Performance Metrics Parameters

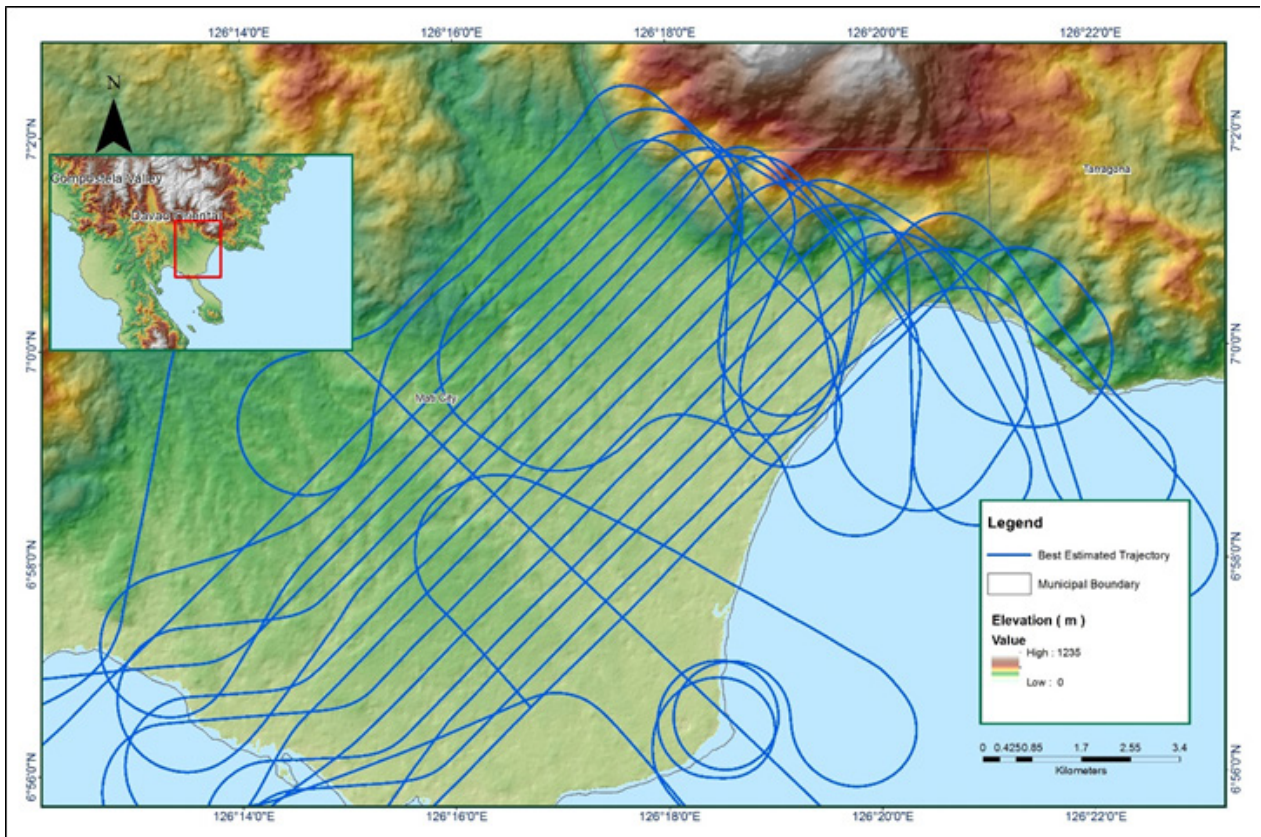


Figure A-8.3. Best Estimated Trajectory

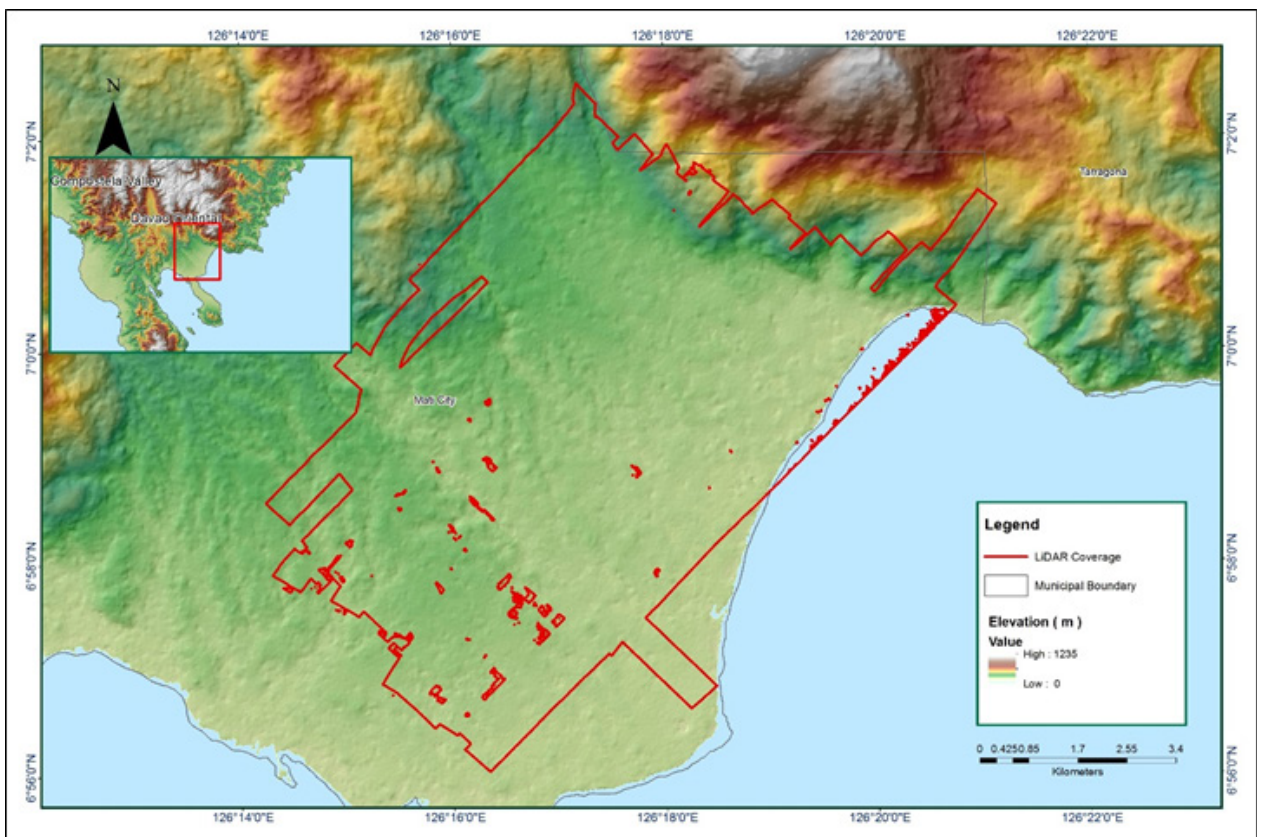


Figure A-8.4. Coverage of LiDAR data

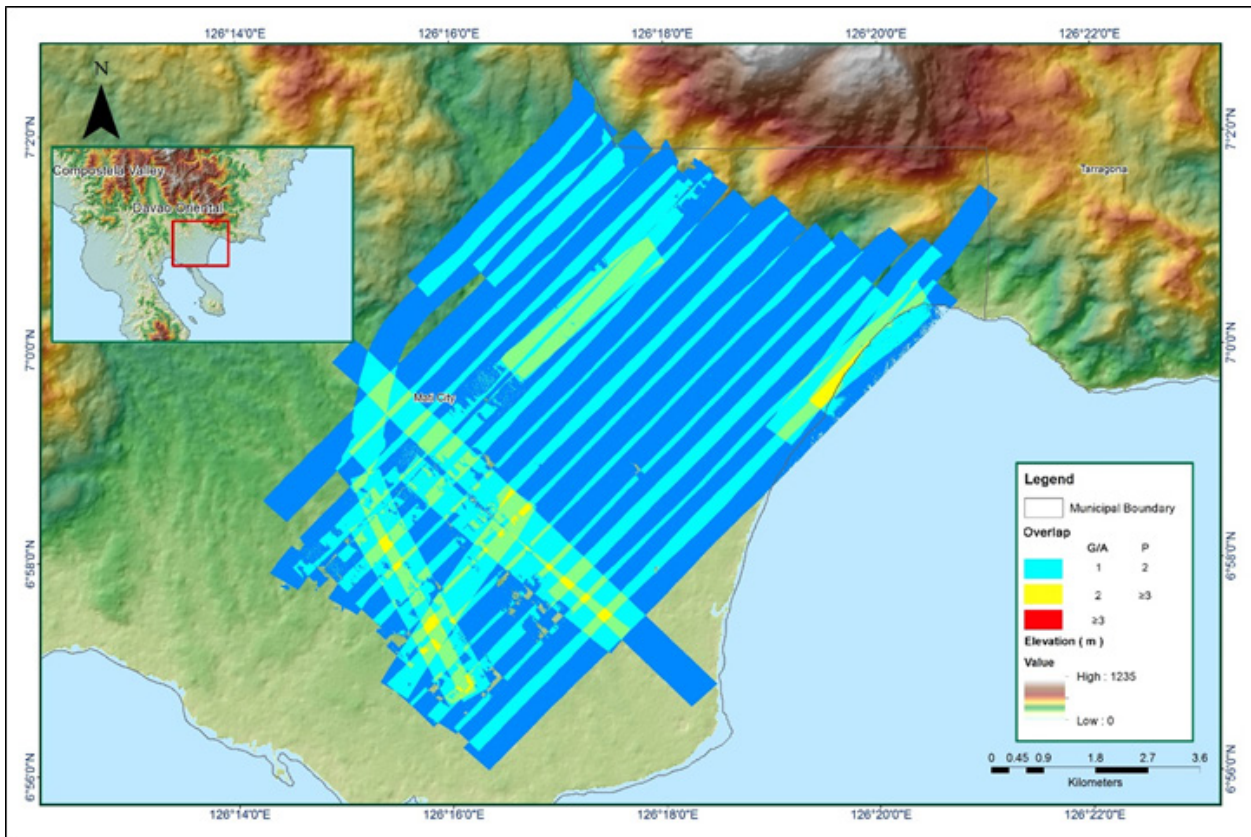


Figure A-8.5. Image of Data Overlap

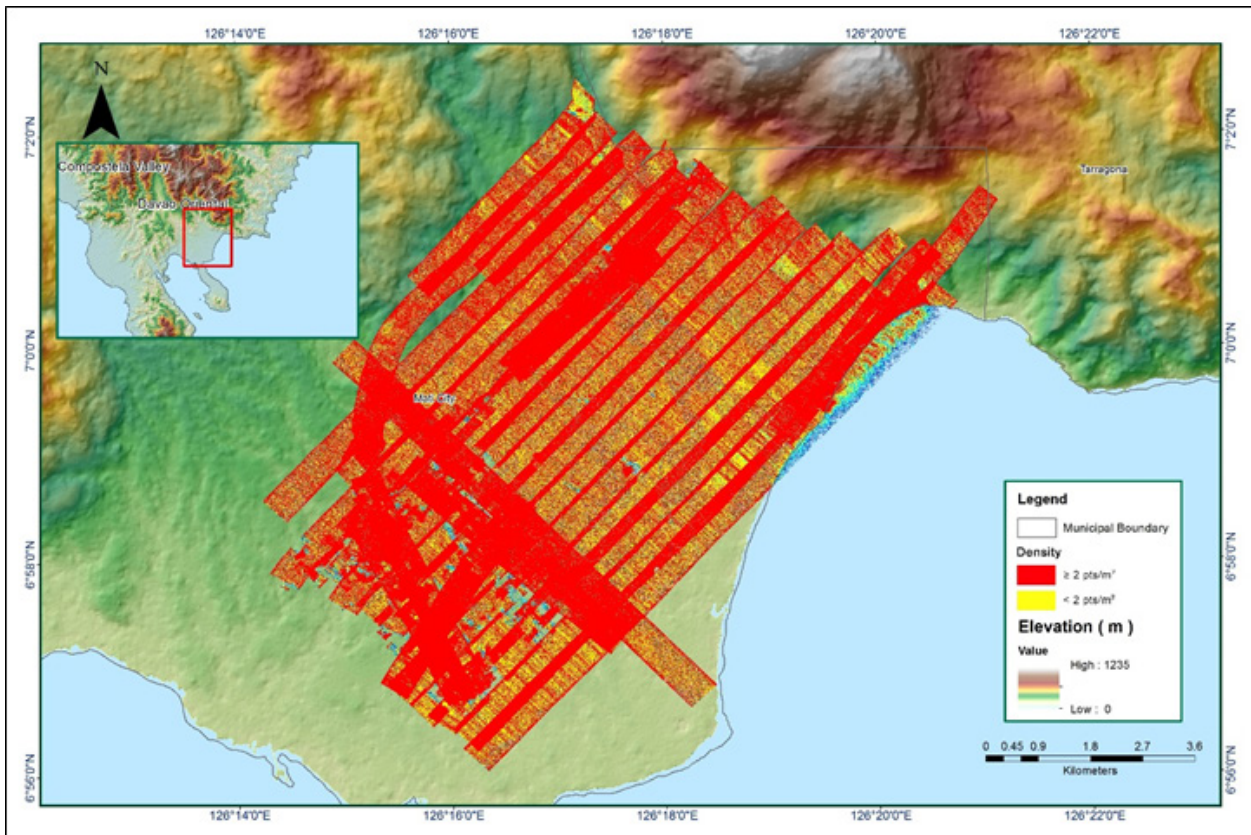


Figure A-8.6. Density map of merged LiDAR data

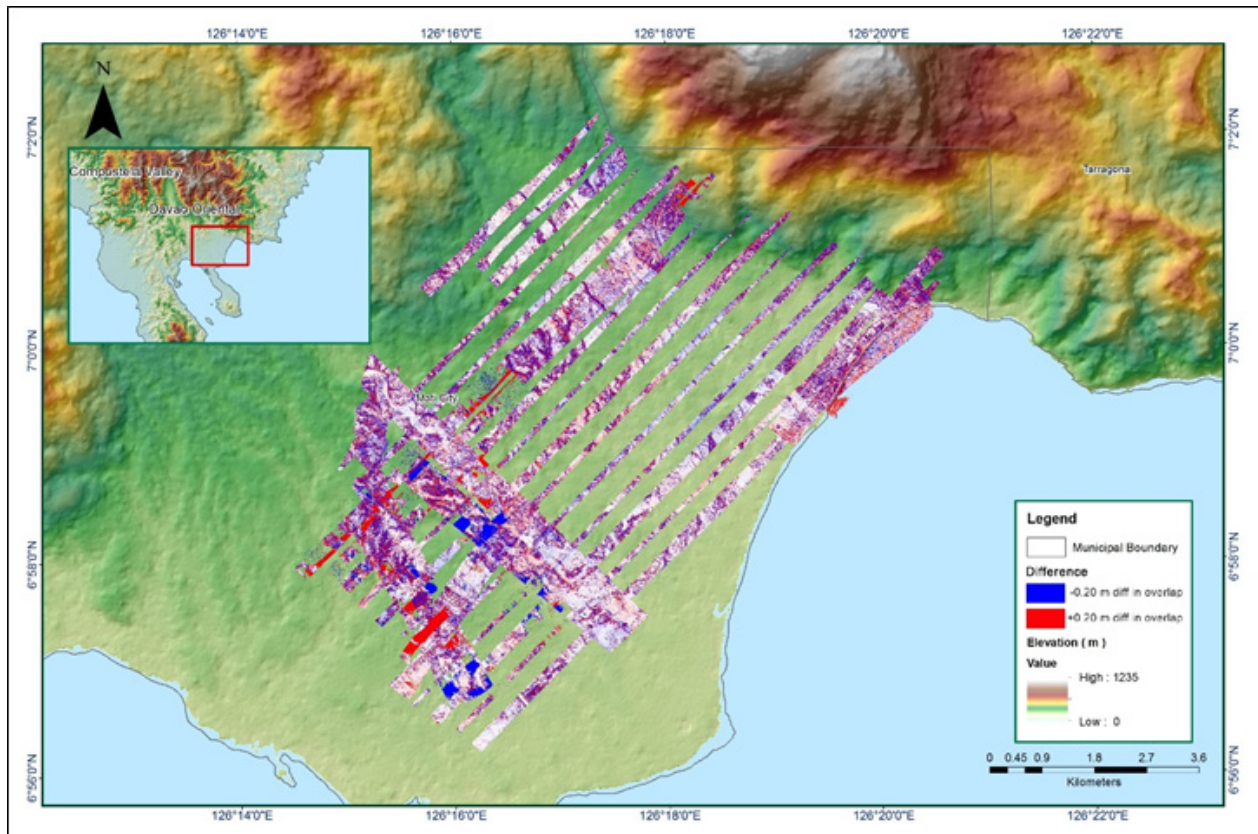


Figure A-8.7. Elevation difference between flight lines

Annex 9. Mayo Model Basin Parameters

Table A-9.1. Mayo Model Basin Parameters

| Basin Number | SCS Curve Number Loss | | | Clark Unit Hydrograph Transform | | | Recession Baseflow | | | | |
|--------------|--------------------------|--------------|----------------|---------------------------------|--------------------------|--------------|--------------------------|--------------------|----------------|---------------|--|
| | Initial Abstraction (mm) | Curve Number | Impervious (%) | Time of Concentration (HR) | Storage Coefficient (HR) | Initial Type | Initial Discharge (M3/S) | Recession Constant | Threshold Type | Ratio to Peak | |
| W460 | 20.729 | 87.447 | 0 | 2.1008 | 47.592 | Discharge | 0.13446 | 0.011284 | Ratio to Peak | 0.02868 | |
| W470 | 30.053 | 38.323 | 0 | 1.4673 | 33.402 | Discharge | 0.13802 | 0.012638 | Ratio to Peak | 0.027261 | |
| W480 | 2.8737 | 99 | 0 | 0.15795 | 682.42 | Discharge | 0.098534 | 0.000869 | Ratio to Peak | 0.043019 | |
| W490 | 15.028 | 99 | 0 | 0.10505 | 46.953 | Discharge | 0.041906 | 0.003161 | Ratio to Peak | 0.043896 | |
| W500 | 21.179 | 99 | 0 | 0.12669 | 47.514 | Discharge | 0.030115 | 0.001747 | Ratio to Peak | 0.019119 | |
| W510 | 11.44 | 73.599 | 0 | 0.13698 | 17.791 | Discharge | 0.041321 | 0.000903 | Ratio to Peak | 0.005441 | |
| W520 | 5.3632 | 35.285 | 0 | 0.036303 | 0.37666 | Discharge | 0.001134 | 0.000253 | Ratio to Peak | 0.003327 | |
| W530 | 17.904 | 40.851 | 0 | 0.15615 | 63.113 | Discharge | 0.237818 | 0.055439 | Ratio to Peak | 0.31 | |
| W540 | 22.207 | 53.616 | 0 | 0.11542 | 18.516 | Discharge | 0.042142 | 0.011278 | Ratio to Peak | 0.0125 | |
| W550 | 9.3957 | 36.679 | 0 | 0.15864 | 29.975 | Discharge | 0.080999 | 0.000783 | Ratio to Peak | 0.001645 | |
| W560 | 23.196 | 35.338 | 0 | 0.16225 | 12.61 | Discharge | 0.130829 | 0.003344 | Ratio to Peak | 0.011756 | |
| W570 | 8.691 | 97.696 | 0 | 0.12382 | 96.127 | Discharge | 0.040348 | 0.001543 | Ratio to Peak | 0.042158 | |
| W580 | 8.8546 | 73.753 | 0 | 0.13106 | 13.875 | Discharge | 0.052798 | 0.000516 | Ratio to Peak | 0.008498 | |
| W590 | 3.822 | 62.211 | 0 | 0.14209 | 20.322 | Discharge | 0.067572 | 0.017892 | Ratio to Peak | 0.094858 | |
| W600 | 49.233 | 60.847 | 0 | 0.72783 | 34.053 | Discharge | 0.10564 | 0.007639 | Ratio to Peak | 0.13943 | |
| W610 | 2.36 | 66.068 | 0 | 0.10861 | 13.119 | Discharge | 0.03593 | 0.023873 | Ratio to Peak | 0.018362 | |
| W620 | 12.198 | 57.499 | 0 | 0.13802 | 36.543 | Discharge | 0.058984 | 0.005114 | Ratio to Peak | 0.02868 | |
| W630 | 12.424 | 91.992 | 0 | 0.097509 | 2.6029 | Discharge | 0.034415 | 0.000345 | Ratio to Peak | 0.001548 | |
| W640 | 17.617 | 65.036 | 0 | 0.0986 | 3.9405 | Discharge | 0.024706 | 0.000364 | Ratio to Peak | 0.00158 | |
| W650 | 13.414 | 42.675 | 0 | 0.12973 | 66.795 | Discharge | 0.1265 | 0.019578 | Ratio to Peak | 0.0618 | |
| W660 | 21.357 | 37.503 | 0 | 0.030484 | 0.016667 | Discharge | 0.001312 | 0.000888 | Ratio to Peak | 0.013 | |
| W670 | 24.325 | 37.503 | 0 | 0.096453 | 0.068933 | Discharge | 0.008798 | 0.000259 | Ratio to Peak | 0.011 | |
| W680 | 8.8549 | 51.821 | 0 | 0.15795 | 0.70068 | Discharge | 0.096251 | 0.00082 | Ratio to Peak | 0.000305 | |

| Basin Number | SCS Curve Number Loss | | | Clark Unit Hydrograph Transform | | Recession Baseflow | | | | | |
|--------------|--------------------------|--------------|----------------|---------------------------------|--------------------------|--------------------|--------------------------|--------------------|----------------|---------------|--|
| | Initial Abstraction (mm) | Curve Number | Impervious (%) | Time of Concentration (HR) | Storage Coefficient (HR) | Initial Type | Initial Discharge (M3/S) | Recession Constant | THreshold Type | Ratio to Peak | |
| W690 | 46.509 | 37.259 | 0 | 0.1169 | 10.457 | Discharge | 0.031954 | 0.004528 | Ratio to Peak | 0.064529 | |
| W700 | 2.7889 | 71.859 | 0 | 0.13268 | 0.36755 | Discharge | 0.122426 | 0.000114 | Ratio to Peak | 0.000144 | |
| W710 | 20.199 | 53.743 | 0 | 0.15315 | 31.801 | Discharge | 0.037121 | 0.028252 | Ratio to Peak | 0.003777 | |
| W720 | 98.891 | 43.592 | 0 | 0.13356 | 1.5559 | Discharge | 0.048933 | 0.000572 | Ratio to Peak | 0.000459 | |
| W730 | 17.862 | 66.407 | 0 | 0.15104 | 0.4251 | Discharge | 0.10778 | 0.000345 | Ratio to Peak | 0.000217 | |
| W740 | 8.5201 | 42.607 | 0 | 0.16523 | 43.475 | Discharge | 0.181356 | 0.02414 | Ratio to Peak | 0.21778 | |
| W750 | 8.031 | 40.333 | 0 | 0.070513 | 0.88694 | Discharge | 0.05439 | 0.001465 | Ratio to Peak | 0.000212 | |
| W760 | 4.6894 | 68.631 | 0 | 0.060041 | 0.66673 | Discharge | 0.04565 | 0.004714 | Ratio to Peak | 0.000459 | |
| W770 | 2.4646 | 44.653 | 0 | 2.1169 | 0.34525 | Discharge | 0.175854 | 0.000258 | Ratio to Peak | 0.000212 | |
| W780 | 4.7621 | 72.887 | 0 | 0.095601 | 0.7242 | Discharge | 0.047338 | 0.00279 | Ratio to Peak | 0.000458 | |
| W790 | 4.8915 | 76.427 | 0 | 0.10597 | 0.3248 | Discharge | 0.067478 | 0.000111 | Ratio to Peak | 0.000318 | |
| W800 | 5.9774 | 70.048 | 0 | 0.065995 | 0.52202 | Discharge | 1.06E-02 | 0.000171 | Ratio to Peak | 0.000145 | |
| W810 | 9.3092 | 38.512 | 0 | 0.12093 | 2.2524 | Discharge | 4.38E-02 | 0.00291 | Ratio to Peak | 0.000459 | |
| W820 | 2.3349 | 82.118 | 0 | 0.63796 | 1.7592 | Discharge | 0.13877 | 0.000171 | Ratio to Peak | 0.000674 | |
| W830 | 5.4976 | 66.722 | 0 | 0.13554 | 1.3393 | Discharge | 0.043451 | 0.000381 | Ratio to Peak | 0.000312 | |
| W840 | 5.968 | 68.664 | 0 | 0.084639 | 1.5795 | Discharge | 0.024107 | 0.000586 | Ratio to Peak | 0.000133 | |
| W850 | 0.10232 | 99 | 0 | 0.034699 | 1.6554 | Discharge | 0.000955 | 0.000172 | Ratio to Peak | 0.005018 | |
| W860 | 0.0972639 | 99 | 0 | 0.16295 | 1.3004 | Discharge | 0.025373 | 7.57E-05 | Ratio to Peak | 0.001494 | |
| W870 | 0.20808 | 85.865 | 0 | 0.016667 | 1.4112 | Discharge | 0.035965 | 0.000114 | Ratio to Peak | 0.000144 | |
| W880 | 0.75083 | 79.471 | 0 | 0.016667 | 0.83537 | Discharge | 0.093719 | 7.57E-05 | Ratio to Peak | 0.000991 | |
| W890 | 1.851 | 64.999 | 0 | 0.14292 | 0.80387 | Discharge | 0.030846 | 7.57E-05 | Ratio to Peak | 0.000674 | |
| W900 | 5.6319 | 99 | 0 | 0.14046 | 1.0867 | Discharge | 0.016936 | 0.000387 | Ratio to Peak | 0.000495 | |

Annex 10. Mayo Model Reach Parameters

Table A-10.1.1. Mayo Model Reach Parameters

| Reach Number | Muskingum Cunge Channel Routing | | | | | | |
|--------------|---------------------------------|------------|----------|-------------|-----------|----------|------------|
| | Time Step Method | Length (m) | Slope | Manning's n | Shape | Width | Side Slope |
| R100 | Automatic Fixed Interval | 1556.4 | 0.12667 | 0.053 | Trapezoid | 230.5381 | 1 |
| R140 | Automatic Fixed Interval | 1381.2 | 0.074397 | 0.053 | Trapezoid | 230.5381 | 1 |
| R160 | Automatic Fixed Interval | 668.7 | 0.0189 | 0.053 | Trapezoid | 230.5381 | 1 |
| R170 | Automatic Fixed Interval | 4499.3 | 0.18029 | 0.053 | Trapezoid | 230.5381 | 1 |
| R190 | Automatic Fixed Interval | 110.71 | 0.042634 | 0.053 | Trapezoid | 230.5381 | 1 |
| R200 | Automatic Fixed Interval | 6226.7 | 0.074297 | 0.053 | Trapezoid | 230.5381 | 1 |
| R210 | Automatic Fixed Interval | 419.71 | 0.061422 | 0.053 | Trapezoid | 230.5381 | 1 |
| R230 | Automatic Fixed Interval | 3411.9 | 0.05174 | 0.053 | Trapezoid | 230.5381 | 1 |
| R250 | Automatic Fixed Interval | 1859.9 | 0.035417 | 0.053 | Trapezoid | 230.5381 | 1 |
| R280 | Automatic Fixed Interval | 1617.8 | 0.18162 | 0.053 | Trapezoid | 230.5381 | 1 |
| R320 | Automatic Fixed Interval | 5351.9 | 0.042381 | 0.053 | Trapezoid | 230.5381 | 1 |
| R330 | Automatic Fixed Interval | 590.42 | 0.000196 | 0.053 | Trapezoid | 230.5381 | 1 |
| R340 | Automatic Fixed Interval | 4278.2 | 0.029266 | 0.053 | Trapezoid | 230.5381 | 1 |
| R350 | Automatic Fixed Interval | 4662.2 | 0.079639 | 0.053 | Trapezoid | 230.5381 | 1 |
| R370 | Automatic Fixed Interval | 4603.5 | 0.015812 | 0.053 | Trapezoid | 230.5381 | 1 |
| R380 | Automatic Fixed Interval | 1279.5 | 0.028183 | 0.053 | Trapezoid | 230.5381 | 1 |
| R390 | Automatic Fixed Interval | 283.14 | 0.018293 | 0.053 | Trapezoid | 230.5381 | 1 |
| R410 | Automatic Fixed Interval | 509.41 | 0.012169 | 0.053 | Trapezoid | 230.5381 | 1 |
| R430 | Automatic Fixed Interval | 3822.7 | 0.014283 | 0.053 | Trapezoid | 230.5381 | 1 |
| R450 | Automatic Fixed Interval | 1754.6 | 0.001 | 0.053 | Trapezoid | 230.5381 | 1 |
| R50 | Automatic Fixed Interval | 104.85 | 0.12017 | 0.053 | Trapezoid | 230.5381 | 1 |
| R70 | Automatic Fixed Interval | 1101.5 | 0.092725 | 0.053 | Trapezoid | 230.5381 | 1 |

Annex 11. Mayo Field Validation Points

Table A-11.1. Mayo Field Validation Points

| Point Number | Validation Coordinates (in WGS84) | | Model Var (m) | Validation Points (m) | Error | Event/Date | Rain Return / Scenario |
|--------------|-----------------------------------|------------|---------------|-----------------------|--------|--|------------------------|
| | Lat | Long | | | | | |
| 1 | 6.974279 | 126.30853 | 0.08 | 0 | 0.0064 | | 25-Year |
| 2 | 6.973988 | 126.307539 | 0.09 | 0 | 0.0081 | | 25-Year |
| 3 | 6.973413 | 126.308363 | 0.11 | 0.02 | 0.0081 | Pablo/ December 2012 | 25-Year |
| 4 | 6.972282 | 126.3076 | 0.12 | 0 | 0.0144 | | 25-Year |
| 5 | 6.985238 | 126.317336 | 0.37 | 0.2 | 0.0289 | Pablo/ 2012 | 25-Year |
| 6 | 6.984663 | 126.313777 | 0.5 | 0.3 | 0.04 | Pablo/ 2012 | 25-Year |
| 7 | 6.984199 | 126.313981 | 0.52 | 0.4 | 0.0144 | Pablo/ 2012 | 25-Year |
| 8 | 6.980696 | 126.314164 | 0.54 | 0 | 0.2916 | | 25-Year |
| 9 | 6.985014 | 126.317948 | 0.67 | 0.3 | 0.1369 | Pablo/ 2012 | 25-Year |
| 10 | 6.987839 | 126.319441 | 0.81 | 0.3 | 0.2601 | Pablo/ December 2012 | 25-Year |
| 11 | 6.984549 | 126.317165 | 0.71 | 0.4 | 0.0961 | Pablo/ 2012 | 25-Year |
| 12 | 6.984118 | 126.317511 | 0.87 | 0.5 | 0.1369 | Pablo/ 2012 | 25-Year |
| 13 | 6.981716 | 126.315047 | 0.87 | 0.1 | 0.5929 | Pablo/ 2012 | 25-Year |
| 14 | 6.985821 | 126.318184 | 0.97 | 0.4 | 0.3249 | Pablo/ 2012 | 25-Year |
| 15 | 6.97524 | 126.309945 | 1.33 | 0.6 | 0.5329 | Pablo/ December 2012 | 25-Year |
| 16 | 6.990538 | 126.308827 | 1.22 | 0 | 1.4884 | | 25-Year |
| 17 | 6.991178 | 126.30924 | 1.3 | 0.5 | 0.64 | | 25-Year |
| 18 | 6.991321 | 126.308467 | 1.37 | 0.5 | 0.7569 | Pablo/ 2012 | 25-Year |
| 19 | 6.97602 | 126.309794 | 1.76 | 1.2 | 0.3136 | Pablo/ 2012 | 25-Year |
| 20 | 6.995603 | 126.305303 | 1.66 | 0.2 | 2.1316 | Pablo/ 2012 | 25-Year |
| 21 | 6.978806 | 126.312746 | 1.98 | 1 | 0.9604 | | 25-Year |
| 22 | 6.977517 | 126.311134 | 2.31 | 1 | 1.7161 | Typhoon/ 2014 | 25-Year |
| 23 | 6.988607 | 126.319967 | 0.72 | 0.4 | 0.1024 | Pablo and Yolanda/ 2012 and 2013 | 25-Year |
| 24 | 6.989011 | 126.320332 | 1 | 0.5 | 0.25 | Pablo/ 2012 | 25-Year |
| 25 | 7.010394 | 126.324075 | 0.03 | 0 | 0.0009 | | 25-Year |
| 26 | 7.009526 | 126.323785 | 0.03 | 0 | 0.0009 | | 25-Year |
| 27 | 7.011579 | 126.324253 | 0.04 | 0 | 0.0016 | | 25-Year |
| 28 | 7.009109 | 126.323549 | 0.57 | 0.4 | 0.0289 | Intense local rainfall/ 2014 | 25-Year |
| 29 | 7.008279 | 126.323624 | 0.7 | 0.6 | 0.01 | Typhoon | 25-Year |
| 30 | 7.008929 | 126.323762 | 0.7 | 0.5 | 0.04 | Intense local rainfall/ 2014 | 25-Year |
| 31 | 6.997212 | 126.326405 | 1.02 | 0.1 | 0.8464 | Buhawi | 25-Year |
| 32 | 7.001417 | 126.331303 | 1.15 | 0 | 1.3225 | | 25-Year |
| 33 | 7.001763 | 126.331299 | 1.21 | 0 | 1.4641 | | 25-Year |
| 34 | 7.007067 | 126.323533 | 0.86 | 0.5 | 0.1296 | Buhawi/ 2015 | 25-Year |

| Point Number | Validation (in WGS84) | Coordinates (Long) | Model Var (m) | Validation Points (m) | 0.636804 | Event/Date | 100-Year Return/Scenario |
|--------------|-----------------------|--------------------|---------------|-----------------------|----------|-----------------------------------|--------------------------|
| 76 | 10.52101 | 123.71755 | 0.771 | 2.1 | 1.766241 | Senyang | 100-Year |
| 77 | 10.52127 | 123.71753 | 0.99 | 1 | 0.0001 | Yolanda | 100-Year |
| 78 | 6.998877 | 126.328052 | 1.716 | 1.5 | 0.614656 | Yolanda | 100-Year |
| 79 | 6.998519 | 126.327724 | 1.808 | 0.2 | 0.369864 | Senyang | 100-Year |
| 80 | 6.999474 | 126.328637 | 1.379 | 0.8 | 0.229441 | Pablo/ 2015 Senyang | 25-Year |
| 81 | 6.991798 | 126.326826 | 1.38 | 0.7 | 0.6644 | Intense local rainfall Ruping | 100-Year |
| 82 | 10.51771 | 123.71789 | 0.199 | 2 | 3.243601 | Senyang | 100-Year |
| 39 | 6.999203 | 126.328384 | 1.15 | 0.8 | 0.1225 | Pablo/ 2015 | 25-Year |
| 40 | 7.005789 | 126.322994 | 0.98 | 0.9 | 0.0064 | Buhawi/ 2015 | 25-Year |
| 41 | 7.008601 | 126.324032 | 1.17 | 0.6 | 0.3249 | Typhoon | 25-Year |
| 42 | 6.99546 | 126.327247 | 1.34 | 0.5 | 0.7056 | Intense local rainfall/ 2011 | 25-Year |
| 43 | 6.998247 | 126.327661 | 1.55 | 0 | 2.4025 | | 25-Year |
| 44 | 7.001958 | 126.31637 | 1.65 | 1.1 | 0.3025 | Buhawi/ 2013 | 25-Year |
| 45 | 7.003001 | 126.331372 | 1.76 | 0 | 3.0976 | | 25-Year |
| 46 | 6.996178 | 126.325119 | 1.76 | 1.1 | 0.4356 | Buhawi/ 2011 | 25-Year |
| 47 | 6.991995 | 126.322718 | 1.94 | 0.4 | 2.3716 | Yolanda/ 2013 | 25-Year |
| 48 | 6.996371 | 126.326099 | 2.05 | 0.55 | 2.25 | Buhawi/ 2013 | 25-Year |
| 49 | 7.002776 | 126.331257 | 2.05 | 0 | 4.2025 | | 25-Year |
| 50 | 6.991728 | 126.321509 | 1.93 | 0.4 | 2.3409 | Yolanda/ 2013 | 25-Year |
| 51 | 7.001004 | 126.317415 | 2.04 | 1.2 | 0.7056 | Buhawi and Yolanda/ 2013 | 25-Year |
| 52 | 6.995878 | 126.325752 | 2.27 | 0.3 | 3.8809 | Agaton/ 2014 | 25-Year |
| 53 | 7.00202 | 126.313883 | 2.45 | 1.5 | 0.9025 | Buhawi/ 2013 | 25-Year |
| 54 | 6.992987 | 126.323231 | 2.56 | 0.6 | 3.8416 | Yolanda and Agaton/ 2013 and 2014 | 25-Year |
| 55 | 7.00249 | 126.331032 | 2.63 | 1.5 | 1.2769 | | 25-Year |
| 56 | 7.002408 | 126.312959 | 2.62 | 1.5 | 1.2544 | Buhawi/ 2013 | 25-Year |
| 57 | 7.005507 | 126.309492 | 3.26 | 2.2 | 1.1236 | Yolanda/ August 14, 2014 | 25-Year |
| 58 | 7.004968 | 126.310067 | 3.26 | 2.3 | 0.9216 | Yolanda/ August 14, 2014 | 25-Year |
| 59 | 7.000783 | 126.330052 | 3.96 | 3.1 | 0.7396 | | 25-Year |
| 60 | 7.002457 | 126.329689 | 4.12 | 3.2 | 0.8464 | Pablo/ December 2012 | 25-Year |
| 61 | 7.006717 | 126.333344 | 0.07 | 0 | 0.0049 | | 25-Year |
| 62 | 7.00647 | 126.333385 | 0.07 | 0 | 0.0049 | | 25-Year |
| 63 | 7.007485 | 126.331752 | 0.09 | 0 | 0.0081 | | 25-Year |
| 64 | 7.007568 | 126.330965 | 0.08 | 0 | 0.0064 | | 25-Year |
| 65 | 7.006458 | 126.334067 | 0.1 | 0 | 0.01 | | 25-Year |
| 66 | 7.006804 | 126.333065 | 0.1 | 0.1 | 0 | Intense local rainfall/ 2014 | 25-Year |
| 67 | 7.007161 | 126.332091 | 0.1 | 0 | 0.01 | | 25-Year |
| 68 | 7.00724 | 126.331443 | 0.11 | 0 | 0.0121 | | 25-Year |

| Point Number | Validation Coordinates (in WGS84) | | Model Var (m) | Validation Points (m) | Error | Event/Date | Rain Return / Scenario |
|--------------|-----------------------------------|------------|---------------|-----------------------|--------|--------------------------------------|------------------------|
| | Lat | Long | | | | | |
| 69 | 7.007136 | 126.331767 | 0.11 | 0 | 0.0121 | | 25-Year |
| 70 | 7.006461 | 126.332877 | 0.11 | 0.4 | 0.0841 | Intense local rainfall | 25-Year |
| 71 | 7.00691 | 126.332607 | 0.11 | 0.1 | 1E-04 | Intense local rainfall/ 2014 | 25-Year |
| 72 | 7.005501 | 126.335614 | 0.12 | 2.1 | 3.9204 | Typhoon/ 2013 | 25-Year |
| 73 | 7.006637 | 126.332471 | 0.12 | 0.3 | 0.0324 | Intense local rainfall | 25-Year |
| 74 | 7.004846 | 126.335627 | 0.13 | 0.51 | 0.1444 | Intense local rainfall | 25-Year |
| 75 | 7.005123 | 126.335483 | 0.18 | 0.51 | 0.1089 | Intense local rainfall | 25-Year |
| 76 | 7.005008 | 126.336078 | 0.22 | 0 | 0.0484 | | 25-Year |
| 77 | 7.005301 | 126.335821 | 0.22 | 0 | 0.0484 | | 25-Year |
| 78 | 7.004637 | 126.335804 | 0.22 | 0.51 | 0.0841 | Intense local rainfall | 25-Year |
| 79 | 7.005772 | 126.33507 | 0.26 | 0.1 | 0.0256 | | 25-Year |
| 80 | 7.005577 | 126.336093 | 0.29 | 2.1 | 3.2761 | Typhoon/ 2013 | 25-Year |
| 81 | 7.006102 | 126.335029 | 0.3 | 0.1 | 0.04 | | 25-Year |
| 82 | 7.005529 | 126.333257 | 0.31 | 0 | 0.0961 | | 25-Year |
| 83 | 7.005008 | 126.335015 | 0.33 | 0 | 0.1089 | | 25-Year |
| 84 | 7.005284 | 126.334964 | 0.35 | 0.1 | 0.0625 | Intense local rainfall | 25-Year |
| 85 | 7.00631 | 126.334353 | 0.37 | 0 | 0.1369 | | 25-Year |
| 86 | 7.00541 | 126.334139 | 0.4 | 0.1 | 0.09 | Intense local rainfall | 25-Year |
| 87 | 7.005241 | 126.333792 | 0.43 | 0.1 | 0.1089 | Intense local rainfall | 25-Year |
| 88 | 7.005434 | 126.334801 | 0.4 | 0.1 | 0.09 | Intense local rainfall | 25-Year |
| 89 | 7.004533 | 126.335459 | 0.47 | 0.1 | 0.1369 | Intense local rainfall | 25-Year |
| 90 | 7.003705 | 126.334729 | 0.45 | 0.5 | 0.0025 | Intense local rainfall/ 2015 | 25-Year |
| 91 | 7.005601 | 126.334854 | 0.43 | 0.1 | 0.1089 | | 25-Year |
| 92 | 7.004112 | 126.335067 | 0.46 | 0.5 | 0.0016 | Intense local rainfall/ October 2016 | 25-Year |
| 93 | 7.005133 | 126.334563 | 0.45 | 0.1 | 0.1225 | Intense rainfall | 25-Year |
| 94 | 7.005268 | 126.334336 | 0.47 | 0.1 | 0.1369 | Intense local rainfall | 25-Year |
| 95 | 7.005345 | 126.334621 | 0.45 | 0 | 0.2025 | | 25-Year |
| 96 | 7.005621 | 126.33449 | 0.5 | 0.1 | 0.16 | Intense local rainfall | 25-Year |

| Point Number | Validation Coordinates (in WGS84) | | Model Var (m) | Validation Points (m) | Error | Event/Date | Rain Return / Scenario |
|--------------|-----------------------------------|------------|---------------|-----------------------|--------|--------------------------------------|------------------------|
| | Lat | Long | | | | | |
| 97 | 7.00582 | 126.334648 | 0.53 | 0 | 0.2809 | | 25-Year |
| 98 | 7.004128 | 126.334891 | 0.61 | 0.41 | 0.04 | Intense local rainfall/ October 2016 | 25-Year |
| 99 | 7.004063 | 126.334629 | 0.64 | 0.5 | 0.0196 | Intense local rainfall/ 2015 | 25-Year |
| 100 | 7.004149 | 126.334814 | 0.64 | 0.41 | 0.0529 | Intense local rainfall/ October 2016 | 25-Year |
| 101 | 7.004086 | 126.333803 | 0.86 | 0.33 | 0.2809 | Yolanda and Intense rainfall/ 2014 | 25-Year |
| 102 | 7.004556 | 126.33513 | 0.71 | 0 | 0.5041 | | 25-Year |
| 103 | 7.004247 | 126.334462 | 0.76 | 0.5 | 0.0676 | Intense local rainfall/ October 2016 | 25-Year |
| 104 | 7.004314 | 126.335304 | 0.75 | 0 | 0.5625 | | 25-Year |
| 105 | 7.00433 | 126.335092 | 0.76 | 0 | 0.5776 | | 25-Year |
| 106 | 7.004782 | 126.334615 | 0.81 | 0 | 0.6561 | | 25-Year |
| 107 | 7.004369 | 126.33526 | 0.79 | 0 | 0.6241 | | 25-Year |
| 108 | 7.004296 | 126.334539 | 0.82 | 0.5 | 0.1024 | Intense local rainfall/ October 2016 | 25-Year |
| 109 | 7.004373 | 126.335151 | 0.83 | 0 | 0.6889 | | 25-Year |
| 110 | 7.004443 | 126.335094 | 0.85 | 0 | 0.7225 | | 25-Year |
| 111 | 7.004398 | 126.335003 | 0.85 | 0 | 0.7225 | | 25-Year |
| 112 | 7.00434 | 126.334246 | 0.97 | 0 | 0.9409 | | 25-Year |
| 113 | 7.004531 | 126.334663 | 0.99 | 0 | 0.9801 | | 25-Year |
| 114 | 7.00472 | 126.334518 | 1.06 | 0 | 1.1236 | | 25-Year |
| 115 | 7.004555 | 126.33426 | 1.1 | 0 | 1.21 | | 25-Year |
| 116 | 7.004647 | 126.334447 | 1.1 | 0 | 1.21 | | 25-Year |
| 117 | 7.00451 | 126.334157 | 1.11 | 0 | 1.2321 | | 25-Year |
| 118 | 7.006501 | 126.286855 | 0.04 | 0 | 0.0016 | | 25-Year |
| 119 | 7.00771 | 126.285747 | 0.07 | 0 | 0.0049 | | 25-Year |
| 120 | 6.997975 | 126.298552 | 1.95 | 0.5 | 2.1025 | Intense local rainfall/ 2013 | 25-Year |
| 121 | 7.01158 | 126.29328 | 2.33 | 0.5 | 3.3489 | Pablo/ 2012 | 25-Year |
| 122 | 6.998382 | 126.298359 | 2.34 | 1.1 | 1.5376 | Typhoon/ 2005 | 25-Year |
| 123 | 6.998051 | 126.299228 | 2.29 | 0.5 | 3.2041 | Intense local rainfall/ 2013 | 25-Year |
| 124 | 7.011619 | 126.291531 | 2.42 | 0.5 | 3.6864 | | 25-Year |
| 125 | 6.999096 | 126.298105 | 2.49 | 0.95 | 2.3716 | Upstream Rainfall/ 2014-2015 | 25-Year |

| Point Number | Validation Coordinates (in WGS84) | | Model Var (m) | Validation Points (m) | Error | Event/Date | Rain Return / Scenario |
|--------------|-----------------------------------|------------|---------------|-----------------------|---------|--|------------------------|
| | Lat | Long | | | | | |
| 126 | 6.998988 | 126.298413 | 2.5 | 0.95 | 2.4025 | Upstream Rainfall/ 2014-2015 | 25-Year |
| 127 | 6.998882 | 126.298181 | 2.56 | 0.95 | 2.5921 | Upstream Rainfall/ 2014-2015 | 25-Year |
| 128 | 6.998706 | 126.298596 | 2.59 | 0.95 | 2.6896 | Upstream Rainfall/ 2014-2015 | 25-Year |
| 129 | 6.998778 | 126.298394 | 2.64 | 0.95 | 2.8561 | Upstream Rainfall/ 2014-2015 | 25-Year |
| 130 | 7.013906 | 126.28712 | 2.83 | 0.4 | 5.9049 | | 25-Year |
| 131 | 7.010927 | 126.2939 | 2.8 | 0.4 | 5.76 | Yolanda/ 2013 | 25-Year |
| 132 | 7.014457 | 126.287727 | 2.97 | 0.5 | 6.1009 | Intense local rainfall/ 2015 | 25-Year |
| 133 | 7.013536 | 126.290221 | 2.85 | 2.1 | 0.5625 | | 25-Year |
| 134 | 7.009008 | 126.294734 | 3.68 | 0.62 | 9.3636 | Intense local rainfall/ September 2012 | 25-Year |
| 135 | 7.010779 | 126.294688 | 3.5 | 2.5 | 1 | | 25-Year |
| 136 | 7.015512 | 126.291201 | 3.64 | 2.5 | 1.2996 | | 25-Year |
| 137 | 7.012633 | 126.29384 | 3.73 | 2.5 | 1.5129 | | 25-Year |
| 138 | 7.009816 | 126.296399 | 3.78 | 2.5 | 1.6384 | | 25-Year |
| 139 | 7.00169 | 126.298331 | 3.86 | 2.5 | 1.8496 | | 25-Year |
| 140 | 7.012455 | 126.294389 | 5.93 | 2.5 | 11.7649 | | 25-Year |
| 141 | 7.00916 | 126.298705 | 5.93 | 2.5 | 11.7649 | | 25-Year |
| 142 | 7.011186 | 126.295793 | 5.87 | 3.5 | 5.6169 | | 25-Year |
| 143 | 7.011367 | 126.295165 | 5.95 | 3.5 | 6.0025 | | 25-Year |
| 144 | 7.012036 | 126.294511 | 6.01 | 3.5 | 6.3001 | | 25-Year |
| 145 | 7.011468 | 126.294653 | 6.02 | 3.5 | 6.3504 | | 25-Year |
| 146 | 7.010536 | 126.297667 | 5.91 | 3.5 | 5.8081 | | 25-Year |
| 147 | 7.015661 | 126.294309 | 6.06 | 3.5 | 6.5536 | | 25-Year |
| 148 | 7.018222 | 126.282032 | 0.04 | 0 | 0.0016 | | 25-Year |
| 149 | 7.017187 | 126.282539 | 0.04 | 0 | 0.0016 | | 25-Year |
| 150 | 7.017831 | 126.282912 | 0.03 | 0 | 0.0009 | | 25-Year |
| 151 | 7.022283 | 126.284617 | 3.27 | 0.6 | 7.1289 | Intense local rainfall/ 2015 | 25-Year |
| 152 | 7.020535 | 126.286512 | 3.29 | 0.5 | 7.7841 | Intense local rainfall/ 2013 | 25-Year |
| 153 | 7.019901 | 126.28644 | 3.37 | 0.5 | 8.2369 | Yolanda/ 2013 | 25-Year |
| 154 | 7.022067 | 126.284877 | 3.44 | 0.6 | 8.0656 | Intense local rainfall/ 2015 | 25-Year |

| Point Number | Validation Coordinates (in WGS84) | | Model Var (m) | Validation Points (m) | Error | Event/Date | Rain Return / Scenario |
|--------------|-----------------------------------|------------|---------------|-----------------------|---------|------------------------------|------------------------|
| | Lat | Long | | | | | |
| 155 | 7.020874 | 126.286301 | 3.47 | 0.5 | 8.8209 | Agaton/ January 2014 | 25-Year |
| 156 | 7.015138 | 126.289108 | 3.4 | 0.5 | 8.41 | Intense local rainfall/ 2013 | 25-Year |
| 157 | 7.020733 | 126.285882 | 3.54 | 0.9 | 6.9696 | Agaton/ 2014 | 25-Year |
| 158 | 7.022895 | 126.284289 | 3.59 | 0.6 | 8.9401 | Intense local rainfall/ 2015 | 25-Year |
| 159 | 7.017107 | 126.288294 | 3.6 | 0.9 | 7.29 | Intense local rainfall/ 2015 | 25-Year |
| 160 | 7.02005 | 126.285465 | 3.73 | 0.9 | 8.0089 | Intense local rainfall/ 2015 | 25-Year |
| 161 | 7.022377 | 126.282931 | 3.89 | 1.5 | 5.7121 | Intense local rainfall/ 2015 | 25-Year |
| 162 | 7.025074 | 126.282397 | 4.06 | 1.5 | 6.5536 | Yolanda & Pablo/ 2012 & 2013 | 25-Year |
| 163 | 7.016235 | 126.289091 | 4.24 | 0.9 | 11.1556 | Intense local rainfall/ 2015 | 25-Year |
| 164 | 7.020525 | 126.28757 | 6.07 | 5 | 1.1449 | Buhawi/ 2011 | 25-Year |
| 165 | 7.025189 | 126.284351 | 6.15 | 5 | 1.3225 | | 25-Year |
| 166 | 7.021992 | 126.287322 | 6.15 | 5 | 1.3225 | | 25-Year |
| 167 | 7.024535 | 126.285114 | 6.27 | 5.5 | 0.5929 | | 25-Year |
| 168 | 7.023099 | 126.286158 | 6.32 | 5.5 | 0.6724 | | 25-Year |
| 169 | 7.020176 | 126.289283 | 6.26 | 5.5 | 0.5776 | | 25-Year |
| 170 | 7.020181 | 126.28779 | 6.34 | 5.5 | 0.7056 | | 25-Year |
| 171 | 7.021901 | 126.290687 | 1.17 | 2 | 0.6889 | | 25-Year |
| 172 | 7.020618 | 126.291168 | 1.93 | 2 | 0.0049 | | 25-Year |
| 173 | 7.023376 | 126.291234 | 2.25 | 2 | 0.0625 | | 25-Year |
| 174 | 7.021703 | 126.292628 | 2.73 | 2 | 0.5329 | | 25-Year |
| 175 | 7.02516 | 126.286052 | 3.92 | 2.5 | 2.0164 | | 25-Year |
| 176 | 7.026591 | 126.284736 | 3.95 | 2.5 | 2.1025 | | 25-Year |
| 177 | 7.026121 | 126.285063 | 4.15 | 2.5 | 2.7225 | | 25-Year |
| 178 | 7.025237 | 126.286791 | 4.41 | 2.5 | 3.6481 | | 25-Year |
| 179 | 7.025757 | 126.285797 | 4.48 | 2.5 | 3.9204 | | 25-Year |
| 180 | 7.020613 | 126.289644 | 6.23 | 4 | 4.9729 | | 25-Year |

Annex 12. Educational Institutions affected by flooding in Mayo Floodplain

Table A-12.1. Educational Institutions in Mati City, Davao Oriental affected by flooding in Mayo Floodplain

| Davao Oriental | | | | |
|---|-------------------|-------------------|---------|----------|
| Mati City | | | | |
| Building Name | Barangay | Rainfall Scenario | | |
| | | 5-year | 25-year | 100-year |
| LIMOT ELEMENTARY SCHOOL | Don Enrique Lopez | High | High | High |
| LIMOT ELEMENTARY SCHOOL (STAGE) | Don Enrique Lopez | High | High | High |
| PAGCOR BUILDING | Don Enrique Lopez | | | |
| MAYO NATIONAL HIGH SCHOOL | Tagabakid | Low | Low | Low |
| VICENTE ALMARIO SR. MEMORIAL SCHOOL | Tagabakid | Low | Low | Low |
| VICENTE ALMARIO SR. MEMORIAL SCHOOL ADMIN BLDG. | Tagabakid | Low | Low | Medium |

Annex 13. Health Institutions affected by flooding in Mayo Floodplain

Table A-13.1. Health Institutions in Mati City, Davao Oriental affected by flooding in Mayo Floodplain

| Davao Oriental | | | | |
|-----------------------------|-----------|-------------------|---------|----------|
| Mati City | | | | |
| Building Name | Barangay | Rainfall Scenario | | |
| | | 5-year | 25-year | 100-year |
| BARANGAY MAYO HEALTH CENTER | Tagabakid | Medium | Medium | Medium |

